

QUANTUM MODELS OF SPACE-TIME BASED ON RECOUPLING THEORY

John P. Moussouris

St. Cross College

Oxford

A thesis submitted in partial fulfillment of the requirements
for the degree of D.Phil. in Mathematics

Michaelmas term 1983

ABSTRACT: Models of geometry that are intrinsically quantum-mechanical in nature arise from the recoupling theory of space-time symmetry groups. Roger Penrose constructed such a model from $SU(2)$ recoupling in his theory of spin networks; he showed that spin measurements in a classical limit are necessarily consistent with a three-dimensional Euclidean vector space. T. Regge and G. Ponzano expressed the semi-classical limit of this spin model in a form resembling a path integral of the Einstein-Hilbert action in three Euclidean dimensions. This thesis gives new proofs of the Penrose spin geometry theorem and of the Regge-Ponzano decomposition theorem. We then consider how to generalize these two approaches to other groups that give rise to new models of quantum geometries. In particular, we show how to construct quantum models of four-dimensional relativistic space-time from the recoupling theory of the Poincare group.

ACKNOWLEDGEMENTS

I would like to thank my supervisor, Prof. Roger Penrose, for his invaluable advice and suggestions, and the IBM Corporation, for supporting the completion of this work during an academic leave of absence from the T.J. Watson Research Center.

ERRATA

p. 23 the middle relation in equation (2.2.9) should be:

$$t_2 = j_3 + j_1 - j_2$$

p. 68 omitted in page numbering

p. 75 in figure 4.11b, the Racah coefficient on the left side of the second line should have dotted lines connecting d and d' to the endpoints of edge x . The label on the edge between the couplings d_1 and d_2 should be j_5 .

p. 108 the following two references should be inserted:

[P.A.M. Dirac 33] "The Lagrangian in Quantum Mechanics" Physikalische Zeitschrift der Sowjetunion, 13, 1

[A.E. Edmonds 57] Angular Momentum in Quantum Mechanics (Princeton University Press, Princeton)

CONTENTS

1. INTRODUCTION	
1.1 Space-time and recoupling theory	1
1.2 Spin networks	4
1.3 Theory of fabrics	8
2. SPIN NETWORKS	
2.1 Basic states and operators	16
2.2 Addition of spin	21
2.3 Geometric relations between spins	30
2.4 The spin geometry theorem	37
3. REGGE-PONZANO THEORY	
3.1 Semiclassical limit of Racah coefficient	46
3.2 Decomposition theorem and path integrals	49
3.3 Regge calculus for quantized spin	55
4. THEORY OF FABRICS	
4.1 Recoupling theory of compact groups	58
4.2 Decomposition theorem	66
4.3 Fabrics	73
5. FABRICS OF THE POINCARÉ GROUP	
5.1 Basic states and operators of the Poincaré group	80
5.2 Relativistic addition of spin and momentum	87
5.3 Semiclassical limit of Racah coefficient	95
5.4 Stationary phase conditions for Poincaré fabrics	101
REFERENCES	108

QUANTUM MODELS OF SPACE-TIME BASED ON RECOUPLING THEORY

I. INTRODUCTION

1.1 Space-time and recoupling theory

Models of space and time that are intrinsically quantum-mechanical in nature arise from the quantum rules for the addition of conserved quantities such as spin and momentum. Roger Penrose constructed such a model from the purely combinatorial calculus of "spin networks" [Penrose 68, 71, 72], based on the non-relativistic rules for addition of quantized spin (i.e. SU(2) recoupling theory). He showed that spin measurements in a classical limit are necessarily consistent with the constraints of a 3-dimensional Euclidean vector space. T. Regge and G. Ponzano developed an analytic approach to the same spin model [Ponzano and Regge 68], expressing the semiclassical limit in a form resembling a path integral of the Einstein-Hilbert action in three Euclidean dimensions. This paper considers how to generalize these two approaches to other groups that give rise to new models of quantum geometries. In particular, we show how to construct quantum models of four-dimensional space-time from the rules for addition of relativistic spin and momentum (Poincare group recoupling theory).

The physical situation described by these models can be illustrated as follows. Suppose we make measurements on an ensemble of test particles or structures in order to probe their space-time relationships. We require these measurements to be invariant under a space-time symmetry group - say, the Poincare group. In this case, given a single particle, all we can measure is its mass and spin. Given two particles, we can measure the mass and spin of the composite system, and also the helicities of each of the two particles in the center-of-momentum frame (these "relative helicities" are also invariants). It turns out that more complicated measurements can be reduced to these simple one- and two-particle observations.

The basic technique for reducing more complicated measurements to one- and two-particle observations is to regard an n-particle system as the coupling of exactly two

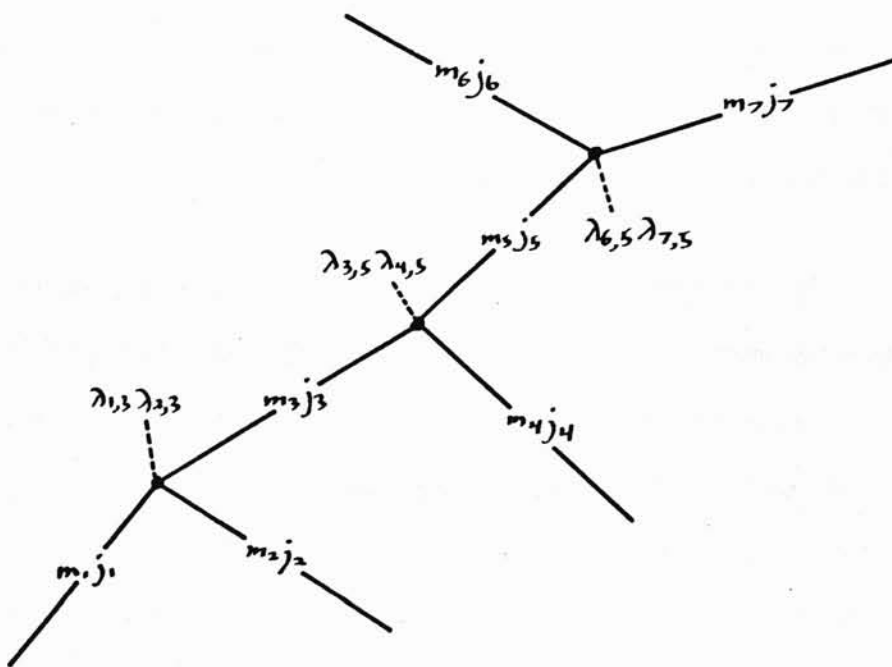
(composite) sub-structures. These in turn are composed of two finer sub-structures, and so on. Hence we can visualize the decomposition as a binary tree. More generally, we can represent both composition and splitting as a cubic graph (fig. 1). The partial masses m , spins j , and helicities λ associated with this graph, as we shall see later, determine all the Poincare invariants of many-particle systems (except for certain discrete ambiguities - e.g. in orientation).

Of course, if we make too many measurements, the system becomes overdetermined, and the space-time we are probing begins to reveal itself. For example, suppose we measure all the pairwise partial masses of n particles. These masses determine the $n \times n$ matrix of scalar products between the momenta, since

$$(P_i \cdot P_j) = \frac{1}{2} [M_{ij}^2 - M_i^2 - M_j^2] \quad (1.1.1)$$

In classical special relativity, this matrix is constrained to have signature (p, q) with $p \leq 1$ and $q \leq 3$, if the momenta are to be imbeddable in $(+---)$ Minkowski vector space. More compli-

Figure 1.1 Poincare Recoupling



cated constraints involving the spins and helicities guarantee the imbeddability of the particle trajectories themselves (and the associated relativistic angular momenta) in an affine Minkowski background. All these constraints are just the conditions for the existence in some reference frame of 4-component momentum vectors and 6-component angular momentum bivectors which are consistent with the observed mass and spin data, and are conserved at the cubic vertices of the recoupling graph. Since we do not observe the background directly, but only through invariant measurements on the test particles, it is convenient to take these kinematic constraints on the invariants as our operational definition of classical Minkowski geometry.

Quantum models of geometry arise from replacing this classical kinematic definition (linear algebra of additively conserved tensor quantities) by its quantum counterpart (the recoupling theory of the group generated by the corresponding tensor operators). In this case, we no longer have the rigid constraints of classical geometry. Instead, we have a prescription (e.g. the recoupling theory of the Poincare group) for assigning a probability measure to graphs like those in figure 1. We can prove, however, that this measure becomes concentrated in the classical limit around values for the measurements that respect the classical constraints. We can also develop a formalism resembling the path integral method for evaluating the semiclassical limit of these quantum models.

The kinematic intricacies of the Poincare group complicate the construction of the quantum model for the full 4-d relativistic space-time. Hence, we will begin with a self-contained review and analysis of earlier models of 3-d Euclidean space based on a much simpler problem: the non-relativistic addition of spin.

1.2 Spin Networks

The physical situation described by spin networks can be illustrated as follows. Imagine an ensemble of spinning structures with relative motions so slow and distances so small that the orbital angular momentum of any two structures is negligible compared with their intrinsic spin. Thus when structures coalesce or split, intrinsic spin is conserved, without any orbital contribution. No matter how complicated the collisions and splittings are, we can always in principle look closely enough to resolve them into cascades of simple exchanges involving only three spins, such as the coalescence of two structures to form a third, or the splitting of a structure into two others. When structures are not colliding or splitting, they are sufficiently isolated from the rest of the universe to have well-defined total spin values. A spin network is a cubic graph, whose edges are labeled with the results of measuring these total spin values, and whose vertices represent the composition of conserved spin.

Note that this is a purely kinematic model. Only the relative orientations of spins are significant in this model: relative positions and velocities are not treated at all. A spin network describes the kinematic addition of spin, abstracted from any details of localization or dynamics.

In classical kinematics, the edges of the spin network correspond to 3-component spin vectors. The total spin label on each edge determines the length of the vector. A vertex joining three edges 1, 2, and 3 represents the vector conservation law:

$$\vec{J}^1 \pm \vec{J}^2 \pm \vec{J}^3 = 0, \quad (1.2.1)$$

where the signs +/- correspond to 2 and 3 out/ingoing at the vertex that produces 1.

In quantum kinematics, the edges of the spin network are labelled by half-integers specifying the quantized total spin in units of \hbar .¹ Associated with an edge labelled j is the Hilbert space spanned by the $2j+1$ distinct directional states of total spin j . Each vertex

represents the requirement that the composition of the three incident spins be spherically symmetric, or satisfy the operator analog of the vector conservation law given in the last paragraph (i.e. it represents the homomorphism from the tensor product of the three Hilbert spaces, regarded as modules over the group, to the trivial module). The spin network as a whole represents a linear functional on the tensor product of all the spaces associated with its external lines. In particular, a closed spin network (one with no external lines) corresponds to a pure number - in fact an integer, with Penrose's definition of the norm.

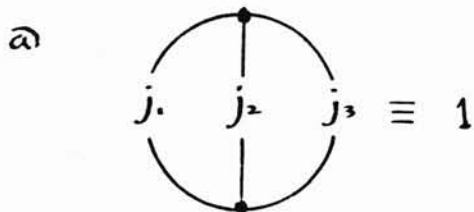
Figure 1.2 lists the four simplest closed spin networks and their values. The numbers of edges and vertices in a closed cubic graph satisfy the relation $2E = 3V$, so the number of distinct spins in these networks is $3n$, with n an integer. Figure 1.2a is the trivial case $n=1$. Figure 1.2b is the simplest non-trivial closed spin network (with $n=2$), the value of which is shown in standard notation as the Racah coefficient, or "6j-symbol".² Figures 2c and 2d show the two possible networks for $n=3$, the first of which corresponds to the standard "9j-coefficient". The second, as we shall see later, evaluates to the simple product of the two Racah coefficients shown.

Roger Penrose invented some combinatorial methods for evaluating the integer values of closed spin networks. These methods include an isomorphism between spinor and "binor" invariants [Penrose 72b], enumeration techniques based on chromatic polynomials [see Moussouris 79], and a collection of reduction formulae [Penrose 71, p.171]. Underlying all these methods is the representation of spin $1/2$ by the simplest (2-d) Hilbert space, and of higher spins by symmetrized products of this basic state space. The homomorphism which enforces spin conservation at each cubic vertex is constructed explicitly from products of the antisymmetric isotropic tensor ϵ_{AB} . Then the value of a network becomes the alternating sum

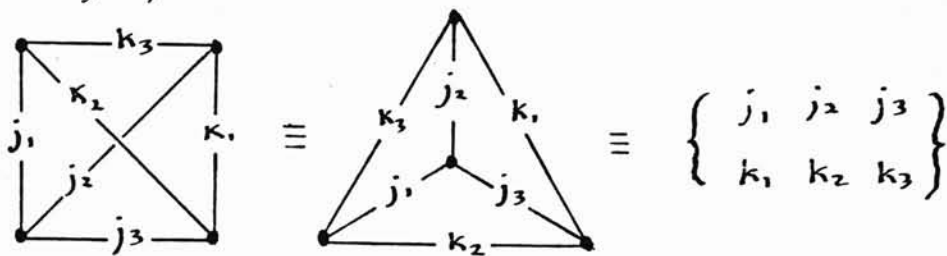
¹ Penrose labels the edges of spin networks with integers specifying spin in units of $1/2 \hbar$. Our convention is more consistent with Regge-Ponzano diagrams and other graphical methods. See the list of other differences in conventions at the end of section 2.2.

² The Racah coefficient and 6j-symbol differ in sign conventions [Edmonds 57, p99].

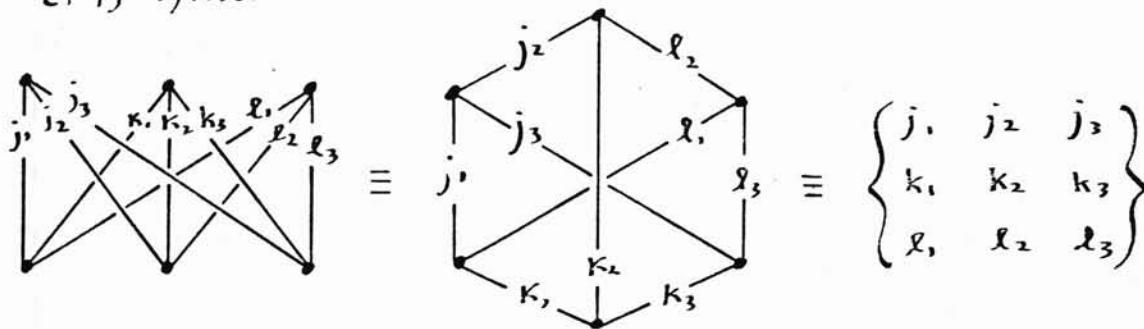
Figure 1.2 Four simplest closed spin networks



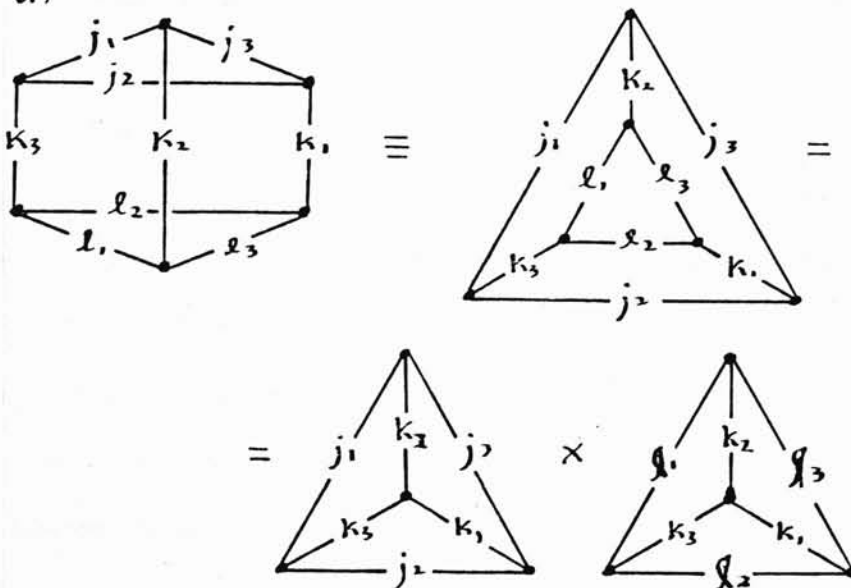
b) $6j$ -symbol or RACA coefficient



c) $9j$ -symbol



d)



of the number of ways individual spin-1/2 subunits can circulate while satisfying the conservation laws. The evaluation methods are primarily devices for handling the cancellation (destructive interference) that occurs because of alternating signs in this superposition.

Chapter 2 begins the analysis of the classical limit of spin networks, by an algebraic method that diverges somewhat from Penrose's approach. We define operators for the scalar product $(\vec{J}^1 \cdot \vec{J}^2)$ between two spins. We then prove that any 4 x 4 matrix of such operators satisfies the identity

$$\det [(\vec{J}^k \cdot \vec{J}^\ell)] \approx 0, \quad (1.2.2)$$

up to terms that result from the commutation of the operators. In a classical limit, where these terms are unimportant, we can then show that any n x n matrix of expectation values of these scalar products must be positive semi-definite with rank no greater than 3. But this is just the condition - the counterpart of the one given earlier for Minkowski momentum space - for the existence of spin vectors imbeddable in a three-dimensional Euclidean "spin space". We discuss the connection between our algebraic proof of this result and a purely combinatorial proof given earlier by Penrose.

Chapter 3 reviews yet another analysis of the semiclassical limit of spin networks, by a method developed by Regge and Ponzano, which resembles the path-integral formulation of quantum mechanics. This method is based on two observations: first, that the Racah coefficient of figure 1.2b is a rapidly oscillating function of each of its six spin lengths (for classically allowed values); second, that any closed network can be decomposed into a product of Racah coefficients, summed over certain "internal" spin values. In the limit of large spins, the frequency of oscillation of the Racah coefficient with variation of one of the spin lengths is proportional to the dihedral angle between the two planes in which that spin couples (the conjugate action-angle variable), as determined by the classical trigonometry of the tetrahedron. An internal spin length appears on the common edge of several tetrahedra,

so the total phase of oscillation will be stationary just when the "defect angle" (the difference between 2π and the sum of all the dihedral angles at that edge) vanishes. But this in turn is just another form of the condition for imbedding spin vectors in a flat 3-d space.

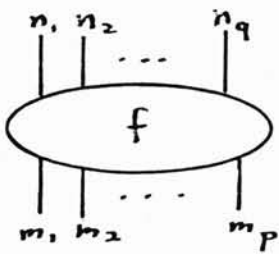
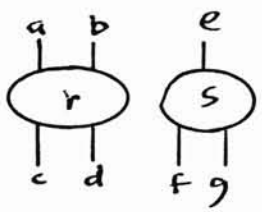
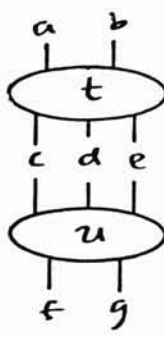

The sum-of-products decomposition in Regge-Ponzano theory is a discrete analog of a path integral. The tetrahedral decomposition is a 3-d simplicial manifold, whose boundary is (the dual of) the original spin network. Summation over the internal spin lengths amounts to integration over the geometries ("paths") spanning this boundary. The phase part of the integrand, as defined above, is formally identical to the 3-d vacuum Einstein action (the integral of the scalar curvature density, or average defect angle) in Regge calculus [Regge 61]. Hence the stationary phase conditions above are Einstein's equations for gravity on a simplicial manifold; and the flatness of the geometry amounts to the well-known fact that these equations admit only solutions with vanishing curvature in three dimensions.

1.3 Theory of Fabrics

The theory of fabrics is introduced in chapter 4 as a formalism for extending the Penrose and Regge-Ponzano analyses of spin to other situations that give rise to new models of quantum geometries. From the point of view of physics, this theory is a natural generalization of the rules for addition of conserved quantities such as spin and momentum. It abstracts from these rules just those properties needed to prove the Regge-Ponzano decomposition theorem in its general form.

As in the special case of a spin network, a fabric is a cubic graph whose edges may be taken to represent (composite) "particles", and whose vertices represent the composition of conserved quantities associated with these particles. In general, the edges of a fabric may be labelled with several values k of ("single-particle") observables, and the vertices may also be labelled with the values d of ("two-particle") observables. For example, figure 1.1 illustrates the edge and vertex labelling in a fabric of the Poincare group.

Figure 1.3 Graphical diagrams for tensors

Tensor	Graphical	Interpretation
$f_{m_1, m_2, \dots, m_p}^{n_1, n_2, \dots, n_q}$		<p>Linear map f from $V_{m_1} \otimes V_{m_2} \otimes \dots \otimes V_{m_p}$ to $V_{n_1} \otimes V_{n_2} \otimes \dots \otimes V_{n_q}$</p>
$r_{cd}^{ab} s_{fg}^e$		<p>Outer Product $r \otimes s$</p>
$t_{cde}^{ab} u_{fg}^{cde}$		<p>Inner Product $t \cdot u$</p>
$\delta_a^{a'}$		<p>Identity operator (Kronecker delta)</p>

The mathematical prototype for the theory of fabrics is recoupling theory. Hence we begin chapter 3 with a graphical formulation of the recoupling theory of compact groups, making use of the graphical calculus for tensor operations developed by Penrose. Figure 1.3 is a glossary of our conventions, which we use throughout this paper. A tensor is represented by a "blob" with "arms" for contravariant indices and "legs" for covariant ones. Tensor (outer) product is indicated simply by placing two or more blobs next to each other. Inner product, by linking the contracted indices (entailing summation, in a component expansion). A line standing alone is an identity operator (or Kronecker delta, in components).

Here we are concerned with the finite-dimensional vector spaces which support irreducible unitary representations of a compact group G , and with tensor products of such irreducible spaces. We define the "coupling tensors" which map the product of two irreducible spaces into its irreducible subspaces. Figure 1.4a is the graphical symbol for such a coupling tensor, mapping the product of spaces identified by k_1 and k_2 into the spaces identified by k_3 . Since multiple copies of the k_3 -space may occur in general in the reduction of $k_1 \otimes k_2$, a "degeneracy index" d is attached to the vertex to distinguish the corresponding coupling tensors.

Coupling tensors are invariant under the action of the group. In fact, the coupling tensors in figure 1.4a, with d ranging over all possible values, form a basis for $\text{Hom}(k_1 \otimes k_2, k_3)$. Natural isomorphisms such as

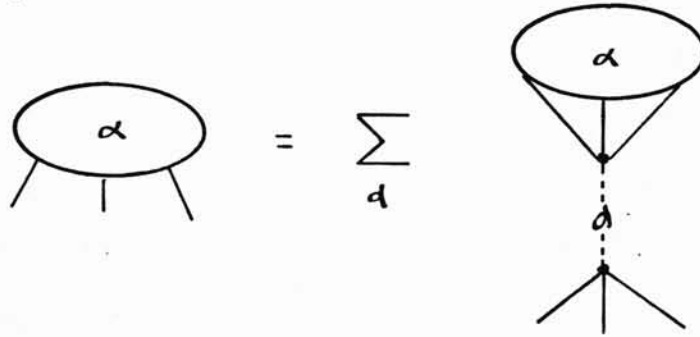
$$\text{Hom}(k_1 \otimes k_2, k_3) \cong \text{Hom}(k_1 \otimes k_2 \otimes k_3^*, \mathbb{C}), \quad (1.3.1)$$

where k_3^* is the irreducible space dual to k_3 (i.e., the space of complex linear functionals on the k_3 -space), allow us to define couplings with different mixtures of covariant and contravariant indices. Figure 1.4b shows how any invariant with 3 covariant indices can be expanded as an explicit sum of covariant coupling tensors (Wigner-Eckart theorem).

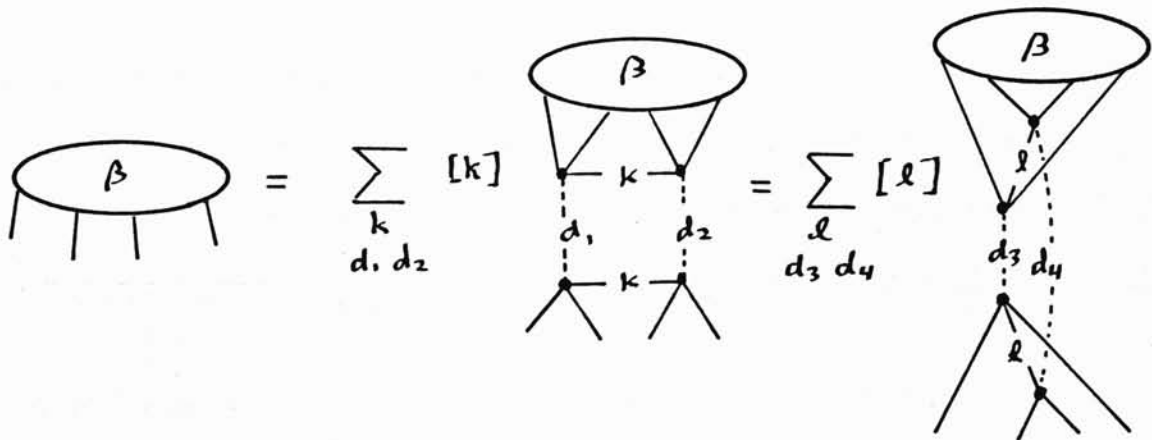
Figure 1.4 Coupling and Recoupling



b) α invariant \Rightarrow



c) β invariant \Rightarrow



A major goal of recoupling theory is to show how invariants with still more indices can be expanded as an explicit sum of "coupling trees", which are contractions of coupling tensors (generalized W-E theorem). Many such bases exist: one for each possible coupling sequence. For example, figure 1.4b shows two different expansions for an invariant with 4 covariant indices. Here $[k]$ is the dimension of the k -space.

A second goal of recoupling theory is to compute the "recoupling coefficients" which transform one coupling basis into another. These coefficients are the values of cubic coupling graphs obtained by contracting together trees of different structural species (i.e. different coupling sequence). For example, the two bases shown in figure 1.4c transform as shown in figure 1.5a by the simplest such graph, corresponding to the Racah coefficient (c.f. the spin network in figure 1.2b). We refer to figure 1.5a as the "crossing identity".

It turns out that any recoupling graph can be evaluated as a sum of products of Racah coefficients. We give a couple of related proofs of this result, which is a generalization of the Regge-Ponzano decomposition theorem. In the "network" version of the proof, we use the crossing identity to rearrange a graph until it contains a cycle with just three vertices. This cycle can then be excised by applying figure 1.4b as shown in 1.5b, yielding a product of Racah coefficients and a graph with fewer vertices. In the "vector" picture, we consider the graph to be imbedded in the surface of a region, and construct the "vector diagram" which is the triangulation of that surface dual to the graph. We use the crossing identity to introduce internal edges that dissect the interior of the region into tetrahedra, which can then be excised by 1.5b. We illustrate this decomposition theorem for some of the basic coupling graphs in Regge-Ponzano theory.

In the last section of chapter 4, we define fabrics as cubic graphs with edges and vertices labelled by variables which take values in arbitrary measure spaces. A fabric valuation is an assignment of complex amplitudes to fabrics satisfying the crossing and excision identities in

Figure 1.5 Crossing and Excision Identities

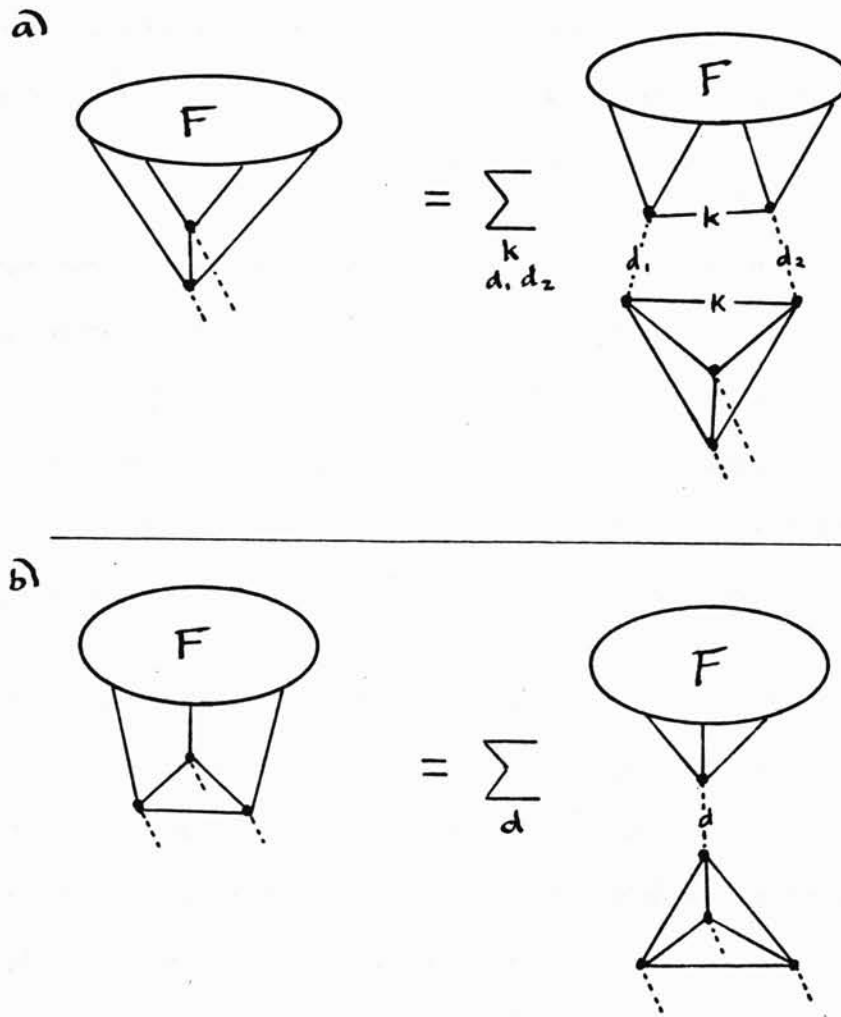
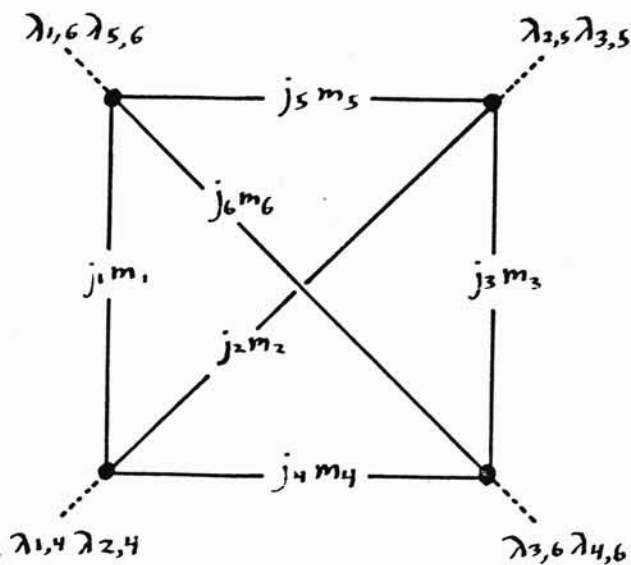


fig. 1.5 (with sums replaced by integrals) needed for the decomposition theorem. We briefly discuss the classification problem and semiclassical limit of fabrics.

In chapter 5, we construct fabrics for affine Minkowski space from the recoupling theory of the Poincare group. We restrict our construction to massive, positive-energy representations in the helicity basis. Helicity has the advantage of being invariant under all Poincare transformations, except boosts in directions transverse to the momentum. The helicity basis, moreover, transforms like ordinary spin states under the three-dimensional "Wigner rotations" of the intrinsic spin entailed by such boosts in the rest-frame of the particle. By working in the

Figure 1.6 Racah coefficient of the Poincare group



center-of-momentum frame of a pair of coupled particles, we can calculate the coupling tensor as a simple product of three rotation matrices. We identify the degeneracy indices of the coupling to be the relative helicities of each particle in this frame.

By contracting together four coupling tensors, we compute the Racah kernel of figure 1.6 in the form

$$e_{64}^1 e_{54}^2 e_{56}^3 e_{26}^4 e_{63}^5 e_{35}^6 \tag{1.3.2}$$

with

$$e_{\ell m}^k \equiv d_{\lambda_{k,\ell} \lambda_{k,m}}^{j_k} (\beta_{k,\ell m}). \tag{1.3.3}$$

where $\lambda_{k,\ell}$ is the helicity of particle k in the frame attached to particle ℓ , $\beta_{k,\ell m}$ is the angle between the 3-momenta of particles ℓ and m in the frame attached to k , and the d -function is the standard y -rotation matrix (only y -rotations appear, because momentum conservation constrains the 3-momenta of all six particles to be coplanar in the frame attached to any one of them).

In the semiclassical limit, the Racah coefficient (1.3.2-3) is a rapidly oscillating function of the masses, spins, and helicities, which we display in manifestly invariant form, with the help of an asymptotic formula for the d -function derived by Regge and Ponzano. We show that the phase of a product of Racah coefficients contains a term proportional to the angle defect in the intrinsic spin plane of each internal particle state. The weights of these terms are such that the phase is stationary just when the ~~curvature~~^{defect} vanishes. The natural way angle defects arise in this model, however, will probably play a role in fabrics for quantizing the curved spaces of general relativity.

2. SPIN NETWORKS

The theory of spin networks is one of several mathematically equivalent graphical methods for treating the recoupling theory of the rotation group [Yutsis, Levinson, and Vanagas 62, ElBaz and Castel 72]. Roger Penrose invented this method while searching for combinatorial models of geometry in quantum physics, so it is distinguished by emphasis on combinatoric techniques that are probably unique in their simplicity and elegance. Underlying these techniques is the representation of spin 1/2 by the simplest (2-d) Hilbert space H_2 , and of higher spins by symmetrized products of this basic space.

In sections 1 and 2, we develop the elementary facts about spin, in a notation compatible with spin networks. In section 3, we define scalar product operators, characterize the constraints imposed upon them in a 3-d Euclidean space, and introduce the notions of ϵ -constraints and δ -classical limit. In the final section, we give an algebraic proof of the spin geometry theorem, sketch Penrose's combinatorial proof, and discuss an alternate approach involving "interior" scalar products.

2.1 Basic States and Operators

The relationship between Minkowski space-time and the spin-1/2 state space H_2 is perhaps most easily seen in the well-known parametrization of the 2x2 Hermitian matrices:

$$H = \begin{pmatrix} t+z & x-iy \\ x+iy & t-z \end{pmatrix} = t \mathbf{1} + \vec{r} \cdot \vec{\sigma}, \text{ where } \vec{r} = (x,y,z) \quad (2.1.1)$$

and

$$\sigma_x = \begin{pmatrix} 0 & 1 \\ 1 & 0 \end{pmatrix}, \sigma_y = \begin{pmatrix} 0 & -i \\ i & 0 \end{pmatrix}, \sigma_z = \begin{pmatrix} 1 & 0 \\ 0 & -1 \end{pmatrix} \quad (2.1.2)$$

are the Pauli spin matrices. The Hermitian property $H = H^\dagger$ and the determinant

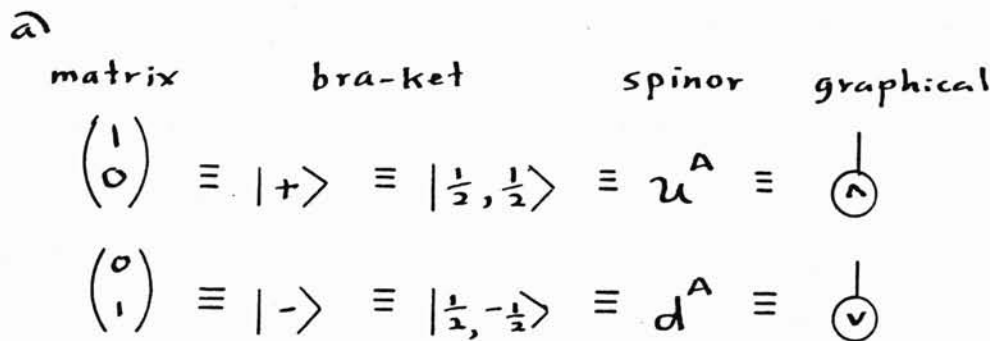
$$\det H = t^2 - x^2 - y^2 - z^2 \tag{2.1.3}$$

are both preserved under the transformation

$$H' = LHL^\dagger, \tag{2.1.4}$$

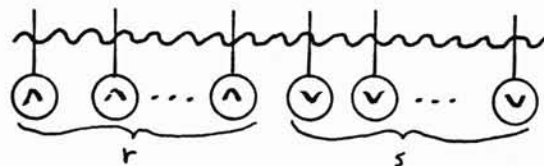
if L is a 2x2 complex matrix with unit determinant. This is the well-known 2-to-1 isomorphism (L and -L produce the same transformation) between SL(2,C) and the identity-connected component of the Lorentz group O(3,1).

Figure 2.1 Basic spin states



b)

$$|j, m\rangle \equiv N_m^j \overset{A}{u} \overset{B}{u} \dots \overset{F}{u} \overset{G}{d} \overset{H}{d} \dots \overset{M}{d}$$



where

$$N_m^j = \left[\frac{(r+s)!}{r! s!} \right]^{\frac{1}{2}}, \quad j = \frac{r+s}{2}, \quad m = \frac{r-s}{2}$$

If L is also restricted to be a unitary matrix U with $UU^\dagger = 1$, then the t-coordinate is also unchanged by the transformation (2.1.4), so the Euclidean norm $x^2 + y^2 + z^2$ is preserved. In fact, the unitary matrices

$$e^{i\theta\sigma_y/2} = \begin{pmatrix} \cos \frac{\theta}{2} & \sin \frac{\theta}{2} \\ -\sin \frac{\theta}{2} & \cos \frac{\theta}{2} \end{pmatrix} \text{ and } e^{i\theta\sigma_z/2} = \begin{pmatrix} e^{i\theta/2} & 0 \\ 0 & e^{-i\theta/2} \end{pmatrix} \tag{2.1.5}$$

which rotate the coordinates (x,y,z) by angle θ around the y and z axes respectively, generate all proper rotations, so the group SU(2) of unitary unimodular matrices is 2-to-1 isomorphic to the group of proper rotations SO(3).

The 2-dimensional Hilbert space H_2 underlying these operators describes the states of a spin-1/2 object. Fig. 2.1a illustrates the two basic vectors of this space in several notations: matrix, Dirac bra-ket (two versions), spinor, and graphical. Noting how σ_z is diagonalized in (2.1.2), we identify the states u^A and d^A as spin "up" and "down" along the z-axis.

The simple combinatorial structure of spin theory stems from the fact that all irreducible unitary representations of SU(2) can be constructed from symmetrized products of H_2 . Figure 2.1b gives an explicit construction of spin-j basis states from the tensor product of 2j half-spins. The round brackets around the spinor indices and the wavy bar in the graphical notation both indicate symmetrizers.

$$\overline{| \uparrow \uparrow \rangle} = \frac{1}{2} (| \uparrow \uparrow + \downarrow \downarrow \rangle), \quad \overline{| \uparrow \uparrow \uparrow \uparrow \rangle} = \frac{1}{6} (| \uparrow \uparrow \uparrow + \downarrow \uparrow \uparrow + \uparrow \downarrow \uparrow + \uparrow \uparrow \downarrow + \uparrow \downarrow \downarrow + \downarrow \uparrow \downarrow \rangle), \quad \text{etc.}$$

The component of spin in the z-direction m, determined by the excess of up to down half-spins, takes all values from j to -j in integer steps. The constants N_m^j make these states orthonormal under the Hermitian product induced from H_2 .

Referring back to (2.1.2) and (2.1.5), we see that $J_1 = \frac{\sigma_x}{2}$, $J_2 = \frac{\sigma_y}{2}$, $J_3 = \frac{\sigma_z}{2}$ are infinitesimal generators forming a Lie algebra su(2) with commutation relations

$$[J_k, J_l] = i\epsilon_{klm} J_m, \tag{2.1.7}$$

where ϵ_{klm} is the totally antisymmetric Levi-Civita tensor with $\epsilon_{123} = +1$. The corresponding operators (satisfying the same relations) on the spin-j Hilbert space $H_{(2j+1)}$ with basis shown in figure 2.1b are the sum of 2j half-spin operators, each being the tensor product of $\frac{\sigma}{2}$ on one of the H_2 spaces with identity operators on the (2j-1) other H_2 spaces in the symme-

trized product. For example, in the spin-3/2 space, we have explicitly

$$J_3 = \frac{\sigma_z}{2} \otimes 1 \otimes 1 + 1 \otimes \frac{\sigma_z}{2} \otimes 1 + 1 \otimes 1 \otimes \frac{\sigma_z}{2}. \quad (2.1.8)$$

From the definition of $|j,m\rangle$ in figure 2.1b, we check that

$$J_3 |j,m\rangle = m |j,m\rangle. \quad (2.1.9)$$

Similarly, if we define the standard operators $J_{\pm} = J_1 \pm iJ_2$ which raise and lower the eigenvalue m , we may check

$$\begin{aligned} J_+ |j,m\rangle &= [(j-m)(j+m+1)]^{1/2} |j,m+1\rangle \\ J_- |j,m\rangle &= [(j+m)(j-m+1)]^{1/2} |j,m-1\rangle. \end{aligned} \quad (2.1.10)$$

The scalar product

$$J^2 \equiv (\vec{J} \cdot \vec{J}) = J_1^2 + J_2^2 + J_3^2 = \frac{1}{2}(J_+ J_- + J_- J_+) + J_3^2 \quad (2.1.11)$$

is an invariant, since (2.1.7) implies it commutes with all J . From (2.1.9-10) we verify that

$$J^2 |j,m\rangle = j(j+1) |j,m\rangle. \quad (2.1.12)$$

The general y -rotation matrix in the spin- j representation can be computed from (2.1.5) and the J_2 definition analogous to (2.1.8):

$$\begin{aligned} d_{mm'}^j(\theta) &\equiv \langle j,m | e^{i\theta J_2} | j,m' \rangle \\ &= \left[\frac{(j+m)!(j-m)!}{(j+m')!(j-m')!} \right]^{1/2} \sum_k \binom{j+m'}{k} \binom{j-m'}{m-m'+k} \times \\ &\quad \times (-1)^k \left(\sin \frac{\theta}{2} \right)^{m-m'+2k} \left(\cos \frac{\theta}{2} \right)^{2j-m+m'-2k}. \end{aligned} \quad (2.1.13)$$

Hence the matrix elements for arbitrary finite rotations are

$$\mathcal{D}_{mm'}^j(\alpha\beta\gamma) \equiv \langle j,m | e^{i\alpha J_3} e^{i\beta J_2} e^{i\gamma J_3} | j,m' \rangle =$$

$$e^{i\alpha m} d_{mm'}^j(\beta) e^{i\gamma m'} \quad (2.1.14)$$

where $\alpha\beta\gamma$ are the Euler angles.

These representations are clearly irreducible, since the operator J_- in (2.1.10) generates all states $|j,m\rangle$ from $|j,j\rangle$. The fact that any irreducible representation is equivalent to one of these can be shown in many ways. Perhaps the simplest is to note the following facts:

1. An irreducible representation must span a single eigenspace of the invariant J^2 . Let the eigenvalue be $j(j+1)$.
2. Then (2.1.11) implies that the J_3 -eigenvalues m in this representation are bounded by $|m| < j + 1$.
3. The commutation relations of J_3 and J_{\pm} imply that the maximal eigenvalues are in fact $m = \pm j$, and that m ranges between them in integer steps.
4. Hence $2j$ is an integer, and we have the spin- j representation of the rotation group.

2.2 Addition of spin

The addition of spin is represented in quantum theory by the composition or tensor product of spin states. The tensor product of spin j_1 and spin j_2 reduces to a direct sum of irreducible subspaces with spin j_3 - where, as we shall see, j_3 ranges between $j_1 + j_2$ and $|j_1 - j_2|$ in integer steps. Physically the direct sum corresponds to the superposition of all possible outcomes of composing j_1 and j_2 , ranging from parallel to antiparallel in steps of the spin quantum. The observation of a particular outcome is represented by an operator, which we display explicitly, following Penrose's construction, with the help of the particular choice of bases in the previous section. These operators are concrete realizations in terms of some simple invariants of the basic coupling tensors of $SU(2)$, the "1-j and 3-j symbols" which are treated in the more general context of compact groups in chapter 4.

The basic ingredient of these constructions is the two-dimensional Levi-Civita symbols:

$$(\epsilon^{AB}) = (\epsilon_{AB}) = \begin{pmatrix} 0 & 1 \\ -1 & 0 \end{pmatrix} \quad (2.2.1)$$

whose invariance is equivalent to the condition that the 2×2 matrices U^A_B in $SU(2)$ have unit determinant:

$$\epsilon^{AB} = U^A_C U^B_D \epsilon^{CD} \text{ or } \epsilon_{CD} = U^A_C U^B_D \epsilon_{AB} \quad (2.2.2)$$

These ϵ 's can be used to raise and lower spinor indices, and establish a canonical isomorphism between spinors and their duals:

$$\begin{aligned} \zeta \begin{matrix} \dots A \dots \\ \dots \dots \end{matrix} &= \epsilon^{AB} \zeta \begin{matrix} \dots \dots \\ \dots B \dots \end{matrix} \\ \zeta \begin{matrix} \dots \dots \\ \dots B \dots \end{matrix} &= \epsilon_{AB} \zeta \begin{matrix} \dots A \dots \\ \dots \dots \end{matrix} \end{aligned} \quad (2.2.3)$$

We also define the identity (or index substitution) operators:

$$\epsilon_A^B \equiv \epsilon_{AC} \epsilon^{BC} = -\epsilon^B_A = \begin{pmatrix} 1 & 0 \\ 0 & 1 \end{pmatrix}. \quad (2.2.4)$$

Because the underlying space H_2 is two-dimensional, a spinor which is skew-

symmetrical in three or more indices must vanish. Hence in particular

$$\epsilon_{AB} \epsilon_{CD} + \epsilon_{AC} \epsilon_{DB} + \epsilon_{AD} \epsilon_{BC} = 0. \quad (2.2.5)$$

From (2.2.3-5) any spinor ζ can be reduced by

$$\zeta^{\dots AB \dots} = \zeta^{\dots (AB) \dots} + \frac{1}{2} \epsilon_{AB} \zeta^{\dots C \dots} \quad (2.2.6)$$

Here the first term on the right is the symmetric part, and the second term is the skew-symmetric part, expressed as a product of ϵ and a contracted spinor of valence lower than ζ .

This identity indicates once again that only totally symmetric spinors are irreducible.

Now composition of two half-spins is the tensor product

$$\zeta_A \eta_B = \zeta_{(A} \eta_{B)} + \frac{1}{2} \epsilon_{AB} (\zeta_C \eta^C). \quad (2.2.7)$$

Here the symmetric part corresponds to parallel composition, giving total spin 1; and the skew-symmetric part, to antiparallel composition, giving the rotationally invariant spin 0.

Similarly, by raising one index in a spinor of valence 2, we get

$$h_A{}^B = h_{(AC)} \epsilon^{BC} + \frac{1}{2} \epsilon_A{}^B (h_C{}^C).$$

Here the two terms correspond to a trace-free vector and trace scalar, as in the equation (2.1.1) with which we began this chapter. Hence we expect that the spin-1 representation is equivalent to the 3-dimensional vector representation of the rotation group. In fact, it is easy to check that the following orthonormal basis transforms as an ordinary 3-vector:

$$e_x = \frac{1}{\sqrt{2}} [|1, -1\rangle - |1, 1\rangle]$$

$$e_y = \frac{i}{\sqrt{2}} [|1, -1\rangle + |1, 1\rangle]$$

$$e_z = |1, 0\rangle. \quad (2.2.8)$$

Strictly speaking, the Hermitian matrix in (2.1.1) is a spinor $h^{AA'}$ where A' is a conjugate spinor index. Conjugate spinors form a space H_2^* of "bra" states related antilinearly to the "kets" in H_2 , and they transform by the adjoint L^\dagger in $SL(2,C)$, as shown in (2.1.4). But in context of $SU(2)$, the matrix

$$\delta^{AA'} = \begin{pmatrix} 1 & 0 \\ 0 & 1 \end{pmatrix}$$

is an invariant because of unitarity, and it provides an isomorphism between H_2^* and H_2 . Hence we may eliminate all reference to conjugate spinors in the theory of $SU(2)$: the simple invariants ϵ^{AB} , ϵ_{AB} , and ϵ_A^B suffice for the construction of all coupling tensors.

Figure 2.2a shows the graphical symbol for ϵ_{AB} . Figure 2.2b shows the "1-j symbol", constructed explicitly from the symmetrized product of 2j ϵ 's. It is a generalization of ϵ_{AB} , in that it produces the spin-0 part of the composition of two systems each with total spin j. The "3-j symbol" in figure 2.2c is an invariant tensor which projects out the spin-0 part from the composition of three spins j_1, j_2, j_3 . The index bundle numbers t_i in this definition are uniquely determined by the j's:

$$t_1 = j_2 + j_3 - j_1; \quad t_2 = j_3 + j_2 - j_1; \quad t_3 = j_1 + j_2 - j_3 \quad (2.2.9)$$

Since these must be positive integers, the j's must satisfy the triangle inequalities

$$j_2 + j_3 \geq j_1; \quad j_3 + j_1 \geq j_2; \quad j_1 + j_2 \geq j_3 \quad (2.2.10)$$

and $j_1 + j_2 + j_3 = t_1 + t_2 + t_3$ must be an integer.

By using the dual isomorphism (2.2.3), we can also define contravariant 1-j and 3-j symbols, as shown in figure 2.3. We interpret these contravariant symbols physically as representing the splitting of a spin-0 system into 2 or 3 higher spin states correlated in such a way that the total spin is 0 (e.g. as in the Einstein-Podolsky-Rosen experiment). These coupling tensors satisfy the standard identities illustrated in figure 2.4, provided that the normalization constants are taken to be

Figure 2.2 Covariant j-symbols

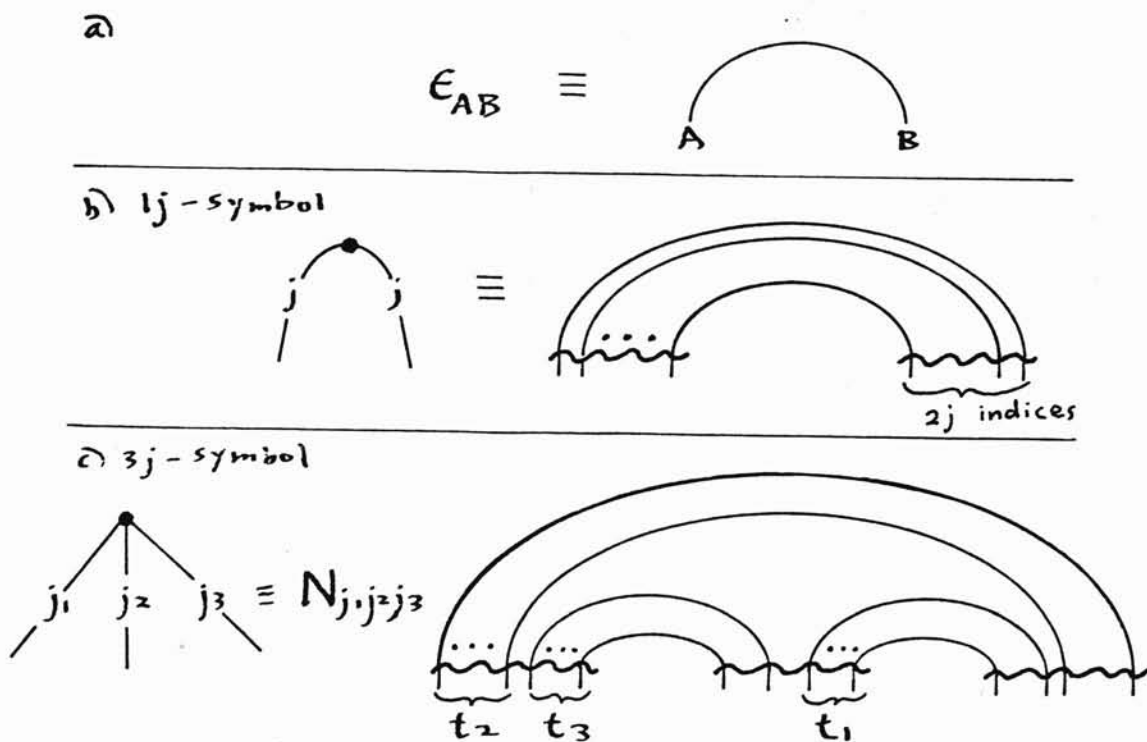
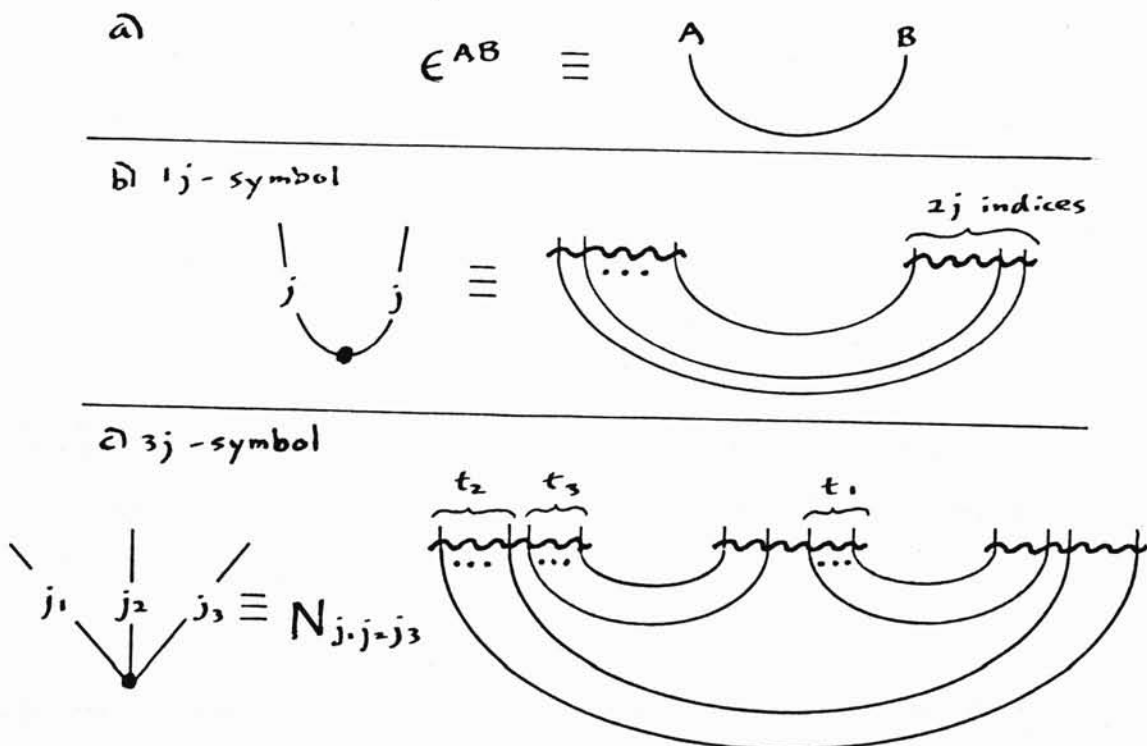


Figure 2.3 Contravariant j-symbols



$$N_{j_1 j_2 j_3} = \left[\frac{(j_1 + j_2 + j_3 + 1)!}{(j_2 + j_3 - j_1)!(j_3 + j_1 - j_2)!(j_1 + j_2 - j_3)!} \right]^{-1/2} \quad (2.2.11)$$

Figure 2.4 Identities between j-symbols

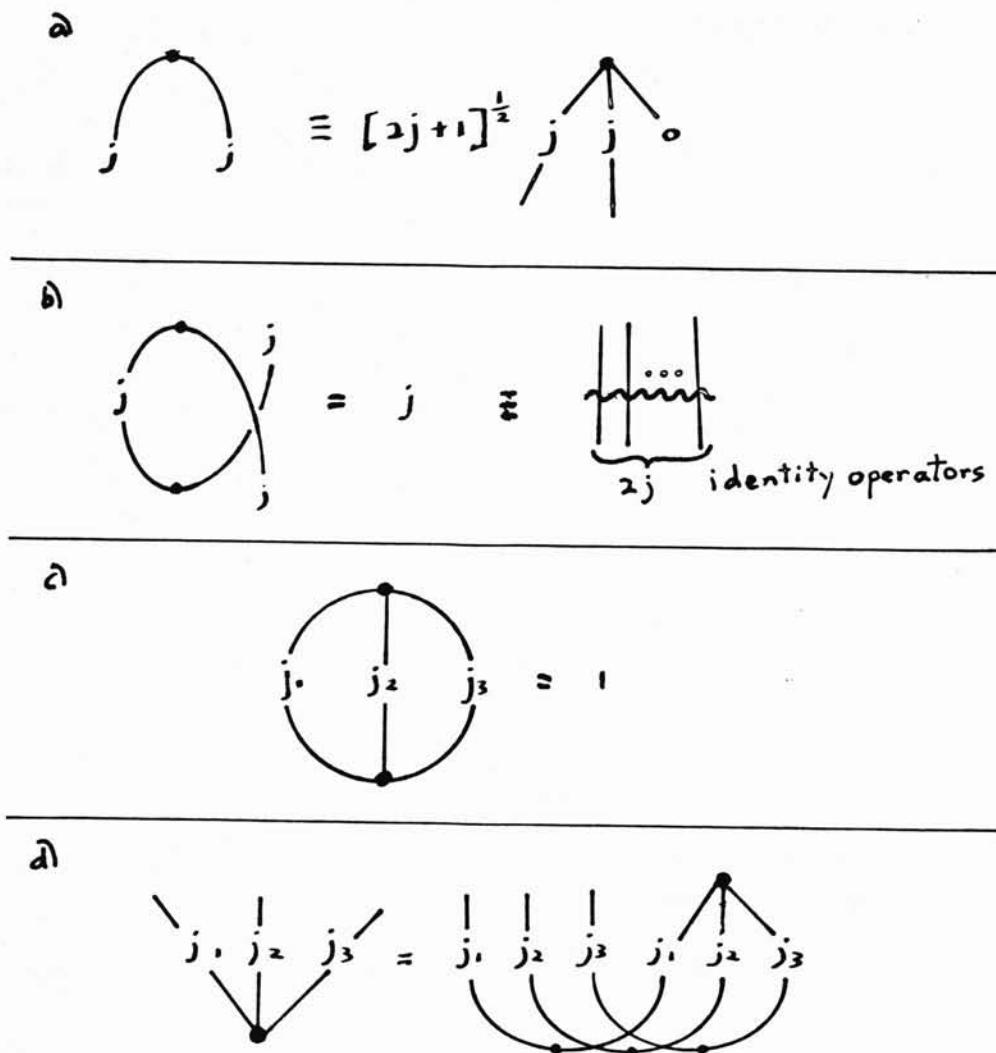


Figure 2.5a is a 3-j symbol of mixed valence, which represents the addition of two spins j_1 and j_2 to produce a third spin j_3 . We see that in our spinor-product basis, this composition is accomplished by the anti-parallel addition of just the right number of half-spin pairs (with $t_3 = j_1 + j_2 - j_3$ skew ϵ 's) so that the remaining half-spins in j_1 and j_2 add in parallel to give j_3 (by the symmetrization of the $t_1 + t_2 = 2j_3$ indices). This coupling tensor and its dual are members of $\text{Hom}(j_1 \otimes j_2, j_3)$ and $\text{Hom}(j_3, j_1 \otimes j_2)$ respectively, where we have used j_1 as a

shorthand for H_{2j_1+1} (see chapter 4 for a definition of the module homomorphisms). By composing these two tensors as shown in figure 2.5b, we define an operator which projects out the irreducible spin- j subspace from the product $j_1 \otimes j_2$. The constraints (2.2.10) imply that $P_j^{(j_1 j_2)}$ can be constructed in this way for j ranging between $j_1 + j_2$ and $|j_1 - j_2|$ in integer steps.

The projector identities

$$P_j P_k = \delta_{jk} P_j \tag{2.2.12}$$

are an immediate consequence of Schur's lemma, shown in Figure 2.5c: the image and kernel of any $\alpha \in \text{Hom}(j, k)$ are both invariant subspaces, so α must vanish unless $j \equiv k$, in which case it must be a multiple of the identity (since the eigenspaces of α are also invariant). The P_j 's are complete as well, since they are independent by (2.2.12), and both sides of the Clebsch-Gordon series defined in figure 2.5d have equal dimensions:

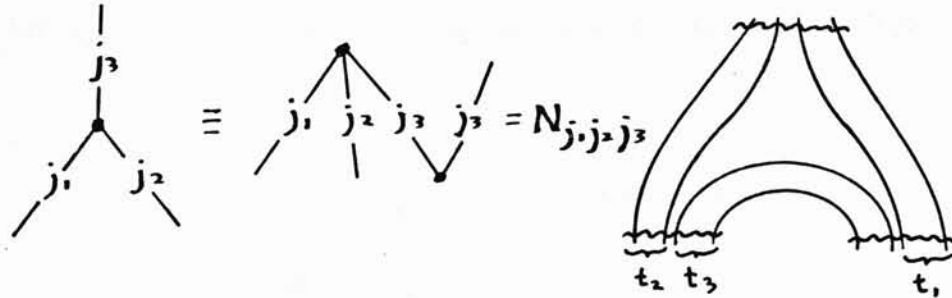
$$(2j_1 + 1) (2j_2 + 1) = \sum_{j=|j_1-j_2|}^{j_1+j_2} (2j + 1). \tag{2.2.13}$$

The completeness of the P_j 's implies the Wigner-Eckart theorem, which states that any $\beta \in \text{Hom}(j_1 \otimes j_2, j_3)$ must be a multiple of the 3-j symbol. For we may decompose the domain $j_1 \otimes j_2$ by projecting out the j -subspaces as shown in figure 2.5e, and then apply Schur's lemma to conclude that only the $j = j_3$ term in the sum is non-vanishing, and that it is proportional to the 3-j symbol.

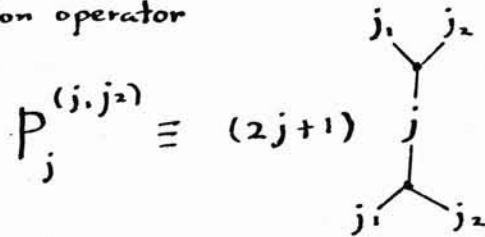
In general, we define a spin network to be an $SU(2)$ -invariant tensor described by a labelled cubic graph which represents the contraction of 3-j symbols according to the graphic conventions in figures 2.2-5. By repeated application of the Clebsch-Gordon decomposition and the Wigner-Eckart theorem, we can prove that any invariant under $SU(2)$ can be expressed as a superposition of spin networks (see the generalized Wigner-Eckart theorem in

Figure 2.5 Coupling Tensor and Classical Theorems

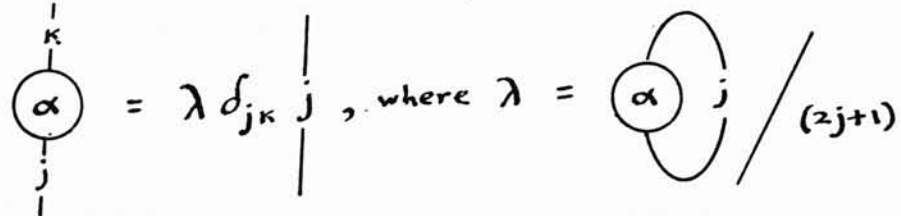
a) Coupling tensor



b) Projection operator



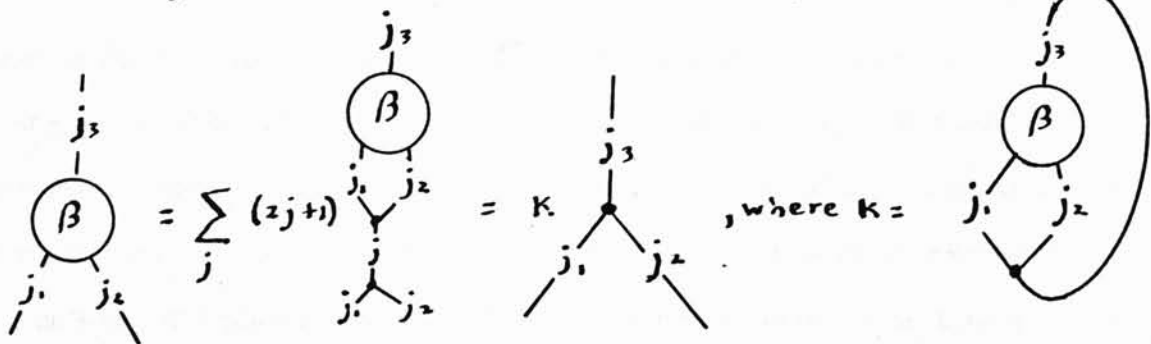
c) Schur's lemma: α invariant \Rightarrow



d) Clebsch-Gordan series

$$j_1, j_2 = \sum_{|j_1 - j_2| \leq j < j_1 + j_2} P_j^{(j_1, j_2)}$$

e) Wigner-Eckart theorem: β invariant \Rightarrow



chapter 4). In fact, a basis for any particular valence can be constructed from a "coupling tree" network of fixed structure by varying the intermediate spins over all possible values. For example, figure 2.6a shows how any invariant of valence 4 can be expanded as a sum over coupling trees with the intermediate spin variable a . Figure 2.6b displays another basis, relying on a different choice of coupling sequence in the tree. By applying the expansion formula in 2.6a to a basis element in 2.6b, we explicitly compute the "recoupling coefficient" shown in figure 2.6c.

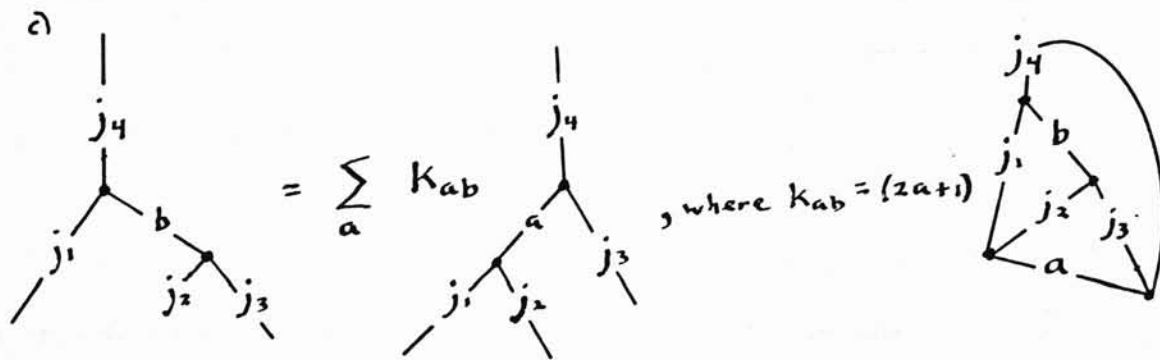
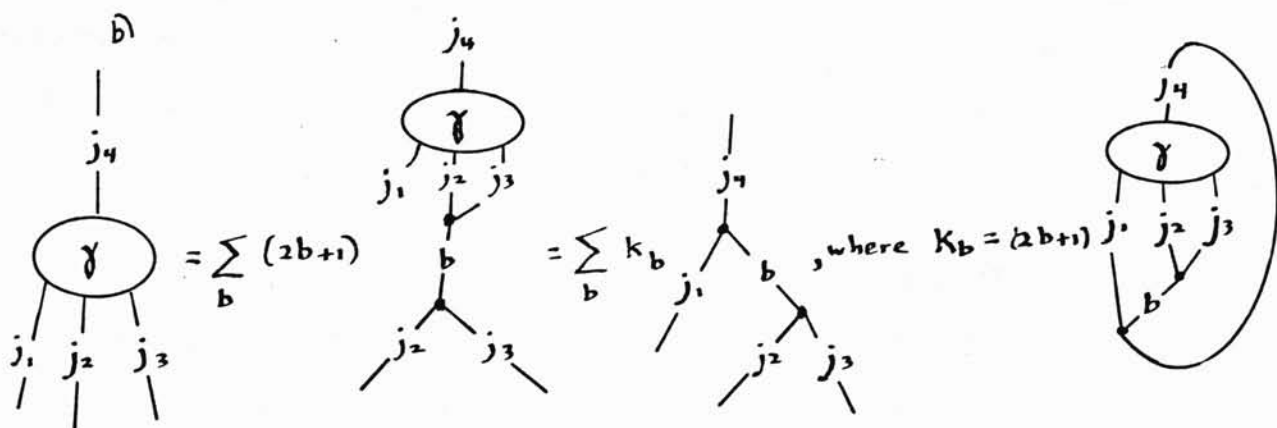
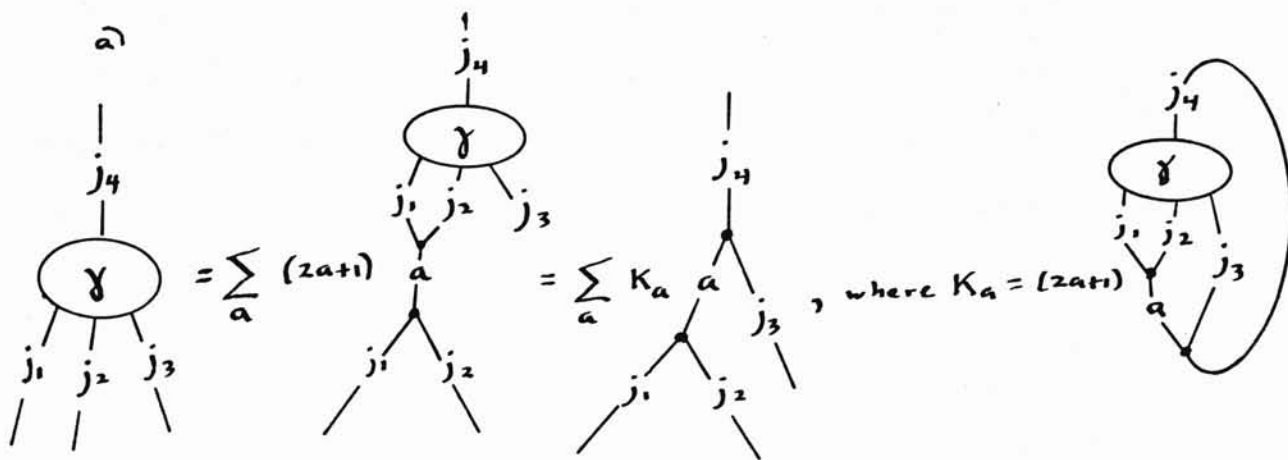
All such recoupling coefficients are closed spin networks obtained by contracting together trees of the same valence but different coupling sequence. The value of any closed network can be computed in principle by using the 3-j definitions in figures 2.3-5 and expanding the ϵ 's in components as in (2.2.1). In practice, there are several techniques for simplifying the evaluation of closed networks, some of which we have described elsewhere [Moussouris 79]. In chapter 4, we supply yet another evaluation method, by proving that all closed networks can be decomposed as a sum of products of the Racah coefficients shown in figure 1.2b.

The graphical conventions of spin networks given here are consistent with chapters 3 and 4 and most diagrammatic methods in the quantum theory of spin. They differ however in a few details from Penrose's conventions, which emphasize combinatorics, e.g. by avoiding all reference to non-integer quantities:

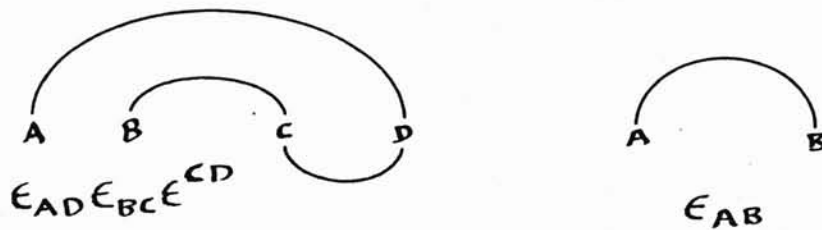
- 1) Penrose labels the edges of a spin network with integers $2j$ specifying the number of half-spins composed to make j .
- 2) Penrose omits the normalization factor (2.2.11) on each vertex, so that the values of closed spin networks become integers.
- 3) Penrose alters the sign conventions for the graphical representation of ϵ 's, so that the value of a closed spin network depends only on the labelled cubic graph, and is unaffected by continuous deformations of its imbedding in the plane.

Figure 2.6 Completeness and Recoupling Coefficients

γ invariant \Rightarrow



We have in fact glossed over certain sign ambiguities that arise in our graphical definition of the j -symbols. For example the two graphical diagrams



are of opposite sign according to (2.2.4), even though they are topologically equivalent. In [Moussouris 79] we described Penrose's modified sign conventions, which alleviate these ambiguities, and result in a formal isomorphism between spinor and "binor" invariants which lead to some elegant evaluation techniques. The geometric analysis of the following sections is independent of sign convention, since the expectation values computed are quadratic in the states.

2.3 Geometric relations between spins

Let $\vec{J}^{(1)}$ and $\vec{J}^{(2)}$ be two spin vector operators. We define the scalar product operator on the tensor product of the two spin spaces:

$$T^{(12)} \equiv (\vec{J}^{(1)} \cdot \vec{J}^{(2)}) \equiv J_1^{(1)} \otimes J_1^{(2)} + J_2^{(1)} \otimes J_2^{(2)} + J_3^{(1)} \otimes J_3^{(2)} \quad (2.3.1)$$

where the superscript ensemble indices are enclosed in parentheses to distinguish them from the 3-d indices. If $\vec{J} = \vec{J}^{(1)} + \vec{J}^{(2)}$,

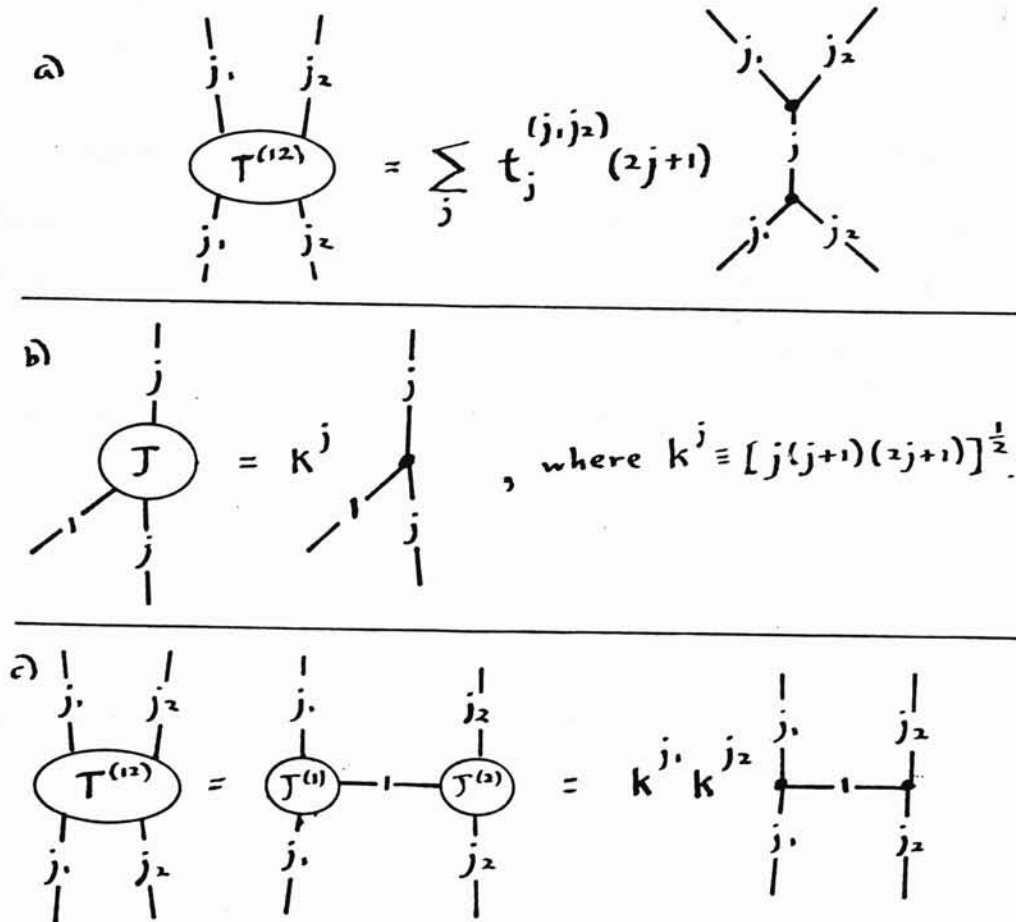
$$T^{(12)} = \frac{1}{2} ([J]^2 - [\vec{J}^{(1)}]^2 - [\vec{J}^{(2)}]^2), \quad (2.3.2)$$

so measurement of the scalar product of two known spins is equivalent to measuring the total spin of the composite system, and T is the sum of Clebsch-Gordon projection operators shown

in figure 2.7a, with

$$t_j^{(j_1 j_2)} = \frac{1}{2} [j(j+1) - j_1(j_1+1) - j_2(j_2+1)]. \quad (2.3.3)$$

Figure 2.7 Scalar Product Operator



A much simpler expression for $T^{(12)}$ arises from applying the Wigner-Eckart theorem to the vector operator \vec{J} . The commutation relations imply that \vec{J} transforms under rotation as follows:

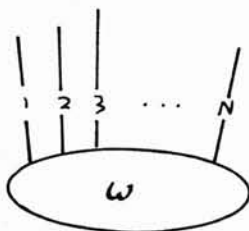
$$\mathcal{D}^j(\alpha\beta\gamma) \vec{J} \mathcal{D}^{j\dagger}(\alpha\beta\gamma) = R \vec{J} \quad (2.3.4)$$

where

$$R = U \mathcal{D}^1(\alpha\beta\delta) U^\dagger \quad (2.3.5)$$

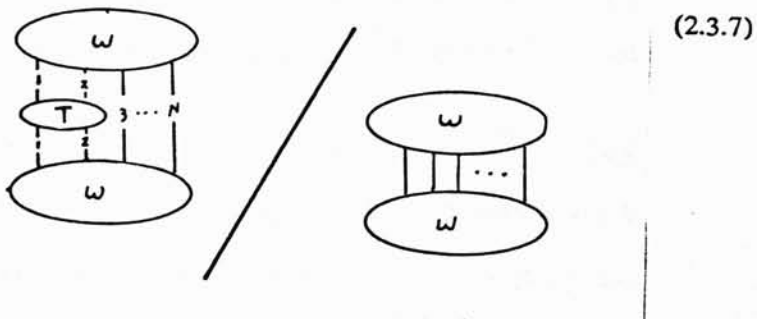
is the 3 x 3 rotation matrix obtained from the spin-1 matrix \mathcal{D}^1 by the basis transformation U given in (2.2.8). Thus the triplet (J_1, J_2, J_3) can be regarded as an element of $\text{Hom}(H_3 \otimes H_{2j+1}, H_{2j+1})$, which must be proportional to the 3-j tensor shown in figure 2.7b. The constant k^j is fixed by $J^2 = j(j+1)$. Hence $T^{(12)}$ is equal to the spin network shown in figure 2.7c.

Suppose now that ω is the state of an ensemble of N spins $\{\vec{J}^{(i)}\}_{i=1}^N$:



The scalar product operator $T^{(12)}$ is defined on ω , provided we multiply (2.3.1) by identity operators on the Hilbert spaces associated with spins 3 through N . We compute the expectation values of T 's on the state ω in the usual way:

$$\langle T \rangle_\omega \equiv \langle \omega | T | \omega \rangle / \langle \omega | \omega \rangle =$$



Our main goal is to show that for states ω approaching the "classical limit", these expectation values are consistent with a 3-dimensional Euclidean vector space.

The following proposition characterizes the constraints a $N \times N$ matrix T^{kf} must satisfy in order to be the matrix of scalar products of N vectors in a 3-d Euclidean space.

Proposition SP (scalar product):

Suppose $T^{k\ell}$ is a real symmetric $N \times N$ matrix.

The following conditions are equivalent:

- 1) There exist 3-d vectors $\{\vec{v}^k\}_{k=1}^N$ such that $T^{k\ell} = (\vec{v}^k, \vec{v}^\ell)$, the Euclidean scalar products.
- 2) $T^{k\ell}$ is positive semi-definite of rank ≤ 3 .
- 3) $x_k T^{k\ell} x_\ell \geq 0$ for all real $\{x_k\}_{k=1}^N$, and the determinants of all symmetric 4×4 submatrices of $T^{k\ell}$ vanish.

(2.3.8)

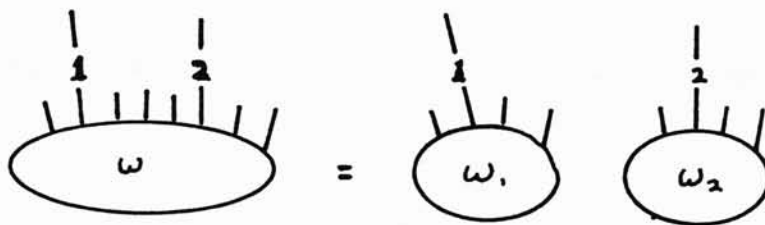
proof: By elementary linear algebra [Herstein, p.310], the real symmetric matrix T can be reduced to diagonal form D by a real orthogonal transformation $D = RTR^T$.

2 \Rightarrow 1: Condition 2 implies that D has no negative elements, and at most three positive elements on the diagonal. We define $D^{1/2}$ by taking positive square roots of the diagonal elements. Then $T = C^T C$, where $C = D^{1/2} R$ can be regarded as a $3 \times N$ real matrix. The columns of C are the components of the 3-vectors $\{\vec{v}^k\}_{k=1}^N$ in condition 1.

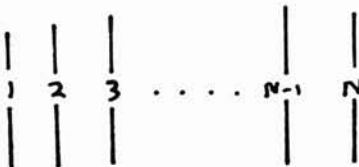
1 \Rightarrow 3: If $T^{k\ell} = (\vec{v}^k, \vec{v}^\ell)$, then $x_k T^{k\ell} x_\ell = (\vec{u}, \vec{u}) \geq 0$, where $\vec{u} = \sum_K x_k \vec{v}^k$. Moreover, any four of the vectors $\{\vec{v}^k\}$ are linearly dependent, so the 4×4 submatrices of T are singular.

3 \Rightarrow 2: $x_k T^{k\ell} x_\ell = (Rx)^T D (Rx) \geq 0$. Since R is non-singular, we can choose Rx to pick out any diagonal element of D , which must therefore be positive semi-definite. The rank of T and the singularity of its 4×4 submatrices are both unchanged under permutations of rows (or columns) of T or addition of a multiple of one row (or column) to another. But these operations are sufficient to reduce T to (upper left) diagonal form while preserving its symmetry [Loomis and Sternberg, p. 114]. Since the determinant of the upper left 4×4 submatrix must vanish, T must be of rank ≤ 3 .

If the spins are too small, then the scalar products are quantized too coarsely to respect these classical constraints. On the other hand, even when the spins are large, the constraints may still be violated, because the state ω provides too little correlation between spins for their geometry to be well defined. For example, suppose ω decomposes into the product of two invariant states ω_1 and ω_2



Then it is easy to see from figure 2.7c that $\langle T^{(12)} \rangle_\omega = 0$, so the spin subspaces associated with ω_1 and ω_2 appear to be orthogonal. In particular, as Penrose noted, the network



describes N completely uncorrelated spins, whose scalar products all have expectation value 0, suggesting an N -dimensional spin space.

In the classical limit, this situation can be avoided by requiring that the state ω contain enough information about the geometric relations between the spins that all the observables T are well-determined. We define the usual root-mean-square uncertainty in an observable A by

$$\sigma_\omega A \equiv [\langle (\Delta_\omega A)^2 \rangle_\omega]^{1/2}, \tag{2.3.9}$$

where

$$\Delta_\omega A \equiv A - \langle A \rangle_\omega. \tag{2.3.10}$$

The operator A is bounded when it has finite norm

$$\|A\| \equiv \lim_{\omega} \sup | \langle A \rangle_{\omega} |.$$

Definition: The bounded observable A is δ -classical for a state ω when

$$\frac{\sigma_{\omega} A}{\|A\|} < \delta.$$

Since the expression (2.3.3) for $T^{(12)}$ attains the maximum value $j_1 j_2$ for $j = j_1 + j_2$, we have

$$\|T^{(12)}\| = j_1 j_2 \tag{2.3.11}$$

and the $T^{(12)}$ are δ -classical when $\sigma_{\omega} T^{(12)} / j_1 j_2 < \delta$.

The uncertainty relations for the T operators imply that they can be δ -classical only if the spins are large. For any Hermitian operators A and B, the Cauchy-Schwartz inequality gives

$$\sigma_{\omega} A \sigma_{\omega} B \geq | \langle \omega | \Delta A \Delta B | \omega \rangle | = | \langle AB \rangle_{\omega} - \langle A \rangle_{\omega} \langle B \rangle_{\omega} |. \tag{2.3.12}$$

Since the commutator $[A, B] = [\Delta A, \Delta B]$, we have the familiar uncertainty relation

$$\sigma_{\omega} A \sigma_{\omega} B \geq \frac{1}{2} | \langle \frac{1}{i} [A, B] \rangle_{\omega} |. \tag{2.3.13}$$

In the case of three spins $\vec{J}^{(1)}, \vec{J}^{(2)}, \vec{J}^{(3)}$,

$$\left[(\vec{J}^{(1)} \cdot \vec{J}^{(2)}), (\vec{J}^{(2)} \cdot \vec{J}^{(3)}) \right] = \tag{2.3.14}$$

$$i \vec{J}^{(1)} \cdot (\vec{J}^{(2)} \times \vec{J}^{(3)}),$$

so

$$\delta^2 > \frac{\sigma_{\omega} T^{(12)}}{j_1 j_2} \frac{\sigma_{\omega} T^{(23)}}{j_2 j_3} \geq \frac{c}{2j_2} \tag{2.3.15}$$

where

$$c = \frac{|\langle \vec{J}^{(1)} \cdot (\vec{J}^{(2)} \times \vec{J}^{(3)}) \rangle_\omega|}{j_1 j_2 j_3}$$

is generically of magnitude $O(1)$.

For spins of finite magnitude, we expect the constraints of proposition SP to be satisfied only approximately. Suppose $T^{k\ell}$ is a real symmetric $N \times N$ matrix which is nearly equal to $(\vec{v}^k, \vec{v}^\ell)$, where $\{\vec{v}^k\}$ are N 3-d vectors. If \vec{v}^k are all non-zero, then $T^{kk} > 0$, and we can normalize to form the matrix

$$\hat{T}^{k\ell} \equiv T^{k\ell} [T^{kk} T^{\ell\ell}]^{-1/2} \quad (2.3.16)$$

Here $\hat{T}^{k\ell}$ is the cosine of the angle between \vec{v}^k and \vec{v}^ℓ . Now if K is a 4-tuple of index elements, the 4-volume spanned by the corresponding four unit vectors is

$$V^{(K)} = |\det [\hat{T}^{k\ell}]_{k,\ell \in K}|^{1/2}. \quad (2.3.17)$$

Definition: The real symmetric $N \times N$ matrix $T^{k\ell}$ satisfies the ϵ -constraints for Euclidean three space if

- a) $T^{kk} > 0$ and $x_k T^{k\ell} x_\ell \geq 0$ for all real $\{x_k\}_{k=1}^N$
- b) $V^{(K)} < \epsilon$ for any 4-tuple K .

2.4 The spin geometry theorem

Spin Geometry Theorem: Let ω be a state of an ensemble of N spins $\{\vec{J}^{(i)}\}_{i=1}^N$, and $T^{(kl)} \equiv (\vec{J}^{(k)} \cdot \vec{J}^{(l)})$ be the $N \times N$ matrix of scalar product operators between these spins. For all $\epsilon > 0$, there exists $\delta > 0$ such that the expectation values $\langle T^{(kl)} \rangle_\omega$ satisfy the ϵ -constraints for Euclidean three space, provided that all the $T^{(kl)}$ are δ -classical in the state ω .

For the proof of this theorem we need the following lemma about expectation values of operator products, which is a weaker form of the bound (2.3.12), applying to three or more operators:

Lemma: Let ω be a state supporting a set of bounded observables $\{A_i\}_{i=1}^n$ with expectation values $\langle A_i \rangle_\omega = \lambda_i$. Then

$$|\langle A_1 A_2 \dots A_n \rangle_\omega - \lambda_1 \lambda_2 \dots \lambda_n| \leq (\|A_1\| \|A_2\| \dots \|A_n\|) \sum_{i=1}^n \frac{\sigma_\omega A_i}{\|A_i\|}$$

proof of Lemma:³ We normalize ω so that $\langle \omega | \omega \rangle = 1$. Then

$$\begin{aligned} & |\langle \omega | A_1 A_2 \dots A_n - \lambda_1 \lambda_2 \dots \lambda_n | \omega \rangle| \\ & \leq \| (A_1 A_2 \dots A_n - \lambda_1 \lambda_2 \dots \lambda_n) | \omega \rangle \| \| \omega \| \\ & = \| (A_1 A_2 \dots A_n - A_1 A_2 \dots A_{n-1} \lambda_n) | \omega \rangle \| \\ & \quad + \| (A_1 A_2 \dots A_{n-1} \lambda_n - A_1 \dots A_{n-2} \lambda_{n-1} \lambda_n) | \omega \rangle \| \\ & \quad + \dots \\ & \quad + \| (A_1 \lambda_2 \lambda_3 \dots \lambda_n - \lambda_1 \lambda_2 \dots \lambda_n) | \omega \rangle \| \end{aligned}$$

³ This proof was suggested by E. B. Davies.

$$\begin{aligned}
 &\leq \|A_1 \dots A_{n-1}\| \|(A_n - \lambda_n)|\omega\rangle\| \\
 &\quad + \|A_1 \dots A_{n-2}\| |\lambda_n| \|(A_{n-1} - \lambda_{n-1})|\omega\rangle\| \\
 &\quad + \dots \\
 &\quad + |\lambda_2 \dots \lambda_n| \|(A_1 - \lambda_1)|\omega\rangle\| \\
 &\leq \|A_1\| \dots \|A_n\| \sum_{i=1}^n \frac{\sigma_\omega A_i}{\|A_i\|}.
 \end{aligned}$$

proof of spin geometry theorem:

First of all, we note that for any real $\{x_k\}_{k=1}^N$,

$$\sum_{k,\ell} x_k \langle T^{(k\ell)} \rangle_\omega x_\ell = \sum_{k,\ell} \langle (x_k \tilde{J}^{(k)} \cdot x_\ell \tilde{J}^{(\ell)}) \rangle_\omega = \sum_{i=1}^3 \langle (H_i)^2 \rangle_\omega \geq 0, \quad (2.4.1)$$

since $H_i \equiv \sum_k x_k J_i^{(k)}$ is Hermitian. Moreover,

$$\langle T^{(kk)} \rangle_\omega = \langle (J^{(k)})^2 \rangle_\omega = j_k(j_k + 1) > 0, \quad (2.4.2)$$

Now we define the operator $\hat{T}^{(k\ell)} \equiv T^{(k\ell)} / j_k j_\ell$ normalized so that $\|\hat{T}^{(k,\ell)}\| \leq 1$. If K is a 4-tuple of indices labelling a subensemble of four spins, we define

$$D^{(K)} \equiv \det [\langle \hat{T}^{(k\ell)} \rangle_\omega]_{k,\ell \in K}$$

Our goal is to show that for any $\epsilon > 0$ there exists $\delta > 0$ such that for all such K

$$\sigma_\omega \hat{T}^{(k\ell)} < \delta \text{ for } k,\ell \in K \Rightarrow |D^{(K)}|^{1/2} < \epsilon. \quad \$(2.4.3)\$$$

Consider the determinant operator

$$\Delta^{(K)} \equiv \frac{1}{4!} \epsilon_{k_1 k_2 k_3 k_4} \hat{T}^{(k_1 \ell_1)} \hat{T}^{(k_2 \ell_2)} \hat{T}^{(k_3 \ell_3)} \hat{T}^{(k_4 \ell_4)} \epsilon_{\ell_1 \ell_2 \ell_3 \ell_4}. \quad (2.4.4)$$

Here there is an implicit summation over the indices k_1, \dots, k_4 and ℓ_1, \dots, ℓ_4 , ranging over the four elements of K . The ϵ 's are totally antisymmetric symbols which have the value +1 for even permutations of K . Applying the lemma to the products of $\hat{T}^{(k\ell)}$ in $\Delta^{(K)}$ we have

$$|\langle \Delta^{(K)} \rangle_\omega - D^{(K)}| \leq 3! \sum_{k, \ell \in K} \sigma_\omega \hat{T}^{(k\ell)} < 96\delta. \quad (2.4.5)$$

Finally, we show that there is a similar bound on $|\langle \Delta^{(K)} \rangle_\omega|$ itself. For consider the antisymmetrized tensor product

$$\widetilde{J}^{(\ell_1)} \widetilde{J}^{(\ell_2)} \widetilde{J}^{(\ell_3)} \widetilde{J}^{(\ell_4)} \epsilon_{\ell_1 \ell_2 \ell_3 \ell_4} = 0. \quad (2.4.6)$$

which vanishes identically, because only products of distinct 3-vector operators occur, and these commute. Therefore

$$\begin{aligned} & \frac{1}{4!} \left[\prod_{k \in K} j_k \right]^{-2} \epsilon_{k_1 k_2 k_3 k_4} J_{i_2}^{(k_2)} (\widetilde{J}^{(k_1)} \cdot \widetilde{J}^{(\ell_1)}) J_{i_2}^{(\ell_2)} \times \\ & \times J_{i_3}^{(\ell_3)} (\widetilde{J}^{(k_4)} \cdot \widetilde{J}^{(\ell_4)}) J_{i_3}^{(k_3)} \epsilon_{\ell_1 \ell_2 \ell_3 \ell_4} = 0. \end{aligned} \quad (2.4.7)$$

But (2.4.7) and (2.4.4) differ by terms of the form

$$A B [C, D]; [A, B] C D; \text{ and } [A, B] [C, D], \quad (2.4.8)$$

where

$$A = \hat{T}^{(k_1 \ell_1)}, \quad B = \hat{T}^{(k_2 \ell_2)}, \quad C = \hat{T}^{(k_3 \ell_3)}, \quad D = \hat{T}^{(k_4 \ell_4)}.$$

Let $[A, B] = E$, $[C, D] = F$. By (2.3.12 - 14),

$$|\langle ABF \rangle_\omega - \langle AB \rangle_\omega \langle F \rangle_\omega| \leq \sigma_\omega(AB) \sigma_\omega F$$

and $|\langle AB \rangle_\omega \langle F \rangle_\omega| \leq 2\delta^2$.

Also

$$\sigma_{\omega}^2(AB) = |\langle ABAB \rangle_{\omega} - \langle AB \rangle_{\omega}^2|$$

$$\leq |\langle ABAB \rangle - \langle ABA \rangle \langle B \rangle| + |\langle ABA \rangle \langle B \rangle - \langle AB \rangle \langle A \rangle \langle B \rangle| +$$

$$|\langle AB \rangle \langle A \rangle \langle B \rangle - \langle AB \rangle^2|$$

$$\leq \sigma_{\omega}(ABA) \sigma_{\omega} B + \sigma_{\omega}(AB) \sigma_{\omega} A + \sigma_{\omega} A \sigma_{\omega} B < 6\delta,$$

since $\|x\| \leq 1 \Rightarrow \sigma_{\omega} x \leq 2$. Similarly, $\sigma_{\omega}^2 F < 24\delta$, so

$$|\langle ABF \rangle_{\omega}| \leq 12\delta + 2\delta^2. \quad (2.4.9)$$

By the same arguments

$$|\langle ECD \rangle_{\omega}| \leq 12\delta + 2\delta^2 \quad (2.4.10)$$

$$|\langle EF \rangle_{\omega}| \leq 24\delta + 2\delta^4. \quad (2.4.11)$$

Now we count the number of terms of each type. A commutator $[T^{(k\ell)}, T^{(k'\ell')}]$ vanishes unless it is of the form $[T^{(12)}, T^{(23)}]$. Given 4 different indices, there are $4 \times 3 \times 4$ commutators of this type. The remaining T's in the term must be $T^{(41)}$ and $T^{(34)}$ or $T^{(31)}$ and $T^{(44)}$ (the latter is excluded in the terms of type $[A,B][C,D]$). Hence there are $4 \times 3 \times 4 \times 4 / 4! = 8$ contributions for each of type (2.4.9) and (2.4.10) and 4 contributions of type (2.4.11).

Thus

$$|\langle \Delta^{(K)} \rangle_{\omega}| \leq 16(12\delta + 2\delta^2) + 4(24\delta + 4\delta^4)$$

Combining this with (2.4.5), we have the bound

$$|D^{(K)}|^{1/2} \leq 4(24\delta + 2\delta^2 + \delta^4)^{1/2} \leq 20\delta^{1/2} \leq \epsilon$$

for sufficiently small δ .

This proof relies only on properties of the observables $\{T^{(k\ell)}\}$. Nothing is assumed about the state ω , except that it contains enough information to make these observables δ -classical. In fact, ω need not even be invariant. Since the observables are invariant, however, we may project out the invariant part of ω (say, by integration over the group manifold), without changing the expectation values of the T 's. In this case, the generalized Wigner-Eckart theorem guarantees that ω is a superposition of spin networks.

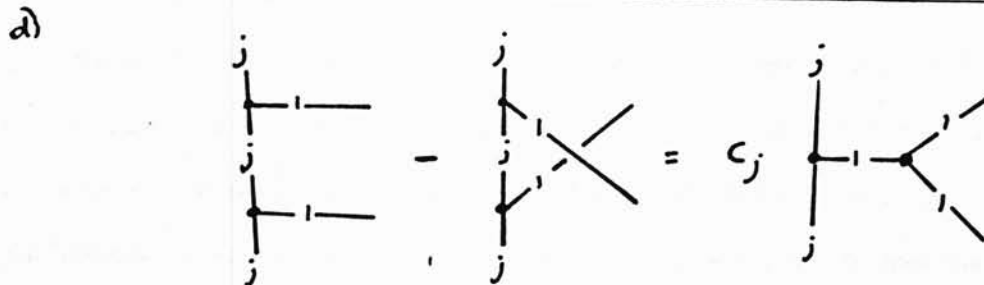
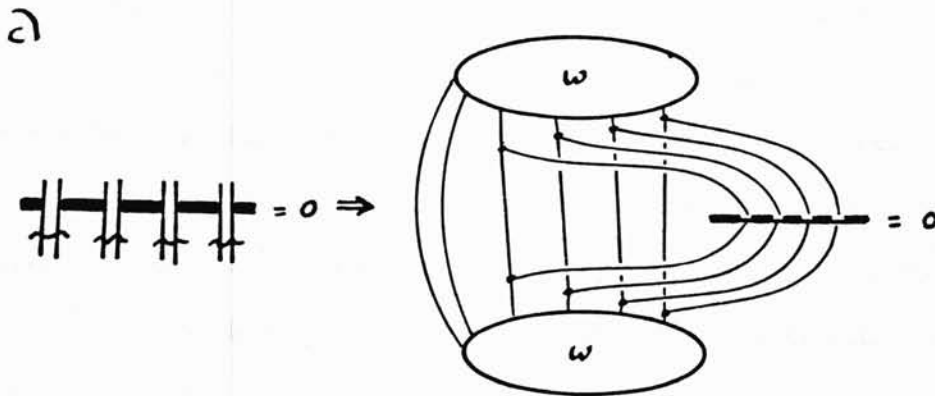
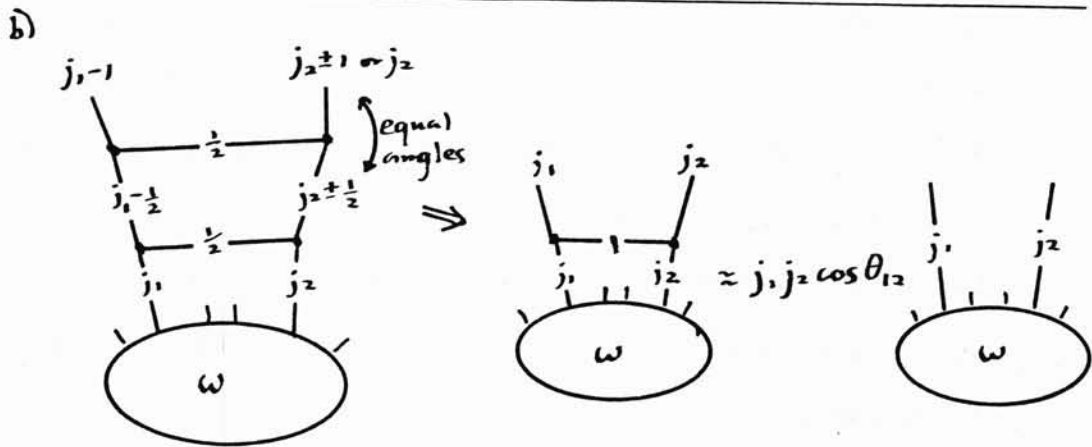
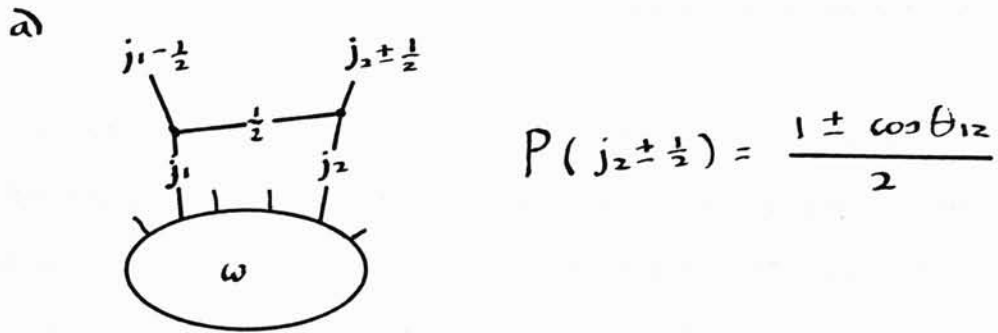
Penrose proved a very similar result by a method emphasizing the combinatorics of the network themselves. Since his proof has not been published, we sketch it here, and show the connections with our method.

Given a network with two free ends j_1 and j_2 , Penrose considers the new network shown in figure 2.8a in which a spin-1/2 unit splits off j_1 and combines with j_2 to form either $j_2 + \frac{1}{2}$ or $j_2 - \frac{1}{2}$. He defines the cosine of the angle between j_1 and j_2 to be the difference between the probabilities of these two outcomes (these probabilities are computed as expectation values of a projection operator as in figure 2.5b).

Penrose notes that if j_1 and j_2 are not connected by ω , then $\cos \theta_{12} = 0$ by this definition. Hence he considers the results of making repeated angle measurements as shown in figure 2.8b. He requires that the angle θ_{12} be well-defined in the sense that the results of successive measurements are approximately the same. He is then able to show that ω is an approximate eigenvector of the spin-1 exchange operator of figure 2.7c, with eigenvalue proportional to $\cos \theta_{12}$, as shown in figure 2.8b.

Since the spin-1 system has only three components, the antisymmetric product of 4 such systems vanishes. Thus the network of figure 2c, which approximates the determinant of the 4x4 matrix of cosines between 4 spins, also vanishes. In order to apply the eigenvector approximation of 2.8b, however, we have to rearrange the order of some spin-1 exchanges as shown in 2.8d, the network analog of the commutation relations (2.3.14). In the limit of very

Figure 2.8 Penrose proof of geometry theorem



large spins, the uncertainty relation (2.3.15) guarantees that these rearrangements make small contributions to the determinant.

Finally, we consider how to extend the spin geometry theorem to make predictions about the interior of a network. As shown in figure 2.9a, we define the expectation value of the scalar product between two interior edges as the fractional change in the amplitude of the network when these edges are linked by a spin-1 exchange operator. If the two edges happen to be coupled, as in figure 2.9b, then we get the expected result (2.3.3). If the edges are not coupled, we may still have the classically expected value. For example, the identity in figure 2.9c guarantees that the expected angles in a tetrahedron take the classical values. In general, the scalar products between any interior edge and each of a coupled triplet of edges satisfy a linear conservation law of this type, thanks to the identity in figure 2.9d. This identity, the operator analog of (1.2.1), is simply the infinitesimal version of the requirement that the $3j$ -symbol be rotationally invariant.

In a closed connected spin network with E edges and V vertices, the $3E$ interior spin components are subject to E quadratic constraints on the spin lengths and $3(V-1)$ linear conservation conditions. Since $2E=3V$, the spin components are algebraically determined by the constraints, up to an overall rotation of the configuration. Because the length constraints are quadratic, however, there may be no real solutions, or a finite multiplicity of solutions, corresponding to discrete ambiguities in the conformation of the spins.

Consider the matrix of expectation values $T^{(k'l')}$ of all the interior scalar products of a closed spin network. Any three rows or columns corresponding to coupled edges are linearly dependent by figure 2.9d. Proposition (SP) implies that real solutions for the underlying spin components exist just when this matrix is positive semidefinite of rank no greater than 3. The argument of the previous paragraph shows that in this "classically allowed" regime there will in general be a finite multiplicity of spin configurations. The multiplicity may cause the

Figure 2.9 Interior geometry of a spin network

a)

$$(\vec{J}^{(a)} \cdot \vec{J}^{(b)}) \equiv k_{j_a} k_{j_b}$$

b)

$$k_{j_1} k_{j_2} \text{ (tetrahedron with edge 1 highlighted) } = (\vec{J}^{(1)} \cdot \vec{J}^{(2)}) \text{ (tetrahedron with edge 2 highlighted)}$$

c)

$$k_{j_1} \text{ (tetrahedron with edge 1 highlighted) } + k_{j_2} \text{ (tetrahedron with edge 2 highlighted) } + k_{j_4} \text{ (tetrahedron with edge 4 highlighted) } = 0$$

$$(\vec{J}^{(1)} \cdot \vec{J}^{(3)}) + (\vec{J}^{(2)} \cdot \vec{J}^{(3)}) + (\vec{J}^{(4)} \cdot \vec{J}^{(3)}) = 0$$

d)

$$k_{j_1} \text{ (tree with edge 1 highlighted) } + k_{j_2} \text{ (tree with edge 2 highlighted) } + k_{j_4} \text{ (tree with edge 4 highlighted) } = 0$$

δ -classical hypothesis of the spin geometry theorem to fail, even for classically allowed networks.

As we shall see in the next chapter, discrete ambiguities in spin configuration are the rule rather than the exception. Regge-Ponzano theory overcomes this difficulty by means of a path-integral technique for evaluating closed networks. Ambiguities in conformation appear as multiple extremal paths. Moreover, this technique accounts for the exponential decay of the amplitude of a network as we "tunnel" into a classically forbidden regime, where there are no extremal spin geometries at all.

3. REGGE-PONZANO THEORY

Regge and Ponzano developed a more detailed analysis of the semiclassical limit of spin networks. Their method has two parts: first, a remarkably accurate analytic approximation to the Racah coefficient; second, an exact path-integral-like decomposition formula for evaluating any spin network as a sum of products of these coefficients. This chapter consists entirely of review of this approach [Ponzano and Regge 68].

3.1 Semiclassical limit of Racah coefficient

In the classical limit, it is convenient to depict spin coupling by means of "vector diagrams", which are graph-theoretic duals of spin networks. Figure 3.1 describes the simplest non-trivial recoupling amplitude, the Racah coefficient: 3.1a is the standard "network" picture; 3.1b is the corresponding vector diagram. The edges in b represent spin vectors, as in classical kinematics. Hence in b the conservation laws are indicated by the closing up of triplets of spin vectors into triangular faces, which correspond one-to-one with the incidence of triplets on cubic vertices in a (the face 012 with vertex A, 130 with B, 203 with C, 321 with D). If we think of the tetrahedra in figure 3.1 as embedded in the surface of a sphere, then a and b are duals in the familiar graph-theoretic sense.

The vector diagram shows two different schemes for coupling the three spins j_1 , j_2 , and j_3 to form the total spin J . In the first scheme, j_1 and j_2 couple (face 012) to form the "partial spin" j_{12} , which couples (on face 203) with j_3 to form J . In the second scheme, j_2 and j_3 couple to form j_{23} , which couples with j_1 to form J . The Racah coefficient is the "recoupling amplitude" which transforms between bases for the 3-spin states labelled by these two different coupling schemes. In standard notation of quantum mechanics [Ponzano and Regge 68, p.9]:

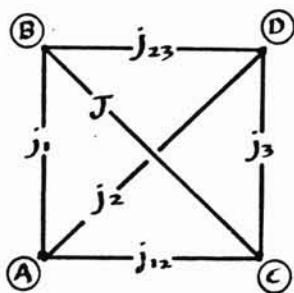
$$\langle (j_1, j_2) j_{12}, j_3 \rangle_J | (j_1, (j_2, j_3) j_{23}) \rangle_J$$

$$\equiv [(2j_{12} + 1)(2j_{23} + 1)]^{1/2} (-1)^{j_1 + j_2 + j_3 + J} \begin{Bmatrix} j_1 & j_2 & j_{12} \\ j_3 & J & j_{23} \end{Bmatrix} \quad (3.1.1)$$

where the normalization factors are chosen to give the 6-j symbol maximal symmetry under the group preserving the tetrahedron. The square of this amplitude can be interpreted as the probability that j_{23} be the sum of the angular momenta j_2 and j_3 , while j_1 and j_2 sum to j_{12} , and both j_{12} , j_3 and j_1 , j_{23} sum to J .

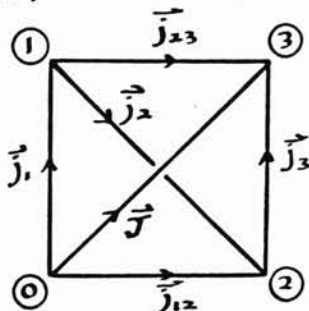
Figure 3.1 Dual Representations of the Racah Coefficient

a) Network:



$$= \begin{Bmatrix} j_1 & j_2 & j_{12} \\ j_3 & J & j_{23} \end{Bmatrix}$$

b) Vector:



$$\begin{aligned} \vec{j}_1 + \vec{j}_2 &= \vec{j}_{12} & \vec{j}_2 + \vec{j}_3 &= \vec{j}_{23} \\ \vec{j}_{12} + \vec{j}_3 &= \vec{J} & \vec{j}_1 + \vec{j}_{23} &= \vec{J} \end{aligned}$$

Wigner reasoned heuristically that, in the limit of large spins, all values of the dihedral angle θ_{02} between the faces (021 and 023) which hinge at j_{12} as j_{23} changes should be equally likely [Wigner 59]. By elementary trigonometry,

$$\frac{d\theta_{02}}{dj_{23}} = \frac{j_{12}j_{23}}{6V} \quad (3.1.2)$$

where V is the volume of the tetrahedron in figure 3.1b. Hence we expect that on the average, in the classical limit

$$\left| \left\{ \begin{matrix} j_1 & j_2 & j_{12} \\ j_3 & J & j_{23} \end{matrix} \right\} \right|^2 \sim \frac{1}{24\pi V} \quad (3.1.3)$$

The actual values of the Racah coefficient $\left\{ \begin{matrix} a & b & c \\ d & J & e \end{matrix} \right\}$ as a function of J oscillate wildly about the average computed by Wigner. Ponzano and Regge accounted for the oscillations with the following analytic approximation:

$$\left[\frac{1}{12\pi V} \right]^{1/2} \cos \left(\sum_e j_e \theta_e + \frac{\pi}{4} \right) \quad (3.1.4)$$

where θ_e is the angle between the outer normals of the faces meeting at edge e , and j_e is the length of the spin associated with that edge.⁴

The phase term in this formula has a simple physical explanation: the angle variables θ are conjugate to the spins j :

$$\frac{1}{i} \frac{\partial}{\partial j} \sim \theta \quad (3.1.5)$$

This correspondence leads us to expect recursion relations for the Racah coefficient of the form

$$\left\{ \begin{matrix} a+1 & b & c \\ d & e & f \end{matrix} \right\} + \left\{ \begin{matrix} a-1 & b & c \\ d & e & f \end{matrix} \right\} = (e^{i\theta_a} + e^{-i\theta_a}) \left\{ \begin{matrix} a & b & c \\ d & e & f \end{matrix} \right\}. \quad (3.1.6)$$

Such relations in fact do exist in the limit of large spins, and the formula (3.1.4) can be derived from them by a finite-differences analog of the WKB method [see also Schulten and Gordon 75]. This method gives accurate approximations to the Racah coefficient even when the 6 spin lengths are not consistent with the classical tetrahedron being embedded in Euclidean 3-space. In this "tunneling" regime, the volume V and angles θ become pure imaginary, and an analytically continued formula similar to (3.1.4) predicts exponential decay of the

⁴ We take the length to be $j + 1/2$, since this is a better approximation to $\sqrt{j(j+1)}$ than j is.

coefficient.

3.2 Decomposition theorem and path integrals

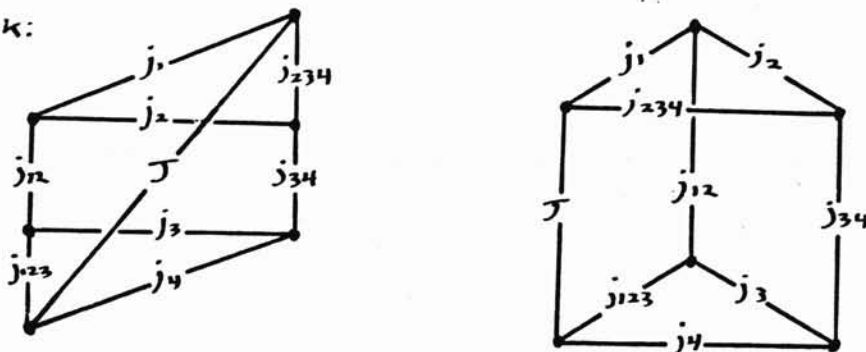
The second part of the Regge-Ponzano method, which we call the decomposition theorem, permits the evaluation of more complicated spin networks, such as shown in figure 3.2a. This network is also planar, so we once again think of it as imbedded in the surface of a sphere, and construct a dual vector diagram 3.2b, triangulating the sphere with six triangular faces, one for each vertex in 3.2a. Figure 3.2c shows that this triangulation can be decomposed into two tetrahedra with the common face 024. In this case, the decomposition theorem implies that the amplitude of a diagram which decomposes into tetrahedra is the product of the corresponding Racah coefficients, resulting in the equation give in figure 1.2d.

Figure 3.3d shows another kind of decomposition of 3.3b, into three tetrahedra which hinge at a new edge j_{23} spanning vertices 1 and 3 in the original vector diagram. In this case, the decomposition theorem implies that the amplitude is the product of the corresponding Racah coefficients, summed over all values of the new edge. Since both methods of evaluating the amplitude must give the same result, we have the classic identity between Racah coefficients derived by Biedenharn and Elliott [Biedenharn 53, Elliott 53] shown in figure 3.3e (the phase factor $(-1)^\phi$ and weight $(2j_{23} + 1)$ are explained in the next chapter). In fact, recursion relations such as (3.1.6) can be derived from this identity.

In general, we may think of any spin network ω as being imbedded in the boundary of a region in some three-dimensional space. We associate with ω a dual vector diagram $D(\omega)$ which triangulates the boundary in a polyhedron with specified edge lengths. Even in the simplest case of planar ω , the geometry of the polyhedron $D(\omega)$ is not completely determined (e.g. it need not be convex). Hence we define a new diagram $C(\omega)$ which has additional information about the lengths x_i , $i = 1, 2, \dots, q$ of a sufficient number of new "internal" edges to dissect the interior of $D(\omega)$ into tetrahedra T_k . We may regard $C(\omega)$ as a three-dimensional

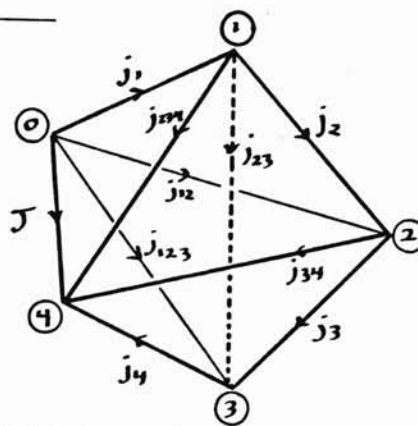
Figure 3.2 Decomposition: the Biedenharn-Elliott Identity

a) Network:

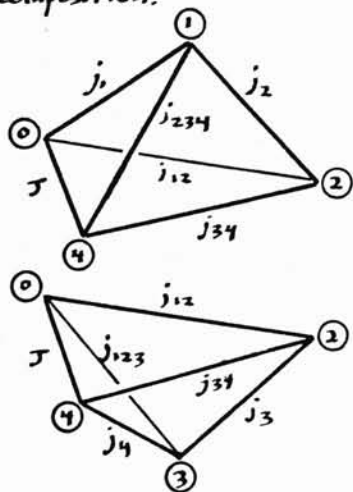


b) Vector:

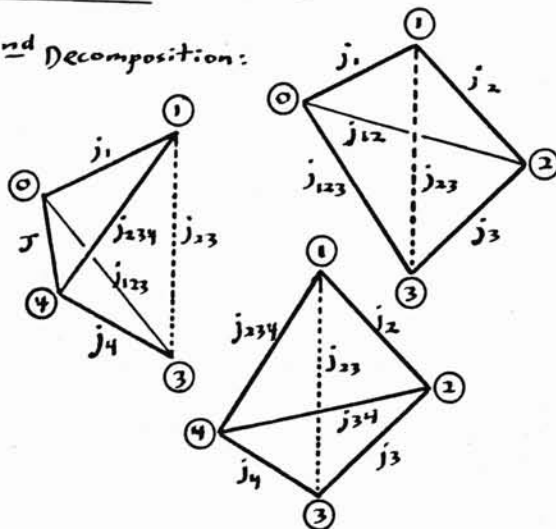
$$\begin{aligned} \vec{j}_1 + \vec{j}_2 &= \vec{j}_{12} & \vec{j}_3 + \vec{j}_4 &= \vec{j}_{34} \\ \vec{j}_{12} + \vec{j}_3 &= \vec{j}_{123} & \vec{j}_2 + \vec{j}_{34} &= \vec{j}_{234} \\ \vec{j}_{123} + \vec{j}_4 &= \vec{j} & \vec{j}_1 + \vec{j}_{234} &= \vec{j} \end{aligned}$$



c) 1st Decomposition:



d) 2nd Decomposition:



e) Biedenharn-Elliott Identity:

$$\begin{aligned} & \left\{ \begin{matrix} j_1 & j_2 & j_{12} \\ j_{34} & \mathcal{J} & j_{234} \end{matrix} \right\} \left\{ \begin{matrix} j_{12} & j_3 & j_{123} \\ j_4 & \mathcal{J} & j_{34} \end{matrix} \right\} \\ &= \sum_{j_{23}} (-1)^{\theta} (2j_{23} + 1) \left\{ \begin{matrix} j_1 & j_2 & j_{12} \\ j_3 & j_{123} & j_{23} \end{matrix} \right\} \left\{ \begin{matrix} j_1 & j_{23} & j_{123} \\ j_4 & \mathcal{J} & j_{234} \end{matrix} \right\} \left\{ \begin{matrix} j_2 & j_3 & j_{23} \\ j_4 & j_{234} & j_{34} \end{matrix} \right\} \end{aligned}$$

combinatorial manifold with boundary $D(\omega)$. We then form the product

$$\Pi(x_1, \dots, x_q) \equiv \prod_{k=1}^p [T_k] (-1)^x \prod_{i=1}^q (2x_i + 1), \quad (3.2.1)$$

where $[T_k]$ is the Racah coefficient associated with T_k and the sign $(-1)^x$ is given by

$$x = \sum_{j=1}^q (p_j - 2) x_j + x_0. \quad (3.2.2)$$

Here p_j is the number of tetrahedra which meet at the internal edge x_j , and x_0 is a constant 0 or 1/2, as required to make x an integer.⁵ The decomposition theorem, which we will prove in a more general context in chapter 4, states that the amplitude $\Psi[\omega]$ of ω is given by

$$\Psi[\omega] = \sum_{x_1} \dots \sum_{x_q} \Pi(x_1, \dots, x_q). \quad (3.2.3)$$

This theorem resembles the path integral approach to quantum theory [Dirac 33, Feynman and Hibbs 65]. In this approach, we compute the transition amplitude $\langle x_t | x_0 \rangle$ (x_0 is an initial state at time 0 and x_t is a final state at time t) by introducing a sequence of intermediate states x_1, \dots, x_q and forming the product

$$\pi(x_1, \dots, x_q) \equiv \langle x_t | x_q \rangle \langle x_q | x_{q-1} \rangle \dots \langle x_2 | x_1 \rangle \langle x_1 | x_0 \rangle. \quad (3.2.4)$$

By repeated application of the completeness theorem for the states x , the original amplitude $\langle x_t | x_0 \rangle$ is equal to the sum (or integral)

$$\langle x_t | x_0 \rangle = \sum_{x_1} \dots \sum_{x_q} \pi(x_1, \dots, x_q) \quad (3.2.5)$$

If x_t evolves according to some Hamiltonian H , it is easy to show that as $dt \rightarrow 0$,

$$\langle x_{t+dt} | x_t \rangle \approx e^{\frac{iLdt}{\hbar}} \quad (3.2.6)$$

⁵ This choice of sign is correct for the planar case only.

where L is the corresponding classical Lagrangian. Hence in the limit of infinitely closely spaced x_i , π becomes a pure phase proportional to the classical action S associated with the "path" defined by the x_i , and (3.2.5) becomes the formal integral over all those paths which span the boundary states x_t and x_o :

$$\langle x_t | x_o \rangle = \int e^{iS/\hbar}, \text{ where } S = \int_0^t L dt. \quad (3.2.7)$$

In the limit $\hbar \rightarrow 0$, only paths near the classical trajectory, for which the action is extremal - and hence stationary - contribute to the amplitude (principle of stationary phase).

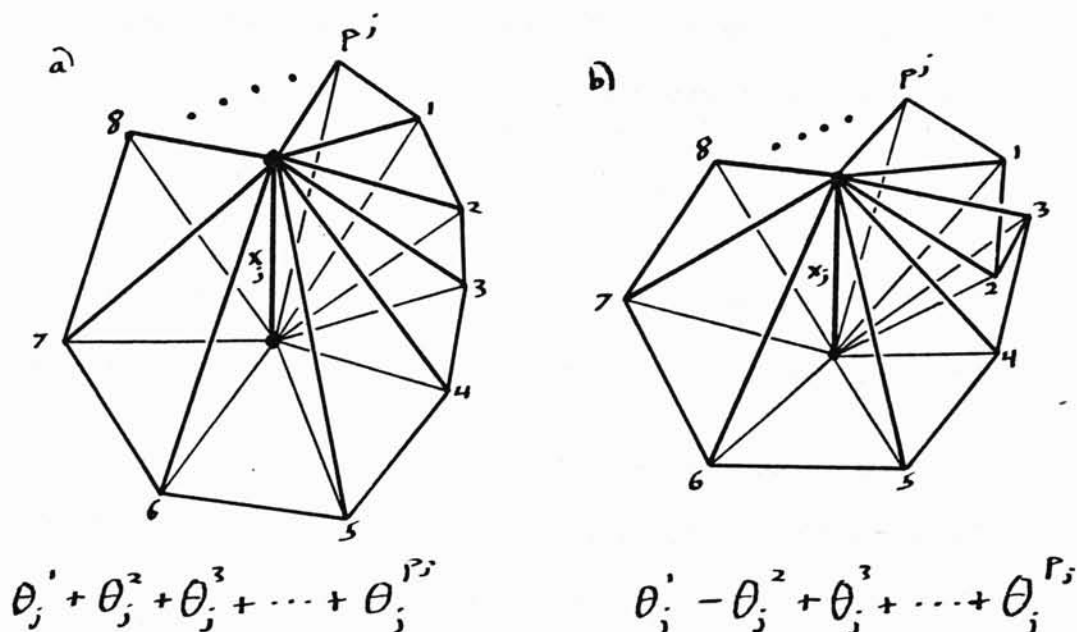
In Regge-Ponzano theory, the analog of (3.2.6) is the semiclassical approximation to the Racah coefficient (3.1.4). Since, moreover, $\cos \phi = (e^{i\phi} + e^{-i\phi})/2$, the substitution of (3.1.4) into the product (3.2.1) for each of the p tetrahedra T_k results in a sum of 2^p different pure phases. A particular internal edge x_j which belongs to p_j different tetrahedra will appear in 2^{p_j} different phases of the form:

$$e^{ix_j \left(\sum_{k=1}^{p_j} \pm \theta_j^k \right)} \quad (3.2.8)$$

where θ_j^k is the external dihedral angle between the faces of tetrahedron k which meet at edge x_j ; and each of the 2^{p_j} different phases correspond to a choice of the signs of these p_j angles.

The physical interpretation of these phases is illustrated in figure 3.3, which shows how they correspond to different orientations of the p_j tetrahedra which hinge at x_j . Each tetrahedron is determined by two vertices that form two triangular faces with the edge x_j and are connected by an edge (which forms the other two faces with the endpoints of x_j). Each of these "equatorial" vertices is shared between two tetrahedra meeting at a common face. Hence there are exactly p_j such vertices in all, connected in a loop which encircles x_j . We number these vertices 1 through p_j around the loop, and let the k th tetrahedron be defined by the two vertices k and $k + 1 \pmod{p_j}$.

Figure 3.3 Phase and Orientation Ambiguities



Now in fig. 3.3a each pair of successive tetrahedra k and $k+1$ are on opposite sides of the common face formed by x_j and vertex $k+1$. Hence the dihedral angles θ_j^k are all of the same sign, and the phase term corresponding to this orientation is $\theta_j^1 + \theta_j^2 + \theta_j^3 + \dots + \theta_j^{P_j}$. In figure 3.3b, however, the tetrahedra 1 and 2 are on the same side of the face defined by x_j and vertex 2. This "retrograde" progression in the loop corresponds to a phase term of the form $\theta_j^1 - \theta_j^2 + \theta_j^3 + \dots + \theta_j^{P_j}$. Each of the 2^{P_j} phase terms corresponds to such an ordering of the loop, once an overall orientation convention is chosen. In fact we may interpret the cosine in the Racah formula (3.1.4) as arising from the superposition of the amplitudes for the two possible orientations of a single tetrahedron.

If we substitute these phase terms in (3.2.3), we arrive at a sum over all orientations of the tetrahedral cells, as well as over all values of x_1, \dots, x_q : i.e., a sum over all geometries consistent with the boundary conditions given by the original spin network ω . Now Regge and Ponzano reason, in formal analogy with the path integral argument, that the geometries that contribute to the sum will be just those for which S is stationary under variation of each x_j .

For the sake of simplicity, we describe what this condition means in the case when an extremal geometry is oriented as shown in fig. 3.4a at all interior edges. Suppose that a particular x_j is integral (the half integral case is similar). Then the effect of x_j in the sign term (3.2.2) can be incorporated into the phase in the form $e^{\pm i\pi(p_j-2)x_j}$, and the total contribution of x_j is

$$e^{ix_j \left[\left(\sum_{k=1}^{p_j} \theta_j^k \right) - \pi p_j + 2\pi \right]} \quad (3.2.9)$$

In this formula the θ_j^k 's are functions of the edge lengths x_j . However, as we shall see in the next section, we can carry out the variation as if the θ_j^k 's were constants. Hence the stationary phase condition is

$$\sum_{k=1}^{p_j} (\pi - \theta_j^k) = 2\pi, \quad (3.2.10)$$

which means that the sum of the internal dihedral angles around x_j is just 2π . But this is the condition for the configuration to be imbeddable in a three-dimensional Euclidean space. Hence we have arrived by this circuitous path at a conclusion very similar to Penrose's spin geometry theorem.

3.3 Regge calculus for quantized spin

We interpret the stationary phase condition (3.2.10) by applying the Regge calculus [Regge 61, Sorkin 75], a discrete coordinate-free approach to describing geometry, to the vector picture of quantized spins. In this approach, a manifold is approximated by a simplectic net with specified edge lengths. For example, a 2-manifold is approximated by a triangulation, a 3-manifold by a tetrahedralization, and in general an n -dimensional manifold by a net of n -simplices ("cells") each rigidly determined by $n(n+1)/2$ edge lengths. The cells meet at $(n-1)$ -simplices called "faces", which join at $(n-2)$ -simplices called "bones". Figure 3.3 is an example of a combinatorial 3-manifold described by p^j tetrahedra which meet at p^j triangular faces, all of which hinge at the bone x^j .

The Regge calculus gives rise to an elegant "finite-element" approximation to Einstein's equations in general relativity. In this context, we assume the usual flat-space parallel transport within each cell and across the face between two cells. Transport around a loop that encircles a bone B will, however, result in an overall rotation around B through a "defect angle" $\eta(B)$ which measures the curvature concentrated at B . The defect $\eta(B)$ is the difference between 2π and the sum of the internal dihedral angles between the successive faces that hinge at B . In fact, explicit calculation of the vacuum Einstein action S gives [Sorkin, p.387]

$$S \equiv -\frac{1}{2} \int R dV = \sum |B| \eta(B) \quad (3.3.1)$$

where $|B|$ is the magnitude of the bone (length, area, volume,...), and the sum is over all the internal bones of the manifold. Einstein's equations are simply the condition for this action S to be stationary under variation of all the internal edges in the simplicial manifold.

These equations are simplified by an identity [Sorkin, p.395] which allows us to perform the variation as if the deficit angles were constants. Let T be the single n -cell with vertices $i = 0, 1, \dots, n$ and volume V . Let F_i be the face opposite vertex i ; B_{ij} the bone opposite i and j (i.e. the intersection of F_i and F_j) and θ_{ij} the dihedral angle contained between F_i and F_j . The

desired identity is

$$\sum_{ij} |B_{ij}| \delta\theta_{ij} = 0 \quad (3.3.2)$$

where $\delta\theta_{ij}$ is the change in θ_{ij} under arbitrary variation of the lengths of edges in T . We compute $\delta\theta_{ij}$ with the help of the elementary facts

$$(F_i \cdot F_j) = -|F_i| |F_j| \cos \theta_{ij} \quad (3.3.3)$$

and

$$|B_{ij}| V = \frac{n-1}{n} |F_i| |F_j| \sin \theta_{ij}. \quad (3.3.4)$$

Thus

$$\begin{aligned} |B_{ij}| \delta\theta_{ij} &= |B_{ij}| \delta(-\cos\theta_{ij}) / \sin \theta_{ij} \\ &= \frac{n-1}{nV} |F_i| |F_j| \delta((F_i \cdot F_j) / |F_i| |F_j|) \\ &= \frac{n-1}{nV} [\delta(F_i \cdot F_j) - (F_i \cdot F_j) \delta \ln |F_i| - (F_i \cdot F_j) \delta \ln |F_j|]. \end{aligned} \quad (3.3.5)$$

Hence the sum (3.3.5) vanishes by Stokes identity $\sum F_i = 0$. Since the defect $\eta(B)$ involves a sum of θ_{ij}^k over all the cells T^k containing B , we conclude that the variation in S is given by

$$\delta S = \sum \eta(B) \delta |B|. \quad (3.3.6)$$

This equation justifies the stationary phase condition (3.2.10) in the previous section. The Regge-Ponzano amplitude for a spin network is simply a formal path integral over the vacuum Einstein action in three dimensions, expressed in terms of the Regge calculus. The vector diagram of the network describes a fixed 2-manifold boundary of a three-dimensional region, and the integral is performed by summing over all "internal" spin lengths introduced by the decomposition theorem (and also over all orientations of the tetrahedra). In three

dimensions, $|B|$ is simply the length of the edges B , so $\delta S = 0$ in (3.3.6) just when $\eta(B) = 0$ at all internal bones. Hence we see that our stationary phase condition (3.2.10) amounts to the well-known fact that Einstein's equations in three dimensions possess only trivial (flat) solutions.

In dimensions $n > 3$, $|B|$ is a more complicated function of the edge lengths (the square root of a Cayley determinant), so Einstein's equations become non-trivial. Recent investigations have shown that a Regge-calculus formulation of quantum gravity is feasible [Rocek and Williams, 81], at least in the weak-field limit. It is tempting to conjecture [Hasslacher and Perry 81] that such a formulation arises from applying the Regge-Ponzano method to the recoupling theory of some larger group.

4. THEORY OF FABRICS

In this chapter, the notion of fabric is introduced as an attempt to extend the Penrose and Regge-Ponzano analyses of spin to other situations that give rise to new models of quantum geometries. In section 1, we review the well-known recoupling theory of compact semisimple groups, in a graphical calculus which is a natural generalization of spin networks. [see also Agrawala and Belinfante 68]. In section 2, we prove the Regge-Ponzano decomposition theorem in this general context, and give some examples of the scope of its application. In section 3, we ~~give axioms for fabrics and their valuations~~ by isolating [↖] those properties needed to prove the decomposition theorem. We briefly discuss the classification problem and semiclassical limit of fabrics. *and generalize these properties ^{into} as axioms for a theory of "fabrics" and their valuations.*

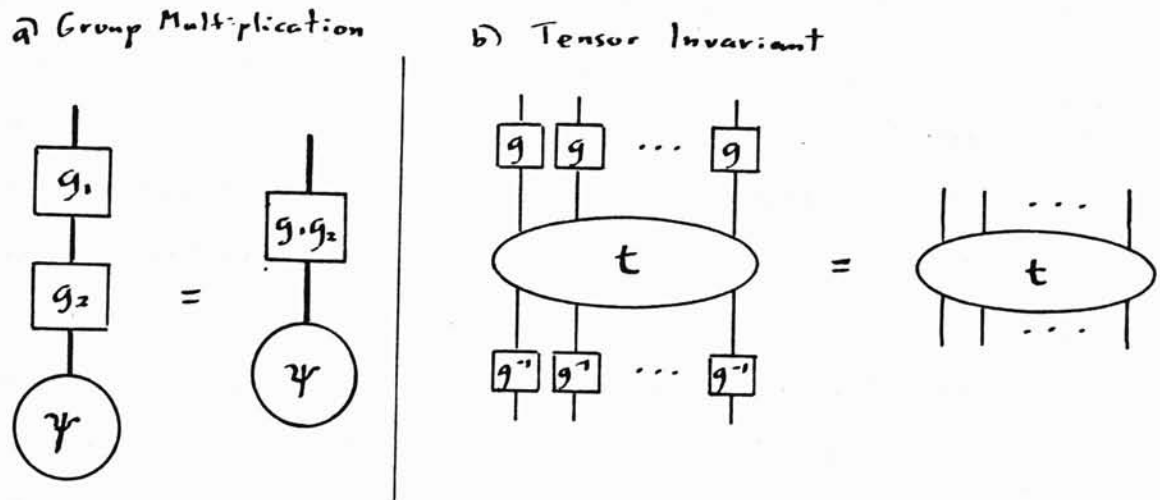
4.1 Recoupling theory of compact semisimple groups

We start with the basic theory of representations of a compact semisimple group G , in the language of modules. A (left) module M over G is a vector space over the field C , along with a continuous map $G \times V \rightarrow V$ through which every element $g \in G$ becomes represented as an invertible linear transformation on V such that $(g_1 g_2)\psi = g_1(g_2\psi)$ for all $\psi \in V$ (figure 4.1a). A submodule is an invariant subspace. A module M is irreducible if its only submodules are C and M .

Compact semisimple groups have the following nice properties:

- a. All modules reduce to a direct sum of irreducible submodules.
- b. All irreducible modules are finite-dimensional.
- c. All finite-dimensional modules are equivalent to unitary ones (we may define an invariant hermitian product on V).

Figure 4.1 Group multiplication and invariance



The space $\text{lin}(M, M')$ of linear maps from M to M' is itself a module over G under the usual action

$$(gt)(\psi) \equiv gt(g^{-1}\psi). \tag{4.1.1}$$

The module homomorphisms $\text{Hom}(M, M')$ are the tensors $t \in \text{lin}(M, M')$ which are invariants under g : $t = gt$. A module isomorphism is a one-one, onto homomorphism.

In analogy with spin theory, we use lower case Latin letters j, k to label isomorphism classes of irreducible modules. Let $M(j)$ be a reference module in the j -class. We adopt the shorthand notation

$$\text{Hom}(k_1 \otimes k_2 \otimes \dots \otimes k_p, k'_1 \otimes k'_2 \otimes \dots \otimes k'_q) \tag{4.1.2}$$

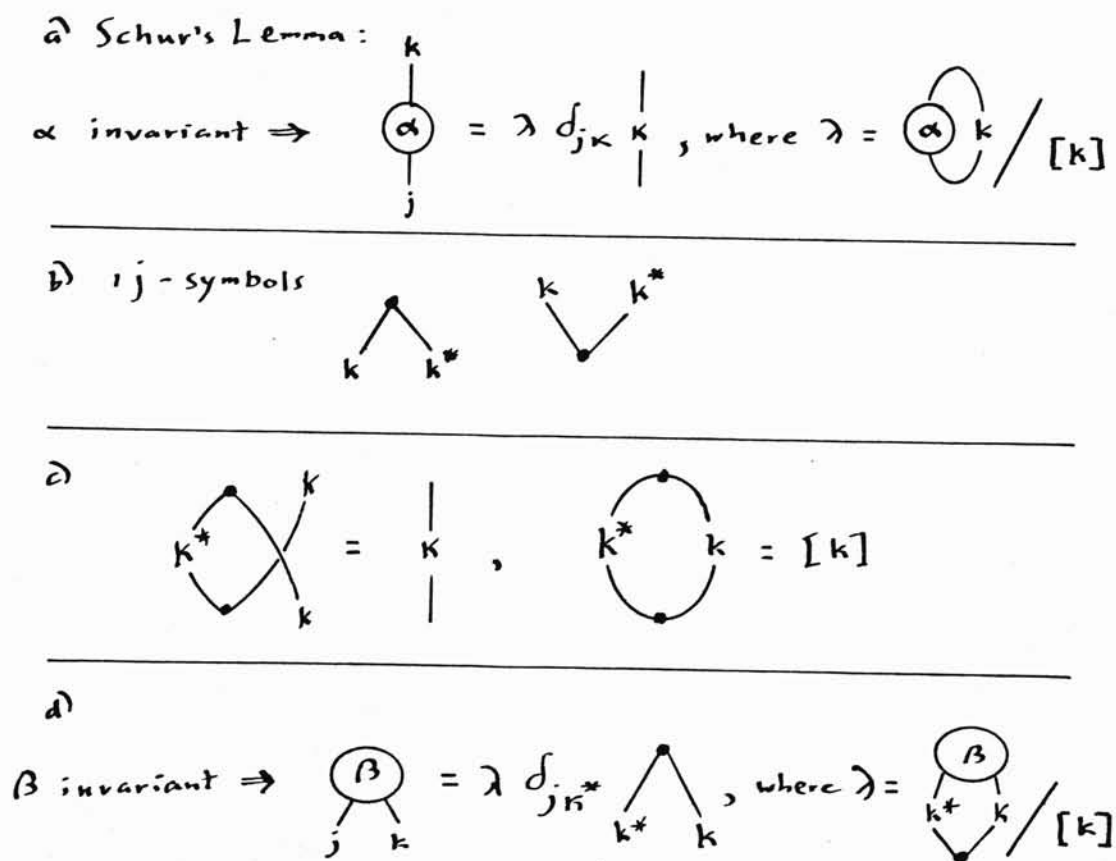
for the space of invariant linear maps between the corresponding products of reference modules (figure 4.1b). We classify such invariants by their valence (p, q) .

There are no non-trivial invariants with one index, by the irreducibility of the modules. Schur's lemmas classify the $(1, 1)$ invariants as follows:

1. $\alpha \in \text{Hom}(j,k)$ vanishes unless $j = k$, since the kernel and image of α are both submodules.
2. $\alpha \in \text{Hom}(k,k)$ must be a multiple of the identity operator, since the eigenspaces of α are submodules.

These lemmas are represented graphically by figure 4.2a. Here we use the shorthand $[k] = \dim M(k)$.

Figure 4.2 Schur's lemmas and 1j-symbols



The module $M^\bullet = \text{lin}(M, C)$ is the dual of M . We have the natural isomorphisms

$$\text{Hom}(M_1 \otimes M_2, C) \cong \text{Hom}(M_1, M_2^\bullet) \cong \text{Hom}(C, M_1^\bullet \otimes M_2^\bullet) \quad (4.1.3)$$

Hence by Schur's lemma $\text{Hom}(k_1 \otimes k_2, C)$ and $\text{Hom}(C, k_1 \otimes k_2)$ vanish unless $k_1 = k_2^\bullet =$ the label of the isomorphism class of $M(k_2)^\bullet$, in which case they are of dimension 1. We define

the generalized covariant and contravariant 1j-symbols (figure 4.2b) to be dual basis elements of the spaces $\text{Hom}(k \otimes k^*, C)$ and $\text{Hom}(C, k \otimes k^*)$ respectively, normalized as shown in figure 4.2c. Figure 4.2d depicts an analog of Schur's lemma for invariants of valence (2,0). The 1j-symbols can be used to raise or lower tensor indices invariantly in any of the recoupling identities that follow.

Another consequence of Schur's lemmas is shown in figure 4.3. The integral with respect to the invariant measure dg on G projects a tensor α onto an invariant tensor, by averaging it over the group manifold. Since α is arbitrary, it can be removed from the identity to give figure 4.3b. This group orthogonality property is the basis for harmonic analysis on G .

Figure 4.3 Group Orthogonality Property

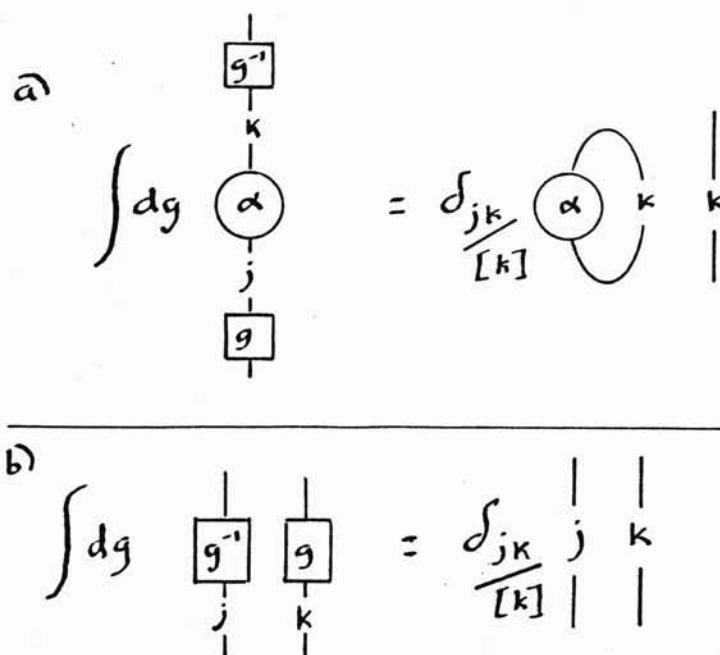


Figure 4.4a is a diagram for a coupling tensor (or generalized 3j-symbol) which maps $k_1 \otimes k_2$ into one of its k_3 -subspaces. In general there are multiple occurrences of k_3 in the product, so a new kind of index d (the 'degeneracy index') is introduced to label an orthonormal basis for the (2,1) invariants $\text{Hom}(k_1 \otimes k_2, k_3)$. Figure 4.4b depicts dual coupling tensors of other valence mixtures, which may be defined with the help of 1j-symbols.

Figure 4.4 Coupling tensors

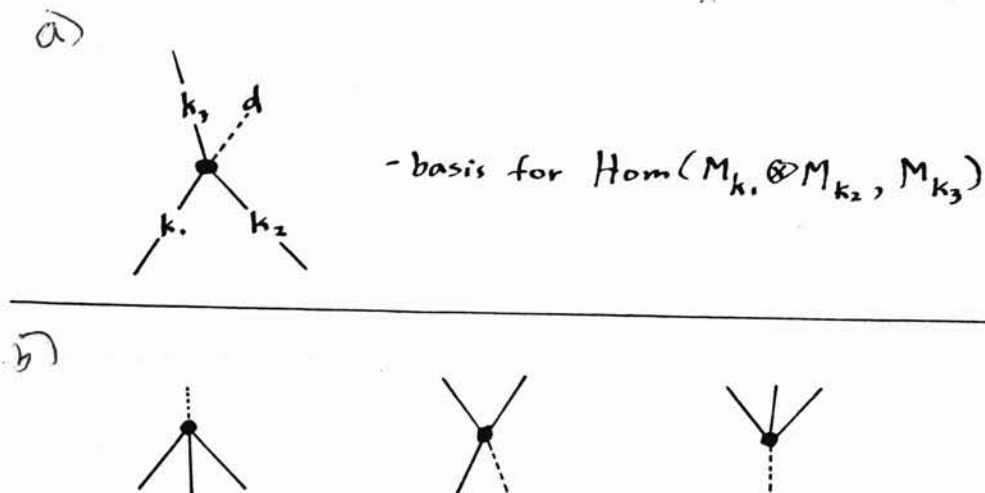




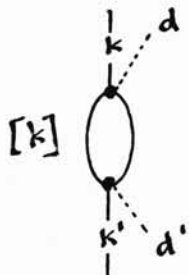
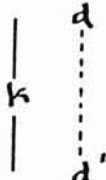
Figure 4.5 shows the results of all possible inner products of two coupling tensors. Figure 4.5a restates our assumption that the covariant and contravariant coupling tensors form dual bases. The orthogonality relation 4.5b arises from Schur's lemmas and an application of 4.5a. The summands on the left side of figure 4.5c are just projection operators into the irreducible subspaces of $k_1 \otimes k_2$. Hence 4.5c is the completeness relation for the reduction of the product. Figure 4.5d illustrates how any invariant with 3 indices can be expressed as an explicit sum of 3j-symbols (the Wigner-Eckart theorem).

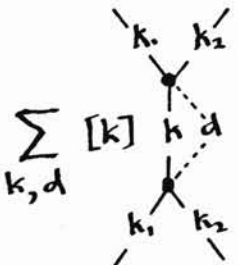
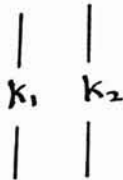
Figure 4.6a shows how to apply these last two identities to give an explicit expansion for any invariant of valence (4,0). In general for an invariant with n indices, we can apply the completeness identity $n-3$ times to get an invariant of valence 3, to which finally we apply the Wigner-Eckart identity. The result is an explicit expansion (generalized Wigner-Eckart theorem) of any invariant tensor with n indices in terms of coupling trees of $n-2$ coupling tensors (figure 4.6b).

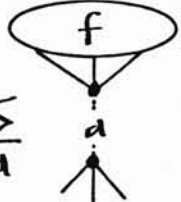
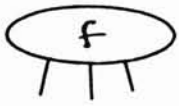
There are many different coupling tree bases for invariants with n indices: one for each choice of coupling sequence. The recoupling coefficients that transform between two such bases are simply the contractions of the two corresponding trees of coupling tensors. The

Figure 4.5 Contractions of coupling tensors

a)  =  ≡ δ_e^d

b)  = $\delta_{kk'}$ 

c) $\sum_{k,d} [k]$  = 

d) \sum_a  =  for f invariant


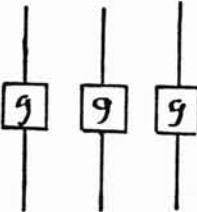
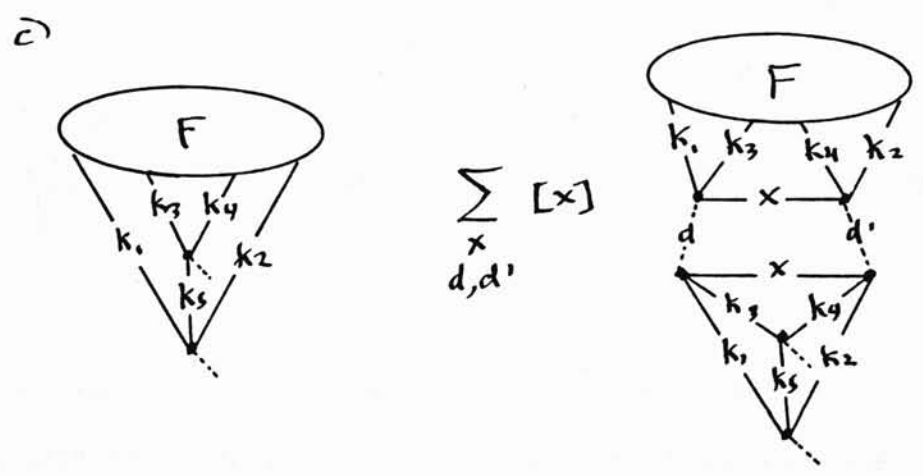
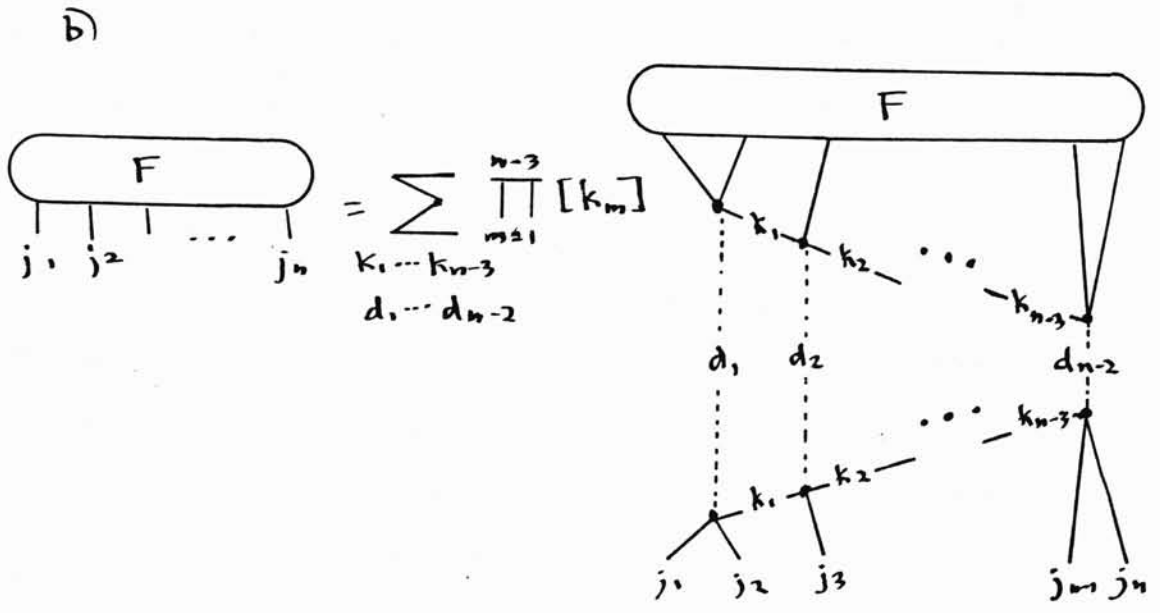
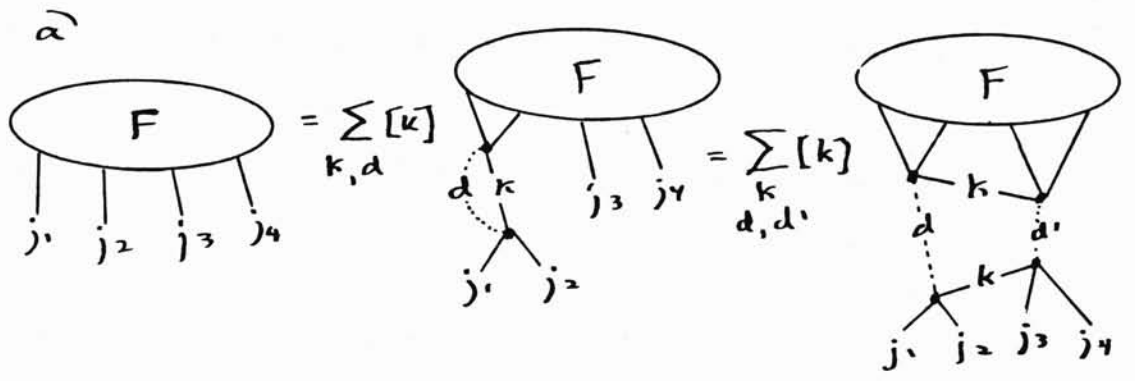
or \sum_a  = $\int dg$ 

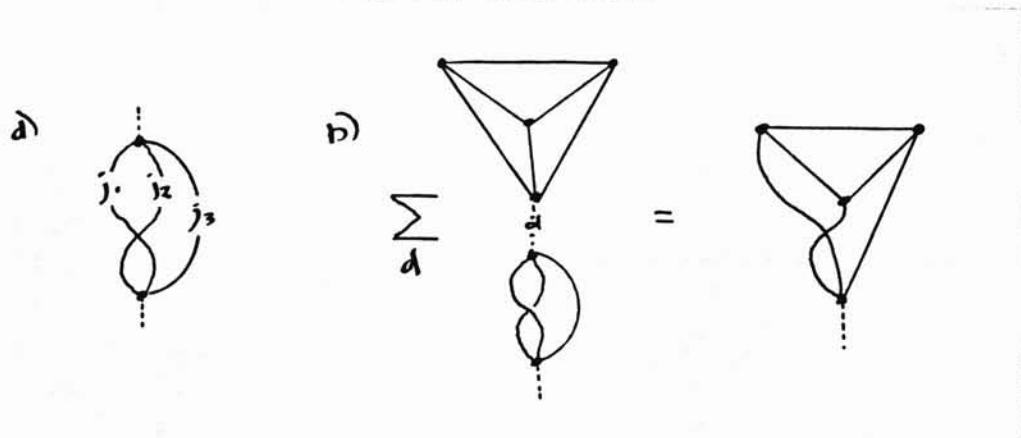
Figure 4.6 Coupling trees and recoupling coefficients



simplest recoupling amplitudes are the Racah coefficients, shown in figure 4.6c. If we identify k_1 and k_2 with the state spaces of ingoing particles in a scattering event, and k_3 and k_4 with outgoing particles, then the Racah coefficients here represent the "crossing symmetry" between s and t channels. With the help of this crossing identity, we show in the following section that any recoupling coefficients can be evaluated as a sum of products of Racah coefficients.

A recoupling graph of the group G is a labelled cubic graph representing a contraction of coupling tensors of G . Such a graph is more general than a recoupling coefficient, since not all cubic graphs split into two trees. Thanks to the dual isomorphisms mediated by the $1j$ -symbols, we may ignore the distinction between covariant and contravariant indices in these tensors. However, the coupling order at the vertices of the graph is significant in general. We may select a coupling basis adapted to the irreducible representations of the permutation group S_3 . In the case of $SU(2)$, only one-dimensional representations of S_3 occur (the identity and alternating ones), so alterations in the coupling order at a vertex will at most change the sign of the recoupling graph. In general, however, the two dimensional rep of S_3 may occur, resulting in more complicated phase factors [Derome 66].

Figure 4.7 Phase factors



These phase factors can be isolated as values of 2-vertex graphs such as shown in figure 4.7a. The Wigner-Eckart theorem determines the phase changes of the Racah coefficient as in 4.7b. In the following sections, the term "recoupling graph" will denote a labelled cubic graph

together with an ordering of the edges at each vertex. Phase factors in the decomposition theorem can be subsumed into the choice of ordering for the Racah coefficients.

4.2 Decomposition theorem

Decomposition Theorem: A recoupling graph F of a compact semisimple group G can always be evaluated as a sum of products of Racah coefficients of G .

proof: (network version)

We use induction on the number of vertices V in F , and the size n of the smallest cycle. A cycle is a sequence of edges e_1, e_2, \dots, e_n such that e_i and $e_{i+1} \pmod{n}$ are coupled in F .

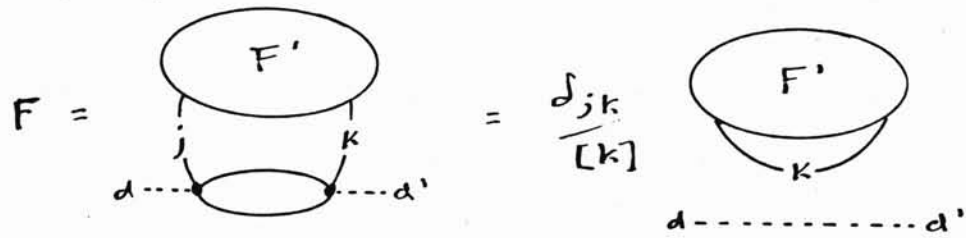
If $V = 2$, F is a phase factor, as in figure 4.7. If $V = 4$, F is a single Racah coefficient (or else two phases). If V is greater than 4, we have the cases shown in figure 4.8:

- a. $n=2$: A 2-cycle is eliminated by the Schur identity (fig. 4.5b), resulting in a graph F' with $V-2$ vertices.
- b. $n=3$: A 3-cycle collapses into a single coupling tensor (by the Wigner-Eckart theorem 4.5d), giving a product of a Racah coefficient and a graph F' with $V-2$ vertices, summed over a common "internal" degeneracy index d .
- c. $n>3$: A cycle with n edges labelled $j_1, j_2, \dots, j_{n-1}, j_n$ reduces to a cycle with $n-1$ edges by the crossing identity (fig. 4.6c). The result is a Racah coefficient multiplied by a graph in which the edge j_n is removed, and a new edge x couples j_1 to j_{n-1} . The product is summed over the "internal" edge x and two internal degeneracy indices d_1 and d_2 . Such a rearrangement can be performed $n-3$ times to produce a graph containing a 3-cycle. Then case b applies to eliminate 2 vertices from this graph.

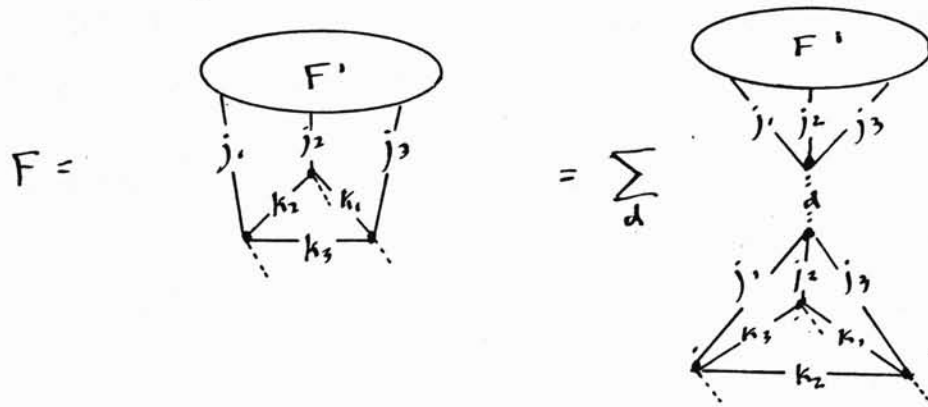
The process of vertex reduction can be repeated until $V=4$. The result is a product of Racah coefficients, summed over all internal variables.

Figure 4.8 Decomposition theorem: network version

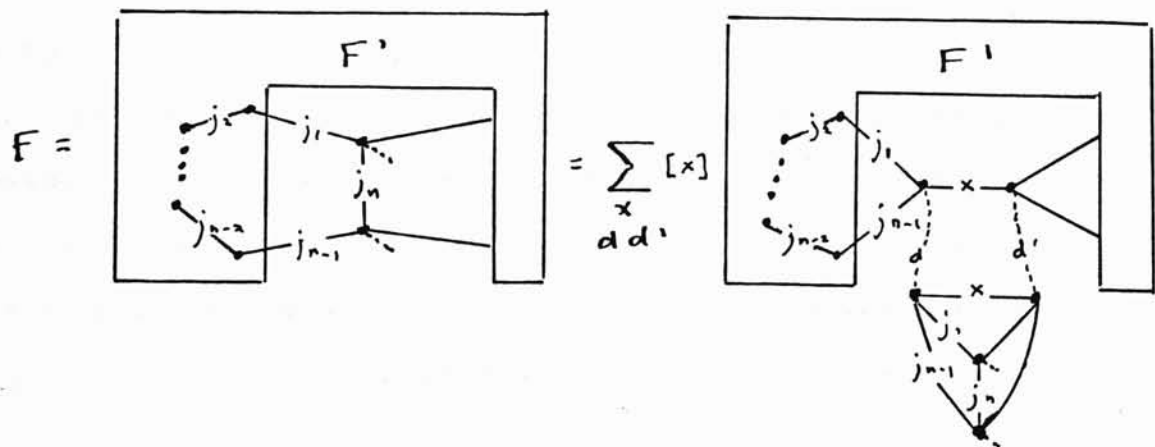
a) Schur



b) Excision



c) Crossing



proof of decomposition theorem: (vector version)

Suppose F is a planar graph, which we regard as being imbedded in the surface of a sphere. The vector diagram $D(F)$ is the graph-theoretic dual of F in this surface. Cubic vertices in F correspond to triangular faces in $D(F)$. Hence $D(F)$ is a triangulation of the sphere, with faces labelled by degeneracy indices.

The decomposition theorem has simple geometric interpretation in this dual vector picture. A cycle is a sequence of edges such that successive pairs belong to the same triangle in $D(F)$. A local cycle is a cycle in which all the edges meet at a common vertex. Figure 4.9a shows that the Schur identity corresponds to the "healing up" of a local 2-cycle: two triangles that share two edges must be congruent on the third as well. Figure 4.9b shows that a local 3-cycle forms the outer three faces of a tetrahedron joined at its base to $D(F)$. The excision identity removes this tetrahedron to expose the internal coupling labelled d on the base triangle, a face of the smaller triangulation $D(F')$. Figure 4.9c illustrates how the crossing identity removes the edge labelled j_n from a local n -cycle by coupling j_{n-1} and j_1 with a new internal edge x .

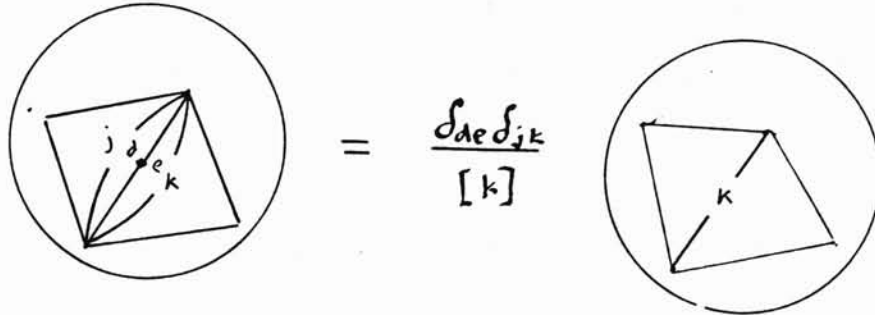
The effect of successive applications of figures 4.9b-c is to add sufficient internal edges to dissect the interior of $D(F)$ into tetrahedra. The result is a combinatorial 3-manifold $C(F)$ which has $D(F)$ as its boundary. We may sharpen the decomposition theorem for this special case as follows:

Decomposition Theorem: (vector version)

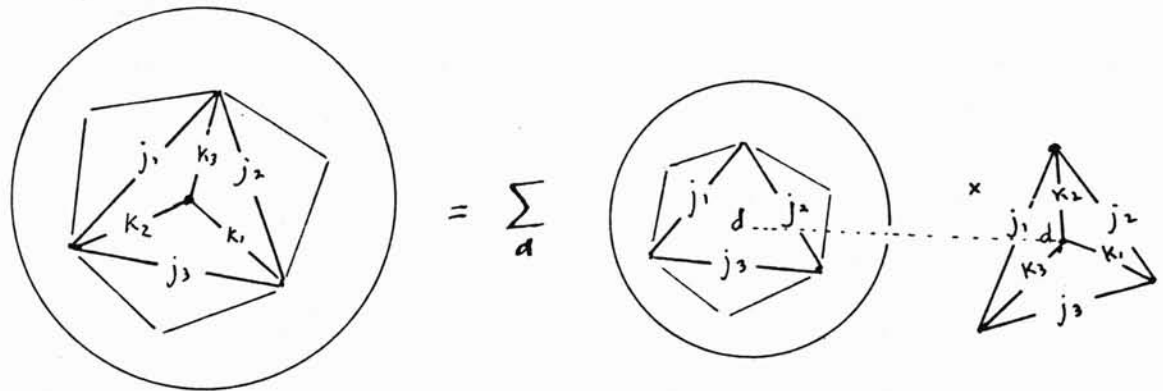
Let F be a planar recoupling graph, $D(F)$ its dual relative to a particular imbedding in the surface of a sphere, and $C(F)$ a combinatorial 3-manifold produced by dissecting $D(F)$ with internal edges labelled x_1, \dots, x_p into tetrahedra T_1, \dots, T_q which meet at internal faces labelled

Figure 4.9 Decomposition theorem: vector version

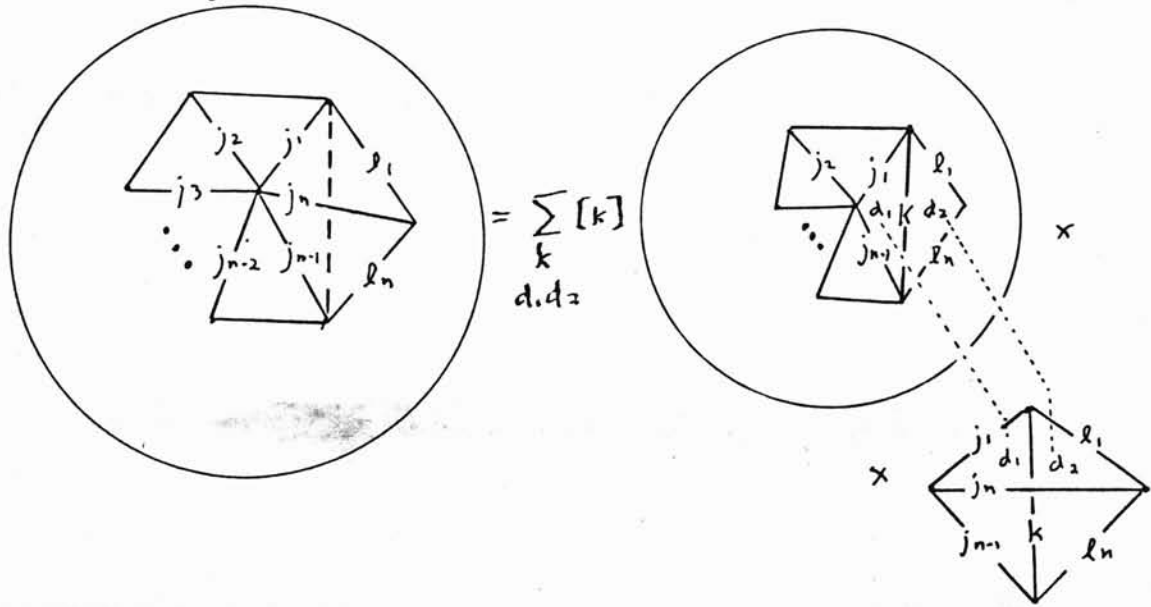
a) Schur



b) Excision



c) Crossing



d_1, \dots, d_r . Then the amplitude $\Psi(F)$ is given by

$$\Psi(F) = \sum_{x_1} \dots \sum_{x_p} \sum_{d_1} \dots \sum_{d_r} \Pi(x_1, \dots, x_p; d_1, \dots, d_r), \quad (4.2.1)$$

where

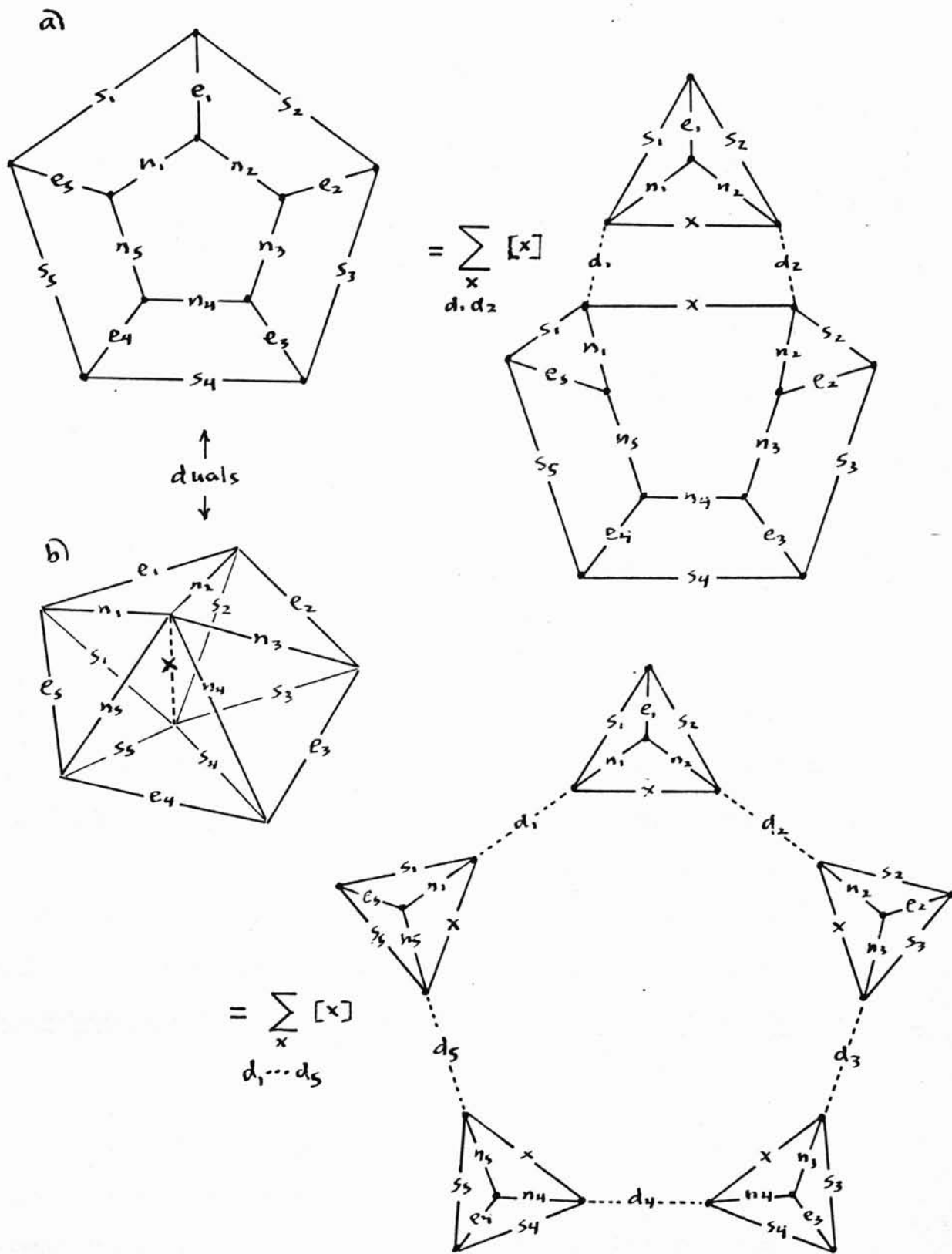
$$\Pi(x_1, \dots, x_p; d_1, \dots, d_r) \equiv \prod_{j=1}^p [x_j] \prod_{k=1}^q R[T_k] \quad (4.2.2)$$

and $R[T_k]$ are the Racah coefficients associated with the tetrahedra T_k .

As an example of the application of the decomposition theorem, we consider the "3nj-coefficients of the first kind". These are recoupling graphs in the form of two n -cycles with corresponding vertices connected by n edges. For example, figure 4.10a is such a graph for $n=5$. On the right, the crossing identity is applied to the edge e_1 . The 3-cycle $s_2 e_2 n_2$ can be removed to produce another 3-cycle $s_3 e_3 n_3$ and so on, until the graph is decomposed into the 5 Racah coefficients shown on the right of figure 4.10b. The left of 4.10b is the dual vector diagram, which triangulates the sphere into 5 "northern hemisphere" triangles and 5 southern ones. The addition of a single internal edge x across the poles dissects the interior of the diagram into 5 tetrahedra hinging at x , which correspond 1-1 to the 5 Racah coefficients on the right. These diagrams are basic in Regge-Ponzano theory, since they describe n cells hinging at an internal bone x , at which the curvature of a simplicial manifold is concentrated (viz. figure 3.3).

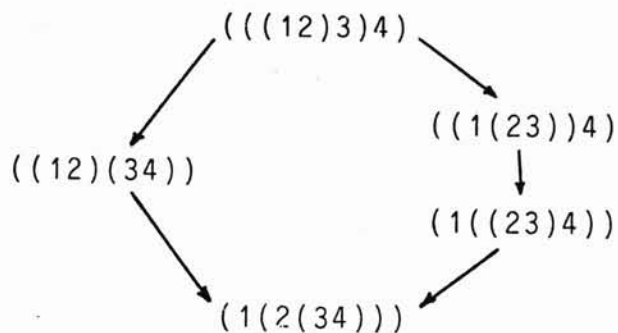
The decomposition process is highly non-unique. For example, a 3nj-coefficient of the first kind with $n=3$ can be decomposed as in figure 4.10 into 3 tetrahedra hinging around a single internal edge x . On the other hand, the three triangles in each hemisphere can be decomposed by the excision identity into two tetrahedra meeting at their common "equatorial"

Figure 4.10 Example: $3nj$ -coefficients of the first kind



face. The equivalence of these two decompositions is the (generalized) Biedenharn-Elliott identity.

As noted in figure 3.2, the B-E graph is the recoupling coefficient between two coupling schemes of the form $((((12)3)4)$ and $(1(2(34)))$. The transition between these coupling trees can be made through intermediate schemes in two different ways as follows:



Here each intermediate step recouples only three states, and therefore involves a single Racah coefficient. The two steps on the left correspond to the left side of the B-E identity in figure 3.2d-e; the three on the right, to the right side. In general, two coupling trees that differ by rearrangement of only three edges are c-equivalent: the crossing identity recouples them with a single Racah coefficient. Thus we have yet another proof of the decomposition theorem for the special case of recoupling coefficients, based on the purely combinatorial fact that the transitive closure of this c-equivalence relation covers the entire set of cubic trees on n objects.

4.3 Fabrics

A fabric F is a triple (C,D,E) , where E is a set of edge labels, D is a set of degeneracy or coupling labels, and C is a well-formed set of couplings. By a coupling we mean a pair $(d,(j,k,l))$ consisting of a coupling label d and a triplet of distinct edge labels. A set of couplings is well-formed if the coupling labels are all distinct, and no edge label occurs more than twice.

A fabric is closed if each edge label in C occurs exactly twice; otherwise it is open. A closed fabric can be depicted as a closed graph with edges and cubic vertices labelled by members of E and D respectively. An open fabric has free ends indicated by the edge labels that occur only once.

We regard the coupling labels D and edge labels E as variables in two measure spaces M and N respectively. With any closed fabric F we associate the measure space $M(F)$ which is the cartesian product of the copies of M and N associated with the distinct coupling and edge labels in F . An amplitude for F is a complex-valued integrable function on $M(F)$. The amplitude of a fabric containing just two couplings is called a phase factor. The amplitude of a fabric containing four couplings with distinct edge triplets (i.e., forming a tetrahedron) is called a Racah kernel.

A fabric valuation (M, N, Ψ) is a choice of measure spaces, along with an assignment of an amplitude $\Psi(F)$ to each closed fabric, satisfying the axioms shown in figure 4.11. The δ -functions in 4.11a are defined by the property

$$\int d\mu(x) \delta(x, y) f(x) = f(y) \quad (4.3.1)$$

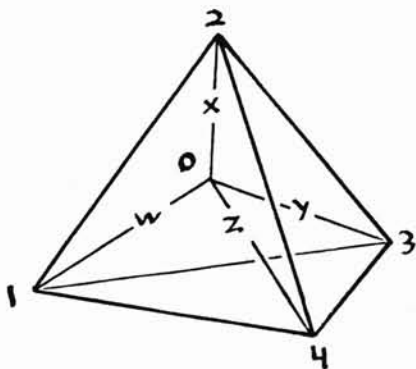
Couplings that have the same coupling label are assumed to be identical: if the ordering of the edge triplets differ, phase factors must be introduced as in figure 4.4.

These axioms are sufficient to prove the decomposition theorem for fabrics, by the arguments of the previous section. Strictly speaking, the axioms are not independent. For example, the excision axiom is an easy consequence of the crossing and Schur axioms, applied to the reduction of the 3-cycle. On the other hand, if we restrict the theory to fabrics which cannot be disconnected at just two edges, we can eliminate the Schur axiom, and avoid some of the complications entailed in δ -functions and the theory of distributions.

We introduce some definitions to clarify the fabric decomposition theorem. A term is a product of Racah kernels. Suppose we designate some subset of coupling variables $\text{Int}(D)$ as internal coupling variables. Internal edge variables are those that occur exclusively in internal couplings. These internal variables will be the ones summed over in the crossing and excision identities. Variables that are not internal are called external. A well-formed term or weft is a term in which all external variables occur in a single Racah kernel, and internal coupling variables occur in identical couplings in exactly two Racah kernels. The boundary $B(w)$ of a weft w is the closed fabric determined by the external couplings of w . We say that a fabric F encloses a weft w , if w can be obtained from F by crossing and Schur deletion. Thus

Fabric Decomposition Theorem: If a fabric F encloses a weft w , then $\Psi(F)$ is the integral of w over all its internal variables.

Figure 4.12 A divergent weft



If a fabric encloses a weft w , then $F = B(w)$. The converse is not true, however. For example, consider the weft made up of the four Racah kernels corresponding to the four tetrahedra which meet at point 0 in the vector diagram of figure 4.12. Here the triangles which meet at 0 are all internal couplings, so the edges w, x, y, z are internal edges. The boundary of the weft is the outer tetrahedron (1234). However, Regge and Ponzano showed in the simple case of an $SU(2)$ fabric, that the integral of this weft over its internal variables diverges.

The source of this divergence is that the sum over w,x,y,z overcounts the possible internal geometries enclosed by the tetrahedron, because of "gauge" freedom in the location of the internal vertex 0. Such internal vertices never arise from the crossing identity, since the new edges introduced by crossing always link external vertices. Regge and Ponzano have shown, however, how to renormalize wefts with internal vertices. They introduce a cutoff r on the magnitude of internal spin variables, then divide the cutoff integral by $\frac{4}{3}\pi r^3$ to compensate for recounting at each internal vertex. The resulting ratio correctly approaches the amplitude of the enclosing fabric as r goes to infinity.

Fabrics derived from recoupling theory of compact groups resemble spin networks in that the edge variable space is discrete. Coupling variables are a new feature that must be introduced to handle multiplicities in the reduction of tensor products, but these too are discrete. Hence the integrals in the decomposition theorem for compact fabrics are simple sums. The usual procedure for making explicit calculations with these fabrics is to label representations with Young patterns which describe maximally symmetrized products of the basic representation. Then contractions of coupling tensors can be computed by purely combinatorial methods, based on the representation theory of the permutation groups.

Fabrics derived from non-compact groups have more complicated label spaces. For example, we shall see in the next chapter that fabrics for the massive representations of the Poincare group have edges labelled by a pair (m,j) , where the spin j is still discrete, but the mass m has continuous spectrum. Each coupling variable in this fabric is a pair of discrete relative helicities.

The problem of classifying all fabric valuations reduces to the classification of all possible Racah coefficients that satisfy the identities arising from the non-uniqueness of decomposition. The simplest of these, the Biedenharn-Elliott identity, guarantees the equivalence of two wefts that differ by one internal edge linking the apices of two tetrahedra that share a common base (in the vector picture). We conjecture that the transitive closure of this equivalence relation

covers the entire set of wefts enclosed by a fabric. In that case, the classification problem would reduce to finding all Racah kernels which solve the B-E equation in the context of a particular choice of label spaces.

Finally, we make some remarks about the classical limit of a fabric F associated with a Lie group G . By the argument that led to figure 2.9d, the invariance of each coupling in F corresponds to a conservation law in the n -dimensional vector space of generators of G (i.e., the Lie algebra). In the classical limit, we expect that the invariants we can construct as polynomials in the generators associated with different edges in F (modulo the ideals generated by commutators) have small uncertainties, and their algebra approaches an ordinary ("c-number") tensor algebra. The edge-labels themselves can be thought of as eigenvalues of k independent Casimir invariants; and the coupling labels, as eigenvalues of m independent "two-particle invariants", which are polynomials of generators in two coupled spaces. In a fabric with V vertices and L edges, these labels impose $mV + kL$ non-linear constraints on the nL vector components. If F is connected, there are $n(V-1)$ independent conservation conditions, so the nL components are algebraically determined, up to an overall n -parameter transformation of the group, just when

$$mV + kL + n(V-1) = nL - n \quad (4.3.2)$$

or

$$n = 3k + 2m, \quad (4.3.3)$$

since $3V = 2L$. In fact, the physically interesting fabrics are algebraically determined in this sense: the rotation group has $n=3$, $k=1$, $m=0$; the Lorentz group has $n=6$, $k=2$, $m=0$; the Poincare group, as we shall see, has $n=10$, $k=2$, $m=2$. Since the conformal group has $n=15$, $k=3$, we expect $m=3$ for this case.

In order to understand these invariants geometrically, it is useful to regard the vector spaces themselves as possessing tensor structure. For example, the generators of the Lie

algebras $so(n)$, $su(n)$, $sp(n)$ transform under the adjoint representation as second rank tensors which are self-adjoint with respect to orthogonal, unitary, and symplectic forms respectively. The Casimir and degeneracy invariants for these groups arise from contracting together these second rank tensor operators, with the help of the corresponding invariant forms and Levi-Civita tensors (spin appears to form a vector in $so(3)$ only because there is a third rank Levi-Civita tensor to dualize the antisymmetric second rank spin tensor). Inhomogeneous Lie groups (e.g. the Poincare group = $ISO(3,1)$) have generators which decompose into a vector operator (e.g. 4-momentum) and a second rank tensor operator (e.g. the spin 6-bivector), resulting in yet more intricate invariant structures.

As in Regge-Ponzano theory, we expect the Racah kernel to be an oscillating function of its edge and coupling variables in a semiclassical limit. The amplitude of a fabric enclosing a weft w can then be approximated by evaluating the integral of w by the method of steepest descents. As in the case of simplicial manifolds, the non-linearity of the edge and coupling invariants is reflected in a multiplicity of stationary phase terms. The fabric decomposition theorem is a natural tool for handling the ambiguities in conformation of a fabric in the classical limit. Moreover, the relation to path integrals suggests a route for incorporating dynamics in geometric models of this type.

5. FABRICS OF THE POINCARÉ GROUP

In this chapter, we show how to construct and evaluate fabrics for the recoupling theory of the Poincaré group, restricted to unitary representations of massive particles with positive energy. The customary mathematical setting for Poincaré recoupling is the theory of induced representations [Klink 71, 75]. Here we give an equivalent self-contained treatment by elementary methods which have more transparent physical interpretation, and help to elucidate the structure of the classical limit.

In section 1, we review some well-known results about the states and operators of massive representations in the helicity basis. In section 2, we define a new two-particle invariant, the relative helicity λ_{ij} : the helicity of particle i in the rest frame of particle j . There are four conservation relations between the six relative helicities at each cubic vertex, and we identify the remaining two independent λ 's as the degeneracy index of the fabric. This identification facilitates a simplified derivation of Wick's formula ^[Wick 62] for the Racah coefficient of the Poincaré group, in a form that makes the tetrahedral symmetries and classical interpretation manifest. In section 3, we compute the semi-classical limit of this Racah coefficient in the oscillatory regime of large spins and helicities. In section 4, we use this limit to compute the pseudo-action in the interior of the fabric. We derive the stationary phase equations, and show that they correspond to vanishing space-time curvature.

5.1 Basic states and operators of the Poincaré group

The Poincaré group \mathcal{P} is the 10-parameter group of transformations preserving intervals $(\Delta s)^2 = \Delta x_\mu g^{\mu\nu} \Delta x_\nu$ in Minkowski space-time, where

$$x_\mu g^{\mu\nu} x_\nu = (x_0)^2 - (x_1)^2 - (x_2)^2 - (x_3)^2.$$

The general element $(a, L) \in \mathcal{P}$ is the semidirect product of a Lorentz transformation L and a translation a :

$$(a,L) : x^\mu \mapsto L^{\mu\nu} x_\nu + a^\mu. \quad (5.1.1)$$

The Lorentz transformations are generated by the relativistic angular momentum $J^{\mu\nu} = -J^{\nu\mu}$, a 6-component bivector; and the translations, by the relativistic momentum P^μ , a 4-component vector. In particular, the hermitian operator

$$G = \delta\epsilon_\nu P^\nu + \frac{1}{2} \delta\omega_{\mu\nu} J^{\mu\nu} \quad (5.1.2)$$

generates the infinitesimal Poincare transformation

$$x^\nu \mapsto x^\nu - \delta x^\nu,$$

where

$$\delta x^\nu = \delta\epsilon_\nu + \delta\omega^{\mu\nu} x_\mu. \quad (5.1.3)$$

Any 4-vector V^μ must transform as x^μ under Lorentz transformations generated by $G' = \frac{1}{2} \delta\omega_{\mu\nu} J^{\mu\nu}$:

$$\begin{aligned} V^\nu &\mapsto V^\nu + \delta\omega^{\mu\nu} V_\mu = (1 - iG') V^\nu (1 + iG') \\ &\approx V^\nu - \frac{1}{i} [V^\nu, G']. \end{aligned} \quad (5.1.4)$$

In particular for P^μ

$$\frac{1}{i} [P_\nu, J_{\kappa\lambda}] = g_{\nu\lambda} P_\kappa - g_{\nu\kappa} P_\lambda. \quad (5.1.5)$$

Similarly, $J_{\mu\nu}$ transforms as the antisymmetric product of two vectors:

$$\frac{1}{i} [J_{\mu\nu}, J_{\kappa\lambda}] = g_{\mu\kappa} J_{\nu\lambda} - g_{\mu\lambda} J_{\nu\kappa} + g_{\nu\lambda} J_{\mu\kappa} - g_{\nu\kappa} J_{\mu\lambda}. \quad (5.1.6)$$

Finally, the translations commute:

$$[P_\mu, P_\nu] = 0. \quad (5.1.7)$$

The mass-squared operator $M^2 = P^\mu P_\mu$ is clearly a Casimir invariant of \mathcal{P} (i.e. commutes with all J's and P's). The Pauli-Lubanski spin vector

$$W_\lambda \equiv \frac{1}{2} \epsilon_{\mu\nu\kappa\lambda} J^{\mu\nu} P^\kappa \quad (5.1.8)$$

commutes with P_μ by (5.1.5). Hence the scalar $W^2 = W_\lambda W^\lambda$ is a second Casimir invariant.

The unitary representations of \mathcal{P} can be classified according to the eigenvalues of M^2 and W^2 [Wigner 39]. Here we will restrict ourselves to the case $M^2 > 0$, corresponding to massive particles. In this case a momentum eigenstate in the rest frame has W^μ proportional to the spatial spin components

$$W^\mu = M(0, J_{23}, J_{31}, J_{12}) = M(0, \vec{J}) \quad (5.1.9)$$

so

$$W^2 = -M^2 J^2.$$

The [J,J] commutation relations (5.1.6) restricted to the spatial components are identical to the SU(2) relations (2.1.7), so the arguments of section 2.1 guarantee that J^2 has eigenvalues $j(j+1)$ with j half-integral.

The [J,P] commutation relation (5.1.5) requires that J transform under translation as an orbital angular momentum

$$L_{\mu\nu} \equiv X_\mu P_\nu - X_\nu P_\mu.$$

In fact, for $M^2 > 0$ we can decompose J explicitly:

$$J^{\mu\nu} = \frac{1}{M^2} (\epsilon^{\mu\nu\rho\sigma} P_\rho W_\sigma) + (Y^\mu P^\nu - Y^\nu P^\mu), \quad (5.1.10)$$

where

$$Y^\mu \equiv J^{\mu\rho} P_\rho / M^2,$$

the skew displacement of the particle trajectory from the origin of angular momentum measurements, transforms as x^μ in (5.1.1-3). This decomposition is an application of the simple combinatoric identity

$$\begin{array}{|c|} \hline \hline \hline \hline \hline \hline \\ \hline \end{array} = 3 \begin{array}{|c|} \hline \hline \hline \hline \hline \hline \\ \hline \end{array} + 2 \begin{array}{|c|} \hline \hline \hline \hline \hline \hline \\ \hline \end{array}$$

Note that

$$W_\mu P^\mu = 0 \text{ and } Y_\mu P^\mu = 0. \tag{5.1.11}$$

Thus (5.1.10) decomposes the 6 components of $J_{\mu\nu}$ into 3 components of skew displacement Y_μ and 3 components of intrinsic spin W_μ .

The sign of the energy $P_0/|P_0|$ is Lorentz-invariant for $M^2 > 0$, so there are two irreducible representations for each mass and spin. Here we will restrict ourselves to the positive-energy massive representations. The sum of two future timelike momenta is also future timelike: hence the tensor product of any two reps in this class will reduce to other reps in this class, and the recoupling theory is self-contained. In particular, we may construct fabrics which describe ensembles consisting only of positive-energy massive particles. The completeness of the corresponding representations under tensor product and reduction will preserve the fabric decomposition properties.

The representation theory of \mathcal{P} is simplified by labelling the basic states with the eigenvalues of a complete set of commuting observables having as much symmetry as possible. We form such a complete set by augmenting the Casimir observables M^2 and J^2 with four translation-invariant operators: the 3-momentum \vec{p} and helicity λ , which is the component of \vec{J} along \vec{P} :

$$\lambda \equiv \vec{J} \cdot \vec{P} / |\vec{P}|. \tag{5.1.12}$$

This particular component of the translation-invariant \vec{W} has the virtue of also being invariant under ~~rotations~~ and boosts along \vec{P} (unless the direction of \vec{P} is reversed, in which case $\lambda \rightarrow -\lambda$), as well as *arbitrary rotations*.

We label our basic states with the eigenvalues of these operators: $|mj, \vec{p}\lambda\rangle$ or more briefly $|p\lambda\rangle$, where p is a 4-vector with $p^2 = m^2$. Since the operators \vec{J} in (5.1.8) have the SU(2) commutation relations, j must be half-integral and λ must range from j to $-j$ in integer steps. The helicity λ in a frame Σ is just the z -component of \vec{J} in a rest frame Σ_0 having z -axis in the direction $-\vec{v}$, where \vec{v} is the relative velocity of Σ in Σ_0 . Using $\vec{p}^0 \equiv (m, 0, 0, 0)$ to denote the 4-momentum in frame Σ_0 , the rest-frame states $|\vec{p}^0\lambda\rangle$ transform under rotations as specified by (2.1.14).

$$R |\vec{p}^0\lambda\rangle = \sum_{\mu} \mathcal{D}_{\mu\lambda}^j(R) |\vec{p}^0\mu\rangle. \quad (5.1.13)$$

(For simplicity, we will use upper case Latin letters R, H, Z, L , etc. both for Lorentz transformations and for the operators which represent them.)

Following Wick [Wick 62], we define the general state

$$|p\lambda\rangle \equiv H(p) |\vec{p}^0\lambda\rangle \quad (5.1.14)$$

with

$$H(p) \equiv R_{\phi\theta_0} Z(p), \quad (5.1.15)$$

where Z is a pure boost in the z -direction

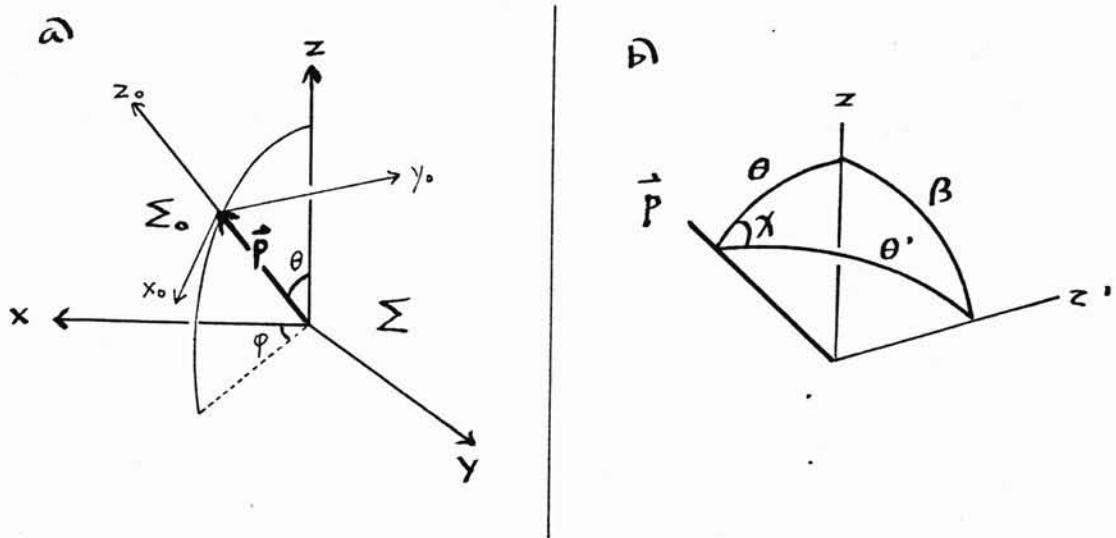
$$Z: \vec{p}^0 = (m, 0, 0, 0) \mapsto (E, 0, 0, |\vec{p}|)$$

and $R_{\phi\theta_0}$ is a rotation of z to the direction \vec{p} :

$$R: (E, 0, 0, |\vec{p}|) \mapsto (E, \vec{p}) = p. \quad (5.1.16)$$

This convention for $H(p)$ corresponds to fixing the ambiguity in possible rest frames Σ_0 (with z_0 -axis along the velocity $-\vec{v}$ of Σ_0 in Σ), by choosing the x_0 -axis so that the z -axis in Σ lies in the $x_0 z_0$ -plane (figure 5.1a).

Figure 5.1 Helicity reference frames



We now compute the transformation law of the states $|p\lambda\rangle$ under arbitrary Poincare transformation (a,L) . Note that

$$Lp = H(Lp) \overset{\circ}{p} = L H(p) \overset{\circ}{p}, \quad (5.1.17)$$

so

$$R \equiv H^{-1}(Lp) L H(p) \quad (5.1.18)$$

fixes $\overset{\circ}{p}$, and is a pure rotation in Σ_0 (a "Wigner rotation").

Hence

$$\begin{aligned} L |p\lambda\rangle &= L H(p) |\overset{\circ}{p}\lambda\rangle = H(Lp) R |\overset{\circ}{p}\lambda\rangle \\ &= H(Lp) \sum_{\mu} \mathcal{D}_{\mu\lambda}^j(R) |\overset{\circ}{p}\mu\rangle = \sum_{\mu} \mathcal{D}_{\mu\lambda}^j(R) |(Lp)\mu\rangle. \end{aligned} \quad (5.1.19)$$

Thus finally the unitary representation $U(a,L)$ of \mathcal{P} on these states is

$$U(a,L) |p\lambda\rangle = e^{ia'p} \sum_{\mu} \mathcal{D}_{\mu\lambda}^j(L,p) |(Lp)\mu\rangle \quad (5.1.20)$$

where

$$\mathcal{D}_{\mu\lambda}^j(L,p) \equiv \mathcal{D}_{\mu\lambda}^j(Lp,L) \equiv \mathcal{D}_{\mu\lambda}^j\{H^{-1}(Lp) L H(p)\}. \quad (5.1.21)$$

The first D-notation on the left describes a Wigner rotation matrix in terms of a Lorentz transformation and the momentum of the particle to which this transformation is applied. The second D-notation is useful for emphasizing the momentum after Lorentz transformation.

We give the Wigner rotation (5.1.21) for some special cases. If $L = R_{\alpha\beta\gamma}$, an ordinary rotation between two frames Σ and Σ' , the axes z_0 and z'_0 coincide, so we have the rotation around these axes

$$\mathcal{D}_{\mu\lambda}^j(R_{\alpha\beta\gamma},p) = \delta_{\mu\lambda} e^{i\lambda\chi}, \quad (5.1.22)$$

where χ is the internal dihedral angle between the pz -plane and the pz' -plane, as shown in figure 5.1b. Since this is a pure phase, we see that the helicity convention (5.1.15) amounts to a choice of phase for the basic states.

As a second example, let $L = Z$, a pure boost in the z -direction. Suppose that p is the zx -plane of Σ . Then p will also be in the $z'x'$ -plane of Σ' , but the azimuthal angles θ and θ' will differ by the angle β between the velocities of the Σ and Σ' systems, as seen from Σ_0 . Hence we have a rotation by β around the y_0 -axis:

$$\mathcal{D}_{\mu\lambda}^j(Z,p) = d_{\mu\lambda}^j(\beta). \quad (5.1.23)$$

Finally, we specify our normalization conventions for the states $|p\lambda\rangle$. We define

$$\tilde{\delta}(p) \equiv 2E \delta_3(\vec{p}), \quad (5.1.24)$$

the δ -function corresponding to the invariant volume element on the mass shell

$$\tilde{d}p \equiv d^3\vec{p} / 2E \approx \delta(p^2 - m^2) d^4p. \quad (5.1.25)$$

Then the convention

$$\langle p' \lambda' | p \lambda \rangle = \delta_{\lambda\lambda'} \tilde{\delta}(p - p') \quad (5.1.26)$$

is consistent with the unitarity of (5.1.20).

5.2 Relativistic addition of spin and momentum

We now compute the 3j-coefficient

$$\langle p_1 j_1 \lambda_1; p_2 j_2 \lambda_2 | p_3 j_3 \lambda_3; d \rangle = \delta_4(p_1 + p_2 - p_3) \langle 12 | 3 \rangle, \quad (5.2.1)$$

which reduces the tensor product of the two states $|p_1 \lambda_1\rangle |p_2 \lambda_2\rangle$ into a sum of irreducible states $|p_3 \lambda_3; d\rangle$ distinguished by degeneracy eigenvalues d . Thanks to the simple form of the transformation law (5.1.20), we can express d in terms of "relative helicities," and compute $\langle 12 | 3 \rangle$ explicitly as a product of ordinary SU(2) rotation matrix elements.

The simplest approach to this computation [Wick 62] is to begin in the "center of momentum" frame such that

$$\vec{p}_3 = (m_3, \vec{0}), \quad \vec{p}_1 = (E_1, q_{12} \hat{z}), \quad \vec{p}_2 = (E_2, -q_{12} \hat{z}), \quad (5.2.2)$$

where q_{12} is the "relative momentum" of p_1 and p_2 . Let $\lambda_{1,3}$ and $\lambda_{2,3}$ be the helicities of particles 1 and 2 respectively in the frame attached to p_3 (the "relative helicities"). We apply a Wigner projection (i.e. harmonic analysis on the rotation group manifold, viz. figure 4.3) to the tensor product $|\vec{p}_1 \lambda_{1,3}\rangle |\vec{p}_2 \lambda_{2,3}\rangle$ to get a new state that transforms under rotation as $|j_3 \lambda_3\rangle$:

$$|\vec{p}_3 j_3 \lambda_3; \lambda_{1,3} \lambda_{2,3}\rangle \equiv$$

$$N \int d\Omega \mathcal{D}_{\lambda\lambda_3}^{j_3^\dagger}(R) R \{ |p_1^0 \lambda_{1,3}\rangle |p_2^0 \lambda_{2,3}\rangle \}, \quad (5.2.3)$$

where $R = R_{\phi\theta_0}$ and the integral is over the 2-sphere

$$0 \leq \phi \leq 2\pi, \quad 0 \leq \theta \leq \pi; \quad d\Omega = \sin \theta d\theta d\phi. \quad (5.2.4)$$

The usual invariant measure on the SU(2) group manifold

$$dR_{\phi\theta\psi} \equiv d\phi \sin \theta d\theta d\psi \quad (5.2.5)$$

is abbreviated to $d\Omega$ because the definition

$$\lambda \equiv \lambda_{1,3} - \lambda_{2,3} = \lambda_{3,2} \quad (5.2.6)$$

guarantees that the integral over the second polar angle is trivial.

Now we go to a general frame by applying $H(p_3)$ of (5.1.15) to both sides of (5.2.3):

$$|p_3 j_3 \lambda_3; \lambda_{1,3} \lambda_{2,3}\rangle = N \int d\Omega \mathcal{D}_{\lambda\lambda_3}^{j_3^\dagger}(R) L \{ |p_1^0 \lambda_{1,3}\rangle |p_2^0 \lambda_{2,3}\rangle \}, \quad (5.2.7)$$

where $L \equiv H(p_3) R$ and

$$L^{-1} : p_3 \mapsto \tilde{p}_3; \quad \tilde{p}_1 \mapsto q_{12} \hat{z} \quad (5.2.8)$$

The 6 components of p_1 and p_2 completely determine the 4 components of p_3 and the 2 angles θ and ϕ , and hence also the Lorentz transformation L . A simple change of variables gives

$$\tilde{dp}_1 \tilde{dp}_2 = \frac{q_{12}}{4m_3} d^4 p_3 d\Omega, \quad (5.2.9)$$

so (5.2.7) can be rewritten, with the help of (5.1.20)

$$\begin{aligned}
 & N_{12,3} \int \tilde{d}p_1 \tilde{d}p_2 \delta_4(p_1 + p_2 - p_3) \mathcal{D}_{\lambda\lambda_3}^{j_3^\dagger}(R) \times \\
 & \times \sum_{\lambda_1\lambda_2} \mathcal{D}_{\lambda_1\lambda_{1,3}}^{j_1}(p_1, L) \mathcal{D}_{\lambda_2\lambda_{2,3}}^{j_2}(p_2, L) |p_1\lambda_1\rangle |p_2\lambda_2\rangle. \quad (5.2.10)
 \end{aligned}$$

It is straightforward to check that this state satisfies the normalization convention (5.1.26) if

$$N_{12,3} = [(2j_3 + 1) m_3 / \pi q_{12}]^{1/2}. \quad (5.2.11)$$

Note also

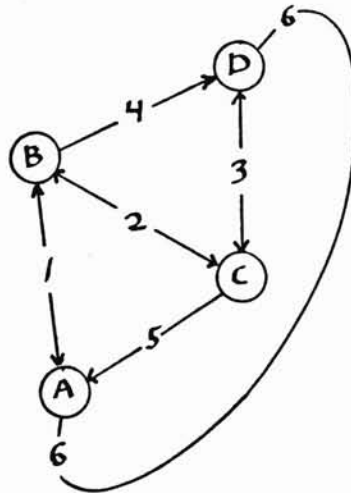
$$R = H^{-1}(p_3) \quad L = H^{-1}(L_p^0) \quad L H(p_3).$$

Thus finally we get the simple result [c.f. Wick 62, eg. (17)].

$$\begin{aligned}
 \langle p_1 j_1 \lambda_1; p_2 j_2 \lambda_2 \mid p_3 j_3 \lambda_3; \lambda_{1,3} \lambda_{2,3} \rangle &= N_{12,3} \delta_4(p_1 + p_2 - p_3) \times \\
 & \times \mathcal{D}_{\lambda_{3,2}\lambda_3}^{j_3^\dagger}(p_3, L) \mathcal{D}_{\lambda_1\lambda_{1,3}}^{j_1}(p_1, L) \mathcal{D}_{\lambda_2\lambda_{2,3}}^{j_2}(p_2, L). \quad (5.2.12)
 \end{aligned}$$

where the momenta determine L by (5.2.8).

Figure 5.2 Recoupling scheme for Racah coefficient



Now we consider two different schemes for coupling together three states, and use the 3j-symbol (5.6.12) to compute the corresponding Racah coefficient. To simplify the indices, suppose that states 1 and 2 couple to form state 4 (rather than state 12 as in figure 3.1); and states 2 and 3 couple to form 5. The composite state 6 of all three particles can be formed either from 4 and 3 or from 5 and 1 (see figure 5.2). The first coupling scheme ((1,2)4,3)6 for state 6 is given by two applications of (5.2.12) as follows {c.f (3.1.1) and (5.2.7)}:

$$\begin{aligned}
 |((1,2)4,3)6\rangle &\equiv |p_6 j_6 \lambda_6; m_4 j_4; \lambda_{4,6} \lambda_{3,6}; \lambda_{1,4} \lambda_{2,4}\rangle \equiv \\
 &N_{43,6} N_{12,4} \int \tilde{d}p_4 \tilde{d}p_3 \delta_4(p_3 + p_4 - p_6) \times \\
 &\times \mathcal{D}_{\lambda_{6,3} \lambda_6}^{j_6 \dagger}(p_6, L_D) \sum_{\lambda_4 \lambda_3} \mathcal{D}_{\lambda_4 \lambda_{4,6}}^{j_4}(p_4, L_D) \mathcal{D}_{\lambda_3 \lambda_{3,6}}^{j_3}(p_3, L_D) \times \\
 &\times \int \tilde{d}p_1 \tilde{d}p_2 \delta_4(p_1 + p_2 - p_4) \times \\
 &\times \mathcal{D}_{\lambda_{4,2} \lambda_4}^{j_4 \dagger}(p_4, L_B) \sum_{\lambda_1 \lambda_2} \mathcal{D}_{\lambda_1 \lambda_{1,4}}^{j_1}(p_1, L_B) \mathcal{D}_{\lambda_2 \lambda_{2,4}}^{j_2}(p_2, L_B) \times \\
 &\times |p_3 \lambda_3\rangle |p_2 \lambda_2\rangle |p_1 \lambda_1\rangle.
 \end{aligned} \tag{5.2.13}$$

Here

$$L_D^{-1}: p_6 \mapsto \overset{\circ}{p}_6; \tilde{p}_4 \mapsto q_{43} \hat{z}$$

and

$$L_B^{-1}: p_4 \mapsto \overset{\circ}{p}_4; \tilde{p}_1 \mapsto q_{12} \hat{z} \tag{5.2.14}$$

Similarly, the adjoint of the second coupling scheme for state 6 is:

$$\begin{aligned}
 \langle (1,(2,3)5)6 | \equiv & \langle p_6' j_6' \lambda_6'; m_5 j_5; \lambda_{1,6} \lambda_{5,6}; \lambda_{2,5} \lambda_{3,5} | \equiv \\
 & N_{15,6} N_{23,5} \int \tilde{d}p_1' \tilde{d}p_5 \delta_4(p_1' + p_5 - p_6') \times \\
 & \times \mathcal{D}_{\lambda_6', \lambda_{6,5}}^{j_6'}(p_6', L_A) \sum_{\lambda_1' \lambda_5} \mathcal{D}_{\lambda_{1,6} \lambda_1}^{j_1^\dagger}(p_1', L_A) \mathcal{D}_{\lambda_{5,6} \lambda_5}^{j_5^\dagger}(p_5, L_A) \times \\
 & \times \int \tilde{d}p_2' \tilde{d}p_3' \delta_4(p_2' + p_3' - p_5) \times \\
 & \times \mathcal{D}_{\lambda_5', \lambda_{5,3}}^{j_5'}(p_5, L_C) \sum_{\lambda_2' \lambda_3'} \mathcal{D}_{\lambda_{2,5} \lambda_2'}^{j_2^\dagger}(p_2', L_C) \mathcal{D}_{\lambda_{3,5} \lambda_3'}^{j_3^\dagger}(p_3', L_C) \times \\
 & \times \langle p_1' \lambda_1' | \langle p_2' \lambda_2' | \langle p_3' \lambda_3' | \quad (5.2.15)
 \end{aligned}$$

where

$$L_A^{-1}: p_6 \mapsto \overset{\circ}{p}_6; \vec{p}_1 \mapsto q_{15} \hat{z}$$

and

$$L_C^{-1}: p_5 \mapsto \overset{\circ}{p}_5; \vec{p}_2 \mapsto q_{23} \hat{z} \quad (5.2.16)$$

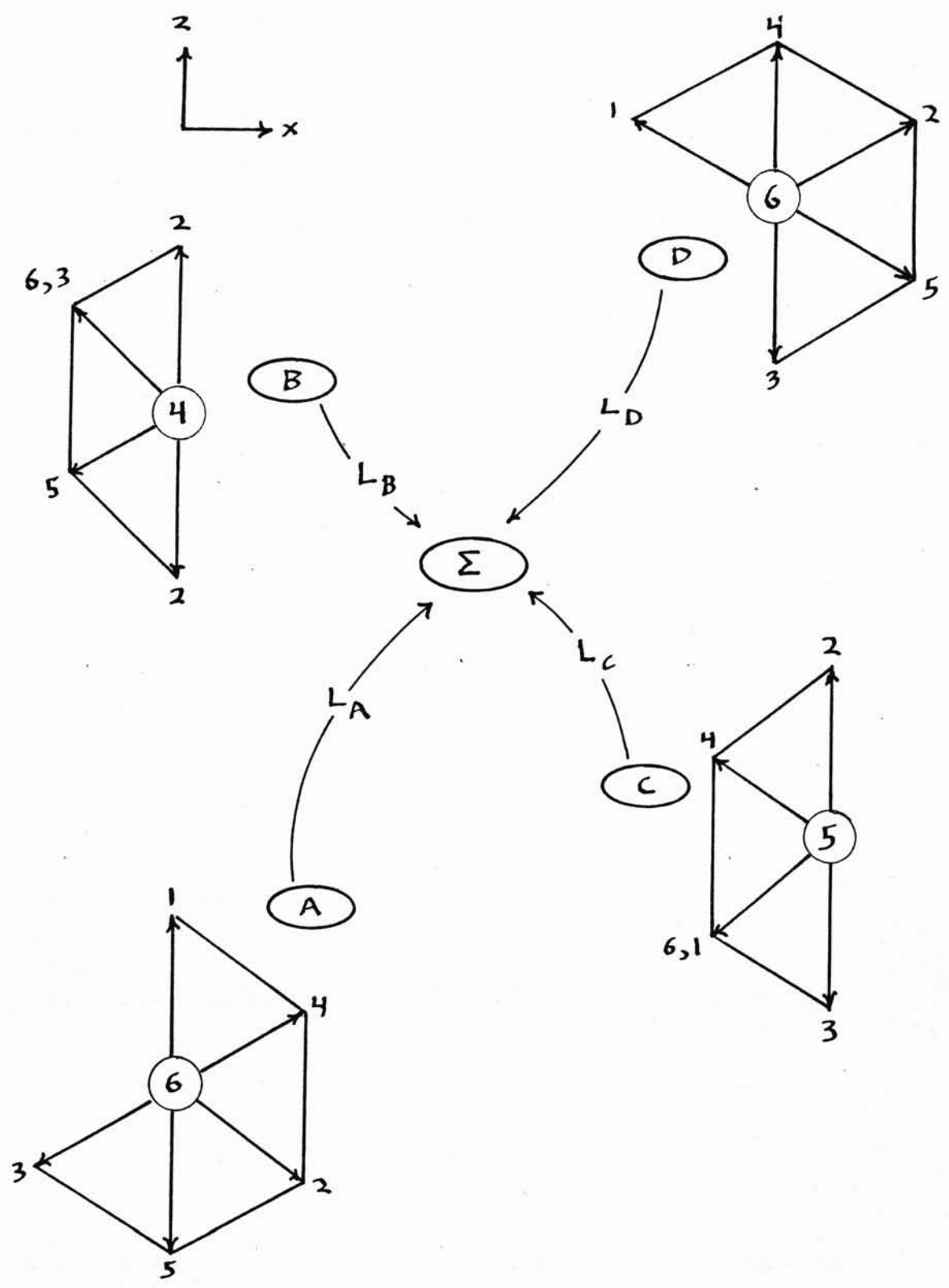
Figure 5.3 summarizes the frames which L_A through L_D transform into the observer's frame.

By Poincare invariance, the inner product of these two states must be of the form

$$\delta_4(p_6 - p_6') \delta_{j_6 j_6'} \delta_{\lambda_6 \lambda_6'} \langle 1(23) | (12)3 \rangle \quad (5.2.17)$$

where the abbreviated recoupling coefficient on the right is a function of the invariants m_i , j_i , and $\lambda_{i,j}$. In fact, we see that this product is a sum over eight helicities and an integral over

Figure 5.3 Coupling frames for the Racah coefficient



eight momenta - namely, of particles 1',2',3', and 1 through 5. However, the normalization conditions

$$\langle p_i' \lambda_i' | p_i \lambda_i \rangle = \delta_{\lambda_i \lambda_i'} \tilde{\delta}(p_i - p_i') \quad (5.2.18)$$

for $i=1,2,3$ eliminate the three primed sums and integrals, and replace the primed variables with the corresponding unprimed ones.

The remaining five momentum integrals can be simplified by noting that (5.2.9) implies

$$\tilde{d}p_1 \tilde{d}p_2 \delta_4(p_1 + p_2 - p_4) \approx \frac{q_{12}}{4m_4} d\Omega_{12}$$

and

$$\tilde{d}p_3 \tilde{d}p_4 \delta_4(p_3 + p_4 - p_6) \approx \frac{q_{34}}{4m_6} d\Omega_{34} \quad (5.2.19)$$

and that (5.1.25) implies

$$\tilde{d}p_5 \delta_4(p_2 + p_3 - p_5) \approx \delta((p_2 + p_3)^2 - m_5^2). \quad (5.2.20)$$

Hence

$$\langle p_6' j_6' \lambda_6'; m_5 j_5; \lambda_{1,6} \lambda_{5,6}; \lambda_{2,5} \lambda_{3,5} | p_6 j_6 \lambda_6; m_4 j_4; \lambda_{4,6} \lambda_{3,6}; \lambda_{1,4} \lambda_{2,4} \rangle$$

$$= N_{15,6} N_{23,5} N_{43,6} N_{12,4} \frac{q_{12}}{4m_4} \frac{q_{34}}{4m_6} \delta_4(p_6 - p_6') \times$$

$$\times \int d\Omega_{12} d\Omega_{34} \delta((p_2 + p_3)^2 - m_5^2) \times$$

$$\times \mathcal{D}_{\lambda_6' \lambda_{6,5}}^{j_6'}(p_6, L_A) \mathcal{D}_{\lambda_{6,3} \lambda_6}^{j_6^\dagger}(p_6, L_D) \times$$

$$\times E_{AB}^1 E_{CB}^2 E_{CD}^3 E_{BD}^4 E_{AC}^5,$$

$$(5.2.21)$$

where

$$E_{AB}^1 \equiv \sum_{\lambda_1} \mathcal{D}_{\lambda_{1,6}\lambda_1}^{j_1 \dagger}(p_1, L_A) \mathcal{D}_{\lambda_1 \lambda_{1,4}}^{j_1}(p_1, L_B) \quad (5.2.22)$$

and the other edge functions are similar. We have

$$E_{AB}^1 = \mathcal{D}_{\lambda_{1,6}\lambda_{1,4}}^{j_1}(L_A^{-1} L_B, q_{12} \hat{z}) = d_{\lambda_{1,6}\lambda_{1,4}}^{j_1}(\beta_{1,64}), \quad (5.2.23)$$

since the boost from frame B to A produces a Wigner rotation of form (5.1.23), where $\beta_{1,64}$ is the angle between \vec{p}_6 and \vec{p}_4 in the frame attached to 1.

Note also that

$$\mathcal{D}_{\lambda_6' \lambda_{6,5}}^{j_6'}(p_6, L_A) = \sum_{\lambda} \mathcal{D}_{\lambda_6' \lambda}^{j_6'}(p_6, L_D) \mathcal{D}_{\lambda \lambda_{6,5}}^{j_6'}(L_D^{-1} L_A, \vec{p}_6). \quad (5.2.24)$$

and

$$d\Omega_{12} d\Omega_{34} = \sin \theta_{12} d\theta_{12} dR_{D6}, \quad (5.2.25)$$

where

$$R_{D6} \equiv H^{-1}(L_D p_6) L_D H(p_6). \quad (5.2.26)$$

The integration over the invariant measure dR_{D6} (viz. 5.2.5) is given by the orthonormality relation (figure 4.3)

$$\int dR \mathcal{D}_{\lambda_6 \lambda_{6,3}}^{j_6 \dagger}(R) \mathcal{D}_{\lambda_6' \lambda}^{j_6'}(R) = \delta_{j_6 j_6'} \delta_{\lambda_6 \lambda_6'} \delta_{\lambda_{6,3} \lambda} \frac{8\pi^2}{2j_6 + 1} \quad (5.2.27)$$

The final integration is

$$\int_0^\pi \sin \theta_{12} d\theta_{12} \delta((p_2 + p_3)^2 - m_5^2) = \frac{m_4}{2m_6 q_{12} q_{34}}. \quad (5.2.28)$$

Putting all this together, we have verified (5.2.17) and have computed the recoupling coefficient (c.f figure 1.6):

$$\langle 1(23) | (12)3 \rangle = \frac{1}{4m_6} \left[\frac{m_4 m_5}{q_{15} q_{23} q_{43} q_{12}} \right]^{\frac{1}{2}} [(2j_4 + 1) (2j_5 + 1)]^{\frac{1}{2}} \times$$

$$\times e_{64}^1 e_{54}^2 e_{56}^3 e_{26}^4 e_{63}^5 e_{35}^6, \quad (5.2.29)$$

where

$$e_{\ell m}^k \equiv d_{\lambda_{k,\ell} \lambda_{k,m}}^{j_k}(\beta_{k,\ell m}). \quad (5.2.30)$$

It is straightforward to check that this formula is equivalent to Wick's [Wick 62] equation (35).

Symmetries and

5.3 Semiclassical limit of Racah coefficient

We identify the symmetrical part of (5.2.29) - namely, the product of the six d's - as the Racah kernel of the Poincare group. The semiclassical limit of this kernel can therefore be deduced from an asymptotic formula for the d-function derived by Regge and Ponzano. In order to understand the symmetries and geometric significance of the Racah coefficient, we first analyze the relative helicities and angles $\beta_{j,k\ell}$ in more detail.

In manifestly invariant form, the relative helicity of particle k in the frame attached to particle ℓ is

$$\lambda_{k,\ell} \equiv \frac{(W_k \cdot P_\ell)}{|P_k \wedge P_\ell|}. \quad (5.3.1)$$

Here the exterior product $P_k \wedge P_\ell$ has magnitude

$$|P_k \wedge P_\ell| = |(P_k \cdot P_\ell)^2 - M_k^2 M_\ell^2|^{\frac{1}{2}}, \quad (5.3.2)$$

a special case of the elementary formula

$$((P_k \wedge P_\ell) \cdot [P_k \wedge P_m]) = M_k^2 (P_\ell \cdot P_m) - (P_k \cdot P_\ell) (P_k \cdot P_m). \quad (5.3.3)$$

The scalar products in (5.3.2-3) are all determined by the masses, as noted in (1.1.1). We also have

$$\cos \beta_{k,\ell m} \equiv - \frac{([\mathbf{P}_k \wedge \mathbf{P}_\ell] \cdot [\mathbf{P}_k \wedge \mathbf{P}_m])}{|\mathbf{P}_k \wedge \mathbf{P}_\ell| |\mathbf{P}_k \wedge \mathbf{P}_m|} \quad (5.3.4)$$

It is easy to check that

$$\lambda_{k,\ell} = (\hat{\mathbf{J}}_k \cdot \hat{\mathbf{P}}_k) / |\hat{\mathbf{P}}_k| \quad (5.3.5)$$

in the frame where $\mathbf{P}_\ell = (M_\ell, 0)$ and that

$$\cos \beta_{k,\ell m} = (\hat{\mathbf{P}}_\ell \cdot \hat{\mathbf{P}}_m) / |\hat{\mathbf{P}}_\ell| |\hat{\mathbf{P}}_m| \quad (5.3.6)$$

and

$$\lambda_{k,\ell} = -(\hat{\mathbf{J}}_k \cdot \hat{\mathbf{P}}_\ell) / |\hat{\mathbf{P}}_\ell| \quad (5.3.7)$$

in the frame where $\mathbf{P}_k = (M_k, 0)$.

Suppose now that we have three particles coupled by the conservation conditions:

$$\mathbf{J}_1 + \mathbf{J}_2 + \mathbf{J}_3 = 0$$

$$\mathbf{P}_1 + \mathbf{P}_2 + \mathbf{P}_3 = 0. \quad (5.3.8)$$

Then

$$|\mathbf{P}_1 \wedge \mathbf{P}_2| = |\mathbf{P}_2 \wedge \mathbf{P}_3| = |\mathbf{P}_3 \wedge \mathbf{P}_1| = q_{12} M_3 = q_{23} M_1 = q_{31} M_2 \quad (5.3.9)$$

is twice the area of the triangle defined by the momenta. Moreover, the six distinct relative helicities between these particles satisfy four identities:

$$\lambda_{1,2} + \lambda_{1,3} = 0$$

$$\lambda_{2,3} + \lambda_{2,1} = 0$$

$$\lambda_{3,1} + \lambda_{3,2} = 0$$

$$\lambda_{1,2} + \lambda_{2,3} + \lambda_{3,1} = 0. \quad (5.3.10)$$

Hence there are only two independent relative helicities associated with each coupling triplet.

In particular, the four couplings of the Racah coefficient have eight independent helicities, as indicate on the left side of (5.2.21). The remaining four helicities in (5.2.29) are

$$\lambda_{4,2} = \lambda_{1,4} - \lambda_{2,4}$$

$$\lambda_{5,3} = \lambda_{2,5} - \lambda_{3,5}$$

$$\lambda_{6,5} = \lambda_{1,6} - \lambda_{5,6}$$

$$\lambda_{6,3} = \lambda_{4,6} - \lambda_{3,6} \quad (5.3.11)$$

Note here that $\lambda_{k,\ell}$ for $k,\ell = 4,5,6$ have signs opposite to those in (5.3.10), because the couplings in figure 5.2 specify these particles to be conserved in conditions like (5.3.8) with reversed signs.

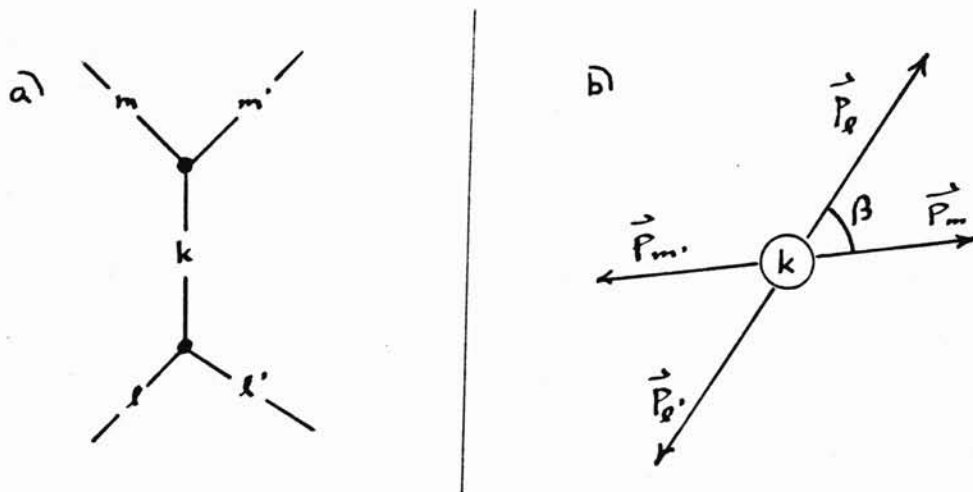
Figure 5.4a shows an edge k and its two couplings $(k\ell\ell')$ and (kmm') . Figure 5.4b is a picture of the corresponding momentum 3-vectors in the rest frame of k . We have

$$\beta_{k,\ell m} = \pi - \beta_{k,\ell' m} = \beta_{k,\ell' m'} = \pi - \beta_{k,\ell m'}. \quad (5.3.12)$$

The well known symmetries

$$\begin{aligned} d_{\lambda\lambda'}^j(\beta) &= (-1)^{j-\lambda'} d_{-\lambda\lambda'}^j(\pi-\beta) = (-1)^{\lambda-\lambda'} d_{-\lambda-\lambda'}^j(\beta) \\ &= (-1)^{j+\lambda} d_{\lambda-\lambda'}^j(\pi-\beta) = (-1)^{\lambda-\lambda'} d_{\lambda'\lambda}^j(\beta) \end{aligned} \quad (5.3.13)$$

Figure 5.4 Scattering diagram for particle k



therefore imply the identities

$$\begin{aligned}
 e_{\ell m}^k &= (-1)^{j_k - \lambda_{k,m}} e_{\ell' m}^k = (-1)^{\lambda_{k,\ell} - \lambda_{k,m}} e_{\ell' m'}^k \\
 &= (-1)^{j_k - \lambda_{k,\ell}} e_{\ell m'}^k = (-1)^{\lambda_{k,\ell} - \lambda_{k,m}} e_{m \ell'}^k.
 \end{aligned}
 \tag{5.3.14}$$

Thus the asymmetries in the edge labels of (5.2.29) are only apparent: any other labelling consistent with the recoupling scheme in figure 5.2 results in a Racah coefficient which differs at most by sign.

In the limit of large j, λ, λ' , it is well known [c.f Edmonds 57, (A.2.2)] that the d -function asymptotically approaches the $SU(2)$ Racah coefficient

$$\begin{aligned}
 d_{\lambda \lambda'}^j(\beta) &\approx (-1)^{a+b+c+j+\lambda} [(2a+1)(2b+1)]^{\frac{1}{2}} \times \\
 &\times \begin{Bmatrix} c & b & a \\ j & a+\lambda & b+\lambda' \end{Bmatrix}
 \end{aligned}
 \tag{5.3.15}$$

provided that a, b, c are all much bigger than j, λ, λ' , and

$$\cos \beta = \frac{a(a+1) + b(b+1) - c(c+1)}{2[a(a+1)b(b+1)]^{\frac{1}{2}}}; \quad 0 \leq \beta \leq \pi.
 \tag{5.3.16}$$

Figure 5.5 Asymptotic d-function

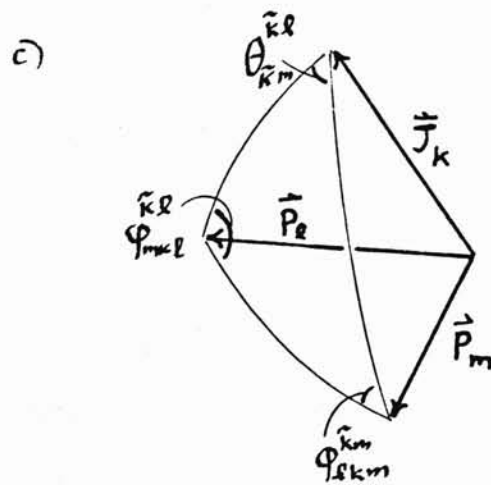
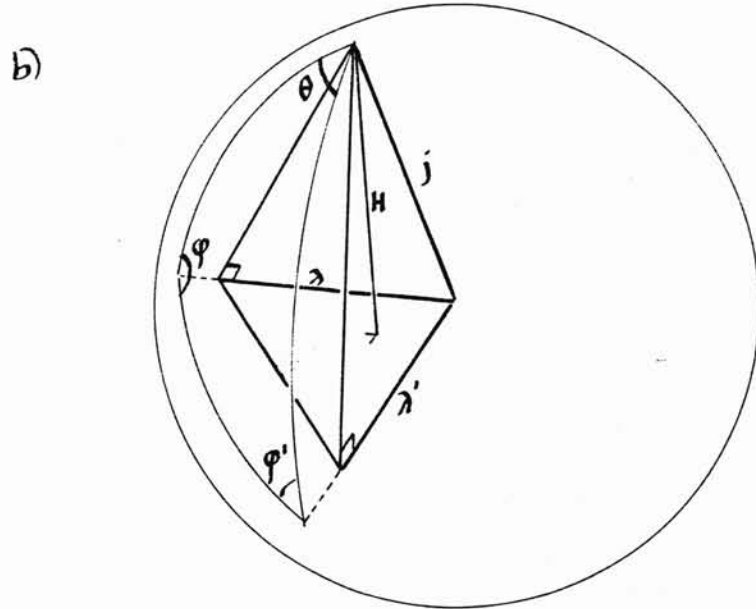
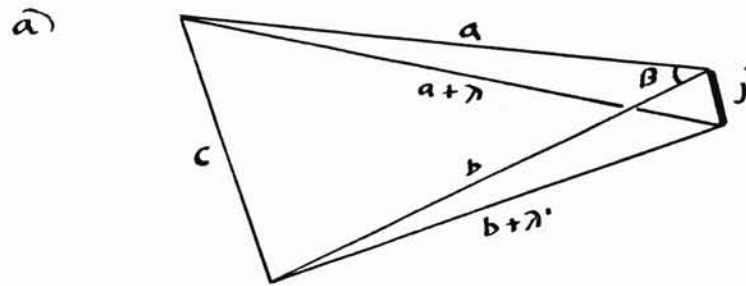


Figure 5.5.a gives a vector diagram for this Racah coefficient. The Regge-Ponzano formula (3.1.4) then implies

$$d_{\lambda\lambda'}^j(\beta) = \left[\frac{2}{\pi H \sin \beta} \right]^{1/2} (-1)^{j-\lambda'} \cos \left(\Phi - \frac{\pi}{4} \right). \quad (5.3.17)$$

with

$$H^2 = j^2 - (\lambda^2 + \lambda'^2 - 2\lambda\lambda' \cos \beta) / \sin^2 \beta \quad (5.3.18)$$

and

$$\Phi = j\theta + \lambda\phi + \lambda'\phi', \quad (5.3.19)$$

where θ, ϕ, ϕ' , are the dihedral angles shown in figure 5.5b. Regge and Ponzano also derive an equivalent formula more directly by a WKB approximation [Regge and Ponzano 68, Appendix G]. The oscillatory solution (5.3.17) is valid only in the classical regime $H^2 > 0$, corresponding to values of j, λ, λ' , and β consistent with the tetrahedron in figure 5.5b (H is the height of this tetrahedron, as shown). For $H^2 < 0$, we have exponential decay in the tunneling region.

Now we apply this approximation to the edge functions in (5.2.30):

$$e_{\ell m}^k \approx \left[\frac{2}{\pi H_{\ell m}^k \sin \theta_{k, \ell m}} \right]^{1/2} (-1)^{j_k - \lambda_{k,m}} \cos \left[\Phi_{\ell m}^k - \frac{\pi}{4} \right] \quad (5.2.20)$$

Here $H_{\ell m}^k$ is the magnitude of the components of \vec{J}_k normal to the plane of \vec{P}_ℓ and \vec{P}_m in the k -frame. Our main interest is the phase term

$$\Phi_{\ell m}^k \equiv j_k \tilde{\theta}_{km}^{k\ell} + \lambda_{k,\ell} \tilde{\phi}_{mk\ell}^{k\ell} + \lambda_{k,m} \tilde{\phi}_{\ell km}^{km}, \quad (5.3.21)$$

where the angles $\tilde{\theta}_{km}^{k\ell}$, $\tilde{\phi}_{mk\ell}^{k\ell}$, and $\tilde{\phi}_{\ell km}^{km}$ are illustrated in figure 5.5c.

For manifestly invariant definitions of these angles, we define the 4-vectors

$$\tilde{V}_{k\ell} \equiv *(W_k \wedge P_k \wedge P_\ell)$$

$$V_{km}^{\sim} \equiv *(W_k \wedge P_k \wedge P_m)$$

$$V_{mk\ell} \equiv *(P_m \wedge P_k \wedge P_\ell) \equiv -V_{\ell km}^{\sim} \tag{5.3.22}$$

Here the operator * indicates the dual to the volume spanned by the three vectors in the exterior product. All of these dual vectors are orthogonal to P_k and hence space-like. Let $u_{k\ell}^{\sim}, u_{km}^{\sim}, u_{mk\ell} = -u_{\ell km}^{\sim}$ be the corresponding "unit" 4-vectors having length -1. In the k -rest-frame, these are the unit normals to the three planes defined by $\vec{J}_k, \vec{P}_\ell,$ and \vec{P}_m in the figure 5.5c. Thus

$$\begin{aligned} \cos \theta_{km}^{\sim k\ell} &= - (u_{k\ell}^{\sim} \cdot u_{kq}^{\sim}) \\ \cos \phi_{mk\ell}^{\sim k\ell} &= - (u_{k\ell}^{\sim} \cdot u_{mk\ell}) \\ \cos \phi_{\ell km}^{\sim km} &= - (u_{km}^{\sim} \cdot u_{\ell km}) \end{aligned} \tag{5.3.23}$$

These scalar products expand into expressions involving $W^2, (W_i \cdot P_j),$ and $(P_i \cdot P_j),$ and are therefore completely determined by the spins, helicities, and masses.

5.4 Stationary phase conditions for Poincare fabrics

Now we consider the semiclassical limit of large Poincare fabrics. The amplitude of such a fabric is an integral of a well-formed product of Racah kernels. In analogy with Regge-Ponzano theory, we expect this integral to be dominated by "extremal geometries" -- that is, by geometries for which the total phase is stationary under variation of all internal variables.

As a prerequisite for computing the stationary phase conditions, we must determine the change in phase Φ of the semiclassical d-function (5.3.14) under variation of spin, helicities, and azimuthal angle. A tedious but straightforward calculation gives ⁶

⁶ There must be a simple derivation along the lines of (3.4.3-6), but I haven't been able to find it.

$$d\Phi = \theta dj + \phi d\lambda + \phi' d\lambda' + Hd\beta. \quad (5.4.1)$$

Here the first three terms indicate that variations in j , λ , and λ' occur as if the conjugate angles θ , ϕ and ϕ' were constants (c.f. (3.3.6)). The final term has a similar action-angle interpretation: H is the component of spin normal to the rotation plane of β . We note in passing that any function $f(\beta) = U \cos \Phi$, where

$$U = [H \sin \beta]^{-\frac{1}{2}}$$

and

$$\dot{\Phi} \equiv \frac{\partial \Phi}{\partial \beta} = H,$$

with H given by (5.3.18) satisfies the differential equation

$$\ddot{f} + \cot \beta \dot{f} + H^2 f = \frac{\ddot{U} + \dot{U} \cot \beta}{U} f.$$

Hence we have verified that in the WKB limit (of slowly changing U with small derivatives) the semiclassical formula (5.3.17) is an approximate solution of the standard differential equation (the J^2 -eigenvalue equation) for the d -function:

$$\left(\frac{d^2}{d\beta^2} + \cot \beta \frac{d}{d\beta} + H^2 \right) d_{\lambda\lambda'}^j(\beta) = 0.$$

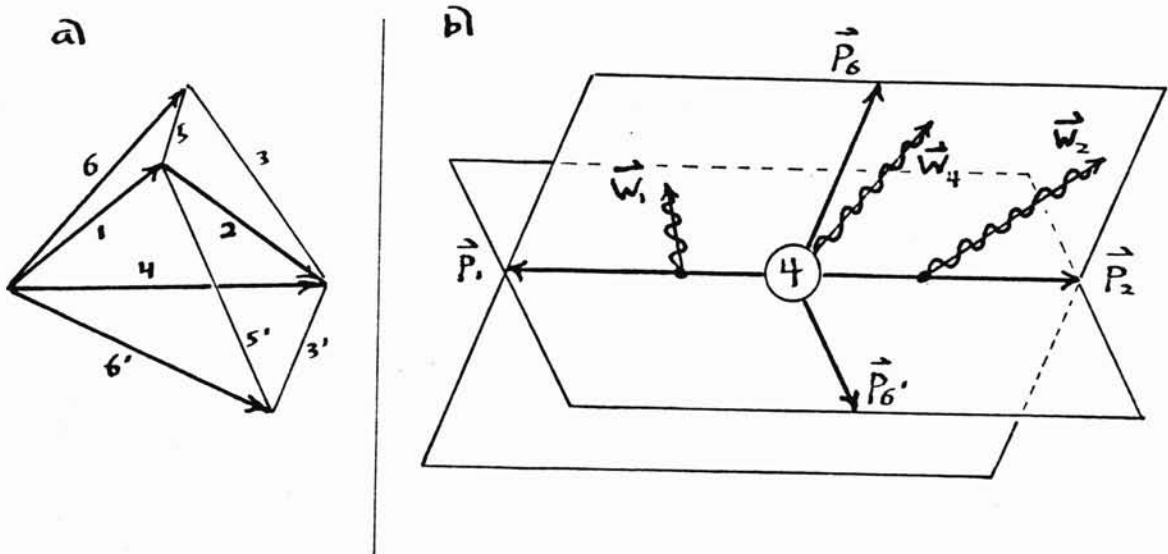
Applying this semiclassical formula (5.3.17) to the Poincare Racah coefficient (5.3.29), we have a sum of 2^6 phase terms of form

$$\pm \Phi_{64}^1 \pm \Phi_{54}^2 \pm \Phi_{56}^3 \pm \Phi_{26}^4 \pm \Phi_{63}^5 \pm \Phi_{35}^6. \quad (5.4.2)$$

As in the $SU(2)$ case, we may interpret this superposition as arising from ambiguity in the orientation of the spin-momenta triad (figure 5.5c) for each of the six particles. The integral over n Racah kernels will be a superposition of 2^{6n} distinct phase terms. As in Regge-Ponzano theory, we analyze the positive-frequency component Φ^+ . We find the conditions for

Φ^+ to be stationary under variation of the internal coupling variables $\lambda_{k,l}$ and the internal edge variables j_k and m_k .

Figure 5.6 Join of two Racah kernels



For the case of the coupling variables $\lambda_{k,l}$, we refer to figure 5.6a, which gives the vector diagram of two Racah kernels T and T' meeting at an internal coupling (124). The apices of the two tetrahedra are generated by adding two different (J,P)-vectors 3 and 3' to 4, giving 6 and 6' and 5 and 5' respectively, in the labelling convention of figures 5.2-3.

The two independent helicities of (124) are $\lambda_{1,4}$ and $\lambda_{2,4}$, which determine $\lambda_{4,2}$ by (5.3.11) The part of the total Φ^+ which depends on $\lambda_{1,4}$ is therefore

$$\Phi_{1,4}^+ \equiv \Phi_{64}^1 + \Phi_{6'4}^1 + \Phi_{26}^4 + \Phi_{26'}^4 \quad (5.4.3)$$

From (5.4.1), we compute

$$\frac{\partial \Phi_{1,4}^+}{\partial \lambda_{1,4}} = \tilde{\phi}_{614}^{14} + \tilde{\phi}_{6'14}^{14} + \tilde{\phi}_{642}^{42} + \tilde{\phi}_{6'42}^{42} = 0 \quad (5.4.4)$$

Similarly, under variation of $\lambda_{2,4}$

$$\frac{\partial \Phi_{2,4}^+}{\partial \lambda_{2,4}} = \tilde{\phi}_{524}^{24} + \tilde{\phi}_{5'24}^{24} - \tilde{\phi}_{642}^{42} - \tilde{\phi}_{6'42}^{42} = 0. \quad (5.4.5)$$

In order to interpret these two conditions, we investigate the imbedding of T in Minkowski space in the classical limit. Recall that the configuration of the three 4-momenta $P_1, P_2,$ and P_3 is completely determined by the masses m_1, m_2, m_3 and the composite masses $m_4, m_5,$ and m_6 -- up to an overall Lorentz transformation. Moreover, the components of W_k in the k-rest-frame are fixed by the length j_k and two projections $\lambda_{k,l}$ and $\lambda_{k,m}$, provided that the "transverse spin squared" H^2 is positive at each edge (and the momenta are not colinear). Hence in the generic case, the configuration in Minkowski space of the six W-vectors and six P-vectors is determined by the conservation laws and 20 invariants associated with the Racah kernel T, up to Lorentz transformation.

Now we investigate the conditions for imbedding both T and T' in the same Minkowski space. In the rest frame of particle 4, the 3-momenta of T fall in a plane, as shown in figure 5.3b. The momenta of T' fall into another plane in the same frame. Figure 5.6b shows the intersection of these two momenta-planes, along with the three intrinsic spin W-vectors associated with the common face (124). In general, this joint configuration is not imbeddable in a single Minkowski space. The requirement that \vec{W}_4 coincide in the T and T' configurations determines the angle between the momenta planes (642) and (6'42) to be

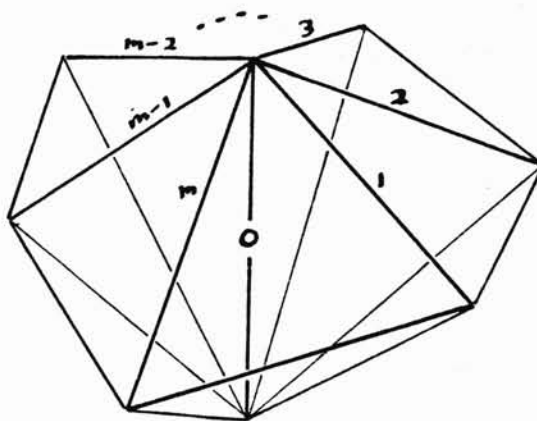
$$\tilde{\phi}_{642}^{42} + \tilde{\phi}_{6'42}^{42} \quad (5.4.6)$$

The conditions for \vec{W}_1 and \vec{W}_2 to coincide as well are precisely (5.4.4) and (5.4.5) respectively. Hence finally

Proposition 1: The phase of two Racah kernels meeting at a common coupling is stationary under variation of the corresponding helicities just when the vector diagrams for the kernels

can be jointly imbedded in Minkowski space.

Figure 5.7 Hinge of m Racah kernels



Now suppose we have n Racah kernels joined up into a web that has phase stationary under variation of all internal variables. Then each pair of adjoining kernels is imbeddable in Minkowski space, but obstructions may arise if we follow a sequence of couplings around in a loop. The basic loops are those that link a single edge. Hence ^{we are led} it suffices to consider the simple case of an internal edge 0 which is the hinge for m Racah kernels T_1, \dots, T_m , as in figure 5.7. From (5.4.1), the stationary phase condition under variation of the spin j_0 is

$$\frac{\partial \Phi^+}{\partial j_0} = \tilde{\theta}_{o2}^{\tilde{o}1} + \tilde{\theta}_{o3}^{\tilde{o}2} + \dots + \tilde{\theta}_{om}^{\tilde{o}m-1} + \tilde{\theta}_{o1}^{\tilde{o}m} = 0. \quad (5.4.7)$$

Here the sum is of all the angles contained between the projections of the successive momenta P_1, P_2, \dots, P_m onto the \tilde{o} -plane: that is, the plane $*(W_o \wedge P_o)$ normal to \vec{J}_o in the o-rest-frame. Since j_0 varies by integer steps, we may introduce into Φ^+ an additional phase factor $-2\pi(j_0 + \chi_o)$, where χ_o is a constant 1/2 or 0, as required to make j_0 an integer. Then (5.4.7) states:

Proposition 2: The phase of m Racah kernels hinging at a common edge 0 is stationary under variation of the spin j_0 just when the successive momenta P_1, P_2, \dots, P_m that couple with 0 produce vanishing defect angle in the $\tilde{0}$ -plane.

Finally, we consider the stationary phase condition under variation of m_0 . From (5.4.1),

$$\frac{\partial \Phi^+}{\partial m_0} = \sum_{k,rs} H_{rs}^k \frac{\partial \beta_{k,rs}}{\partial m_0}, \quad (5.4.8)$$

where the sum is over the $6m$ combinations of edge indices k,rs which occur in the d -functions of the m Racah kernels T_1, \dots, T_m . This sum can be simplified by noting that

$$H_{rs}^k = (W_k \cdot u_{krs}) / m_k. \quad (5.4.9)$$

The derivatives of the β -angles can be computed from (5.3.4), and simplified with the techniques of (3.3.3-5). Despite these simplifications, I have not been able to cast (5.4.8) into a form that admits geometric interpretation as straightforward as propositions 1 and 2. At least some of the conditions (5.4.8) are redundant: in particular, the angles β are unchanged under simultaneous scaling of all the masses.

Recall that the positive-frequency action Φ^+ in the semiclassical limit of n Racah kernels is

$$\Phi^+ = \sum_{k,\ell m} (j_k \tilde{\theta}_{km}^{k\ell} + \lambda_{k,\ell} \tilde{\phi}_{mk\ell}^{k\ell} + \lambda_{k,m} \tilde{\phi}_{\ell km}^{km}), \quad (5.4.10)$$

where the sum is over all $k,\ell m$ combinations occurring in the d -functions of the kernels. The λ -stationarity conditions (5.4.4-5) together with the λ -conservation laws (5.3.10) imply that the summation over the $\lambda\phi$ -terms in (5.4.10) vanishes identically. Except for surface terms, we are left with a summation over $j\theta$ -terms which involves angle defects identical to those arising in the Regge calculus version of the 4-d vacuum Einstein action. However, these angle defects appear in the sum with weights which differ from those in the Einstein case in such a

way that the action is stationary under variation in the spins only when the curvature vanishes.

It remains to be seen how a fabric can be constructed which will correctly model curved spaces in the semiclassical limit. A term must appear in the action to break the mass scale-invariance and account for the inhomogeneous source in Einstein's equations (i.e., the energy-momentum density). A fabric for curved space might correspond to some generalization of the local space-time symmetry group. The natural way scalar curvature arises even in the simple case of the Poincare group will probably play a role in applying fabrics as models in the quantization of gravity.

REFERENCES

- [V.K. Agrawala and J.G. Belinfante 68] "Graphical Formulation of Recoupling Theory for any Compact Group" Annals of Physics 49, 130-170
- [L.C. Biedenharn 53] "An Identity Satisfied by the Racah Coefficients" J.Math.Phys. 31, 287-293
- [J.R. Derome 66] "Symmetry Properties of the 3j-Symbols for an Arbitrary Group" J.Math.Phys. 7, 612-15
- [E. ElBaz and B. Castel 72] Graphical Methods of Spin Algebras (Marcel Dekker, New York)
- [J.P. Elliott 53] Proc.Roy.Soc. A218, 370
- [R.P. Feynman and A.R. Hibbs 65] Quantum Mechanics and Path Integrals (McGraw Hill, New York)
- [B. Hasslacher and M. Perry 81] "Spin Networks are Simplicial Quantum Gravity" Physics Letters 103b 21-24
- [I.N. Herstein 64] Topics in Algebra (Ginn)
- [W.H. Klink 71] "Multiparticle Partial-Wave Amplitudes and Inelastic Unitarity I. General Formalism: Racah Coefficient for the Poincare Group" Phys.Rev. D 4, 2260-80
- [W.H. Klink 75] "Two applications of the Racah Coefficients of the Poincare Group" J.Math.Phys. 16, 1247-52
- [L.H. Loomis and S. Sternberg 68] Advanced Calculus (Addison-Wesley)
- [J.P. Moussouris 79] "Chromatic Evaluation of Spin Networks" in Advances in Twistor Theory, eds. L.P. Hughston and R.S. Ward (Pergamon)
- [R. Penrose 68] "Structure of Space-time", in Battelle Rencontres 1967, eds. C.M. De Witt and J.A. Wheeler (W.A. Benjamin)
- [R. Penrose 71] "Angular Momentum: An Approach to Combinatorial Space-time" in Quantum Theory and Beyond, ed. T. Bastin (Cambridge University Press)
- [R. Penrose 72] "On the Nature of Quantum Geometry", in Magic Without Magic: John Archibald Wheeler, ed. J.R. Klauder (W.H.Freeman & Co., San Francisco)
- [R. Penrose 72b] "Applications of Negative Dimensional Tensors" in Combinatorial Theory and Applications, ed. D. Welsh (Wiley)
- [G Ponzano and T. Regge 68] "Semiclassical Limit of Racah Coefficients" in Spectroscopic and Group Theoretical Methods in Physics, ed. F. Bloch (North Holland Publ. Co., Amsterdam)
- [T. Regge 61] "General Relativity without Coordinates" Nuovo Cimento 19, 558-571
- [M. Rocek and R.M. Williams 81] "Quantum Regge Calculus" Physics Letters 104B, 31-37

[Edmonds 53] >
[Poincaré 33]

[K. Schulten and R.G. Gordon 75] "Semiclassical approximations to 3j- and 6j-coefficients for quantum-mechanical coupling of angular momenta" J.Math.Phys. 16, 1971-89

[R. Sorkin 75] "Time-evolution problem in Regge Calculus" Phys.Rev. D 12, 385-396

[G.C. Wick 62] "Angular Momentum States for Three Relativistic Particles" Annals of Physics 18, 65-80

[Wick 62 39]
[E.P. Wigner 59] Group Theory and its Application to the Theory of Atomic Spectra (Academic Press, New York)

[A.P. Yutsis, I.B. Levinson and V.V. Vanagas 62] Mathematical apparatus of the theory of angular momentum (Israel Program for Scientific Translations, Jerusalem)